

NEUTRON CAPTURE IN THE  
GIANT DIPOLE RESONANCE REGION OF  $^{14}\text{C}$

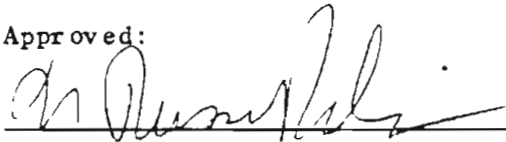
by

Michael Carl Wright

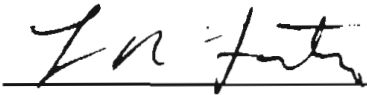
Department of Physics  
Duke University

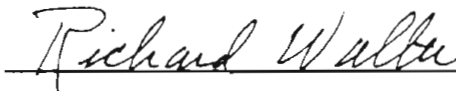
Date: June 24, 1983

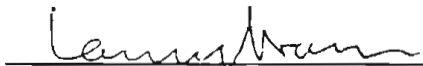
Approved:



N. Russell Roberson, Supervisor









A dissertation submitted in partial fulfillment of  
the requirements for the degree of Doctor  
of Philosophy in the Department of  
Physics in the Graduate School  
of Duke University

1983

Abstract

NEUTRON CAPTURE IN THE  
GIANT DIPOLE RESONANCE REGION OF  $^{14}\text{C}$

by

Michael Carl Wright

Department of Physics  
Duke University

Date: \_\_\_\_\_

Approved:

\_\_\_\_\_

N. Russell Roberson, Supervisor

\_\_\_\_\_

\_\_\_\_\_

\_\_\_\_\_

\_\_\_\_\_

An abstract of a dissertation submitted in partial  
fulfillment of the requirements for the degree  
of Doctor of Philosophy in the Department  
of Physics in the Graduate School  
of Duke University

1983

# NEUTRON CAPTURE IN THE GIANT DIPOLE REGION OF $^{14}\text{C}$

by

Michael Carl Wright

The ninety-degree absolute cross section of the  $^{13}\text{C}(n, \gamma_0)^{14}\text{C}$  reaction was measured in 200 keV steps at neutron energies ranging from 5.6 to 13 MeV and at selected energies between 13 and 17 MeV. The angular distributions of cross section and analyzing power were measured at 7.75, 9.2, 10.0, 10.2, 11, 12, and 13 MeV over an angular range of  $30^\circ$  to  $150^\circ$ . Ninety-degree analyzing powers were measured at 17 energies from  $E_n = 7.75$  MeV to  $E_n = 15$  MeV. Fore-aft asymmetries were measured at 7 energies from  $E_n = 10.2$  MeV to  $E_n = 17$  MeV.

The giant dipole resonance in  $^{14}\text{C}$  was found to be split into two components at excitation energies of 15.45 and 17.85 MeV and with widths of 1.5 and 1.75 MeV, respectively. Two-level doorway state calculations agree well with the measured  $a_2$  and  $b_2$  coefficients and indicate that it is reasonable to parameterize the giant dipole resonance as two different levels of the same spin and parity. After detail balance conversion to photoneutron cross section, the integrated E1 yield exhausted 14 % of the classical dipole sum rule in the  $(\gamma, n_0)$  channel in the region of 13.4 to 24 MeV excitation energy. A model independent E1 transition matrix analysis of the data yielded two solutions, one where the  $d_{3/2}$  matrix element accounted for about 85 % of the E1 cross section, the other where the  $d_{3/2}$  element accounted for about 30 % of the E1 cross section. Direct-semidirect model calculations indicate the dominant

$d_{3/2}$  solution to be the physical one.

The E1-E2-M1 transition matrix element analysis showed that the E2 strength was less than 2 % of the total cross section and that the M1 strength could not be determined by examination of a single angular distribution. The observed E2 strength exhausts  $2.8 \pm 0.6$  % of the isoscalar E2 energy weighted sum rule. The data show little evidence for collective E2 strength in the  $(\gamma, n_0)$  channel.

Structure in the  $90^\circ$  analyzing power and in the Legendre coefficient  $b_1$  near 9.2 and 10.2 MeV neutron energy suggests the existence of narrow M1 resonances at these energies. A direct-semidirect model calculation was in good overall agreement with all of the experimental data when it included two M1 resonances at excitation energies 16.7 and 17.5 MeV, with strengths 0.24 and  $0.17 \mu_0^2$ , and widths less than the 300 keV energy spread of the neutron beam.

## ACKNOWLEDGEMENTS

I would like to thank Dr. Russell Roberson, my thesis advisor, and Dr. Henry Weller for their interest, help, advice, and support during my graduate career. I would also like to thank Drs. Mark Jensen and Ron Tilley for their prior work with this reaction. I am very grateful for the help and friendship of the other students in the capture group, Steve King, George Mitev, Steve Manglos, Linton Ward, Colleen Fitzpatrick, Bob August, and Doug Wagenaar. I also want to thank Kim Murphy for many pleasant hours of algebraic manipulations.

I would like to thank Dr. Tom Clegg for his help with the polarized ion source and its microprocessor, and Dr. Jim Jury for the use of the  $^{13}\text{C}$  target. I am indebted to Sidney Edwards for many discussions of computers and electronics, and to Mike Bailey for her help with the preparation of the figures.

Most of all, I thank my parents, Harvel and Carleta, and my sister, Nancy, for their support and encouragement throughout all of my 22 years of schooling.

## TABLE OF CONTENTS

ABSTRACT . . . . .	iii
ACKNOWLEDGEMENTS . . . . .	v
LIST OF FIGURES . . . . .	viii
LIST OF TABLES . . . . .	ix
1. INTRODUCTION . . . . .	1
2. EXPERIMENTAL EQUIPMENT . . . . .	7
2.1 Overview . . . . .	7
2.2 Beam . . . . .	7
2.3 Target . . . . .	16
2.4 Detectors . . . . .	16
2.5 Electronics . . . . .	17
2.6 Data Acquisition . . . . .	23
3. ANALYZING POWER AND FORE-AFT ASYMMETRY MEASUREMENTS . . . . .	31
3.1 Peak Stripping and Summing . . . . .	31
3.2 Analyzing Power . . . . .	32
3.3 Fore-aft Asymmetry . . . . .	33
3.4 Cross Section . . . . .	38
4. ANGULAR DISTRIBUTIONS . . . . .	54
4.1 Peak Stripping and Summing . . . . .	54
4.2 Angular Distributions of Cross Section . . . . .	55
4.3 Angular Distributions of Analyzing Power . . . . .	56
4.4 Constrained Legendre Polynomial Fits . . . . .	59
5. CONSTRAINED LINEAR LEAST SQUARES . . . . .	65
5.1 Introduction . . . . .	65
5.2 Reexpression of the Function to be Fit . . . . .	66
5.3 Determination of Fitting Coefficients . . . . .	69
5.4 Error on Fitted Coefficients . . . . .	70
5.5 Error on All Coefficients . . . . .	73
6. TRANSITION MATRIX ELEMENT ANALYSIS . . . . .	76
6.1 Introduction . . . . .	76
6.2 E1 Analysis . . . . .	80
6.3 E1-E2 Analysis . . . . .	83
6.4 E1-E2-M1 Analysis . . . . .	85

7.	COMPARISON TO THEORY . . . . .	97
7.1	Sum Rules . . . . .	97
7.2	Direct-Semidirect Model . . . . .	98
7.3	Two Level Doorway State Calculations . . . . .	107
7.4	Summary . . . . .	111
8.	REFERENCES . . . . .	113
APPENDIX A	Excitation Functions . . . . .	119
APPENDIX B	Angular Distributions . . . . .	124
APPENDIX C	Transition Matrix Element Analysis . . . . .	136
APPENDIX D	Comparison to Theory . . . . .	139
APPENDIX E	Polarized Ion Source Microprocessor System . . . . .	142
APPENDIX F	Listing of SENSE Program . . . . .	159

## List of Figures

1-1	Modes of Giant Resonance Oscillation . . . . .	4
2-1	TUNL Van de Graaff Laboratory . . . . .	9
2-2	Deuterium Gas Cell . . . . .	12
2-3	Energy Spread of the Neutron Beam . . . . .	15
2-4	Gas Cell, Target, and $\gamma$ -Ray Detector Geometry . . . . .	19
2-5	$\gamma$ Ray Detection Electronics . . . . .	21
2-6	Typical $^{13}\text{C}(n, \gamma_0)^{14}\text{C}$ Spectra . . . . .	26
2-7	XSYS Box Display . . . . .	29
3-1	$90^\circ$ Analyzing Power Direct Measurement . . . . .	35
3-2	Combined $90^\circ$ Analyzing Power . . . . .	37
3-3	Fore-aft Asymmetry Direct Measurement . . . . .	40
3-4	Combined Fore-aft Asymmetry . . . . .	42
3-5	Comparison of $90^\circ$ Yield Curves . . . . .	46
3-6	Combined $90^\circ$ Yield Curve . . . . .	48
3-7	Total $(n, \gamma_0)$ Yield Curve . . . . .	50
3-8	Total $(\gamma, n_0)$ Yield Curve . . . . .	53
4-1	Angular Distributions of Cross Section . . . . .	58
4-2	Angular Distributions of Analyzing Power . . . . .	64
6-1	Schematic Representation of Transition Matrix Elements . . . . .	78
6-2	E1 Transition Matrix Solutions . . . . .	82
6-3	E1-E2 Transition Matrix Solutions . . . . .	87
6-4	E2-M1 Chi-Square Contour Plot at $E_n = 10.2$ MeV . . . . .	91
6-5	E2-M1 Chi-Square Contour Plot at $E_n = 12$ MeV . . . . .	93



6-6	E1-E2-M1 Transition Matrix Solutions . . . . .	96
7-1	Direct-Semidirect Calculation using an E2 Resonance . . . . .	101
7-2	Direct-Semidirect Calculation using two M1 Resonances . . . . .	103
7-3	DSD Calculation with one and with two M1 Resonances . . . . .	105
7-4	Two-Level Doorway State Calculation . . . . .	109

List of Tables

A-1	90° Analyzing Power . . . . .	119
A-2	Fore-aft Asymmetry . . . . .	120
A-3	90° Cross Section . . . . .	121
A-4	Total ( $n, \gamma_0$ ) Cross Section . . . . .	122
A-5	Total ( $\gamma, n_0$ ) Cross Section . . . . .	123
B-1	Angular Distributions of Cross Section and Analyzing Power . .	124
B-2	Unconstrained Legendre Polynomial Fits . . . . .	128
B-3	Constrained Legendre Polynomial Fits . . . . .	132
C-1	E1 Transition Matrix Solutions . . . . .	136
C-2	E1-E2 Transition Matrix Solutions . . . . .	137
C-3	E1-E2-M1 Transition Matrix Solutions . . . . .	138
D-1	Parameters used in the Direct-Semidirect Calculations . . . .	139

## 1 Introduction

The dominant features of the photonuclear reaction in the excitation energy region of a few MeV up to about 50 MeV are the giant resonances. They are characterized by a peak in the yield curve of the order of 5 MeV wide. The magnitude of the integrated cross section of the individual peaks is, in general, a large fraction of the appropriate sum rule (Fuller, 1981). The giant resonance can be labeled by the angular momentum  $L$  of the absorbed  $\gamma$  ray. The order of the  $\gamma$ -ray multipolarity is given by  $2^L$  so that if, for example,  $L = 1, 2,$  or  $3,$  the absorbed  $\gamma$  radiation is dipole, quadrupole, or octupole, respectively. If the parity change of the nucleus is  $(-1)^L$ , the multipolarity is classified as electric; if the parity change is  $(-1)^{L+1}$ , the classification is magnetic. In this way, the multipolarity of a giant resonance can be written by  $XL$ , where  $X = E$  for electric and  $M$  for magnetic, and  $L$  is the angular momentum of the absorbed  $\gamma$  ray. For example, the giant electric quadrupole resonance is referred to as a giant E2 resonance.

The most prominent and well studied giant multipole resonance is the one associated with electric dipole transitions. The peak of the giant dipole resonance occurs near  $80 A^{-1/3}$  MeV in medium and heavy nuclei and at about 20 MeV in light nuclei. Resonances of higher multiplicities have recently been observed and are of current experimental interest (Bertrand, 1976). Giant resonance cross section measurements have been carried out by a variety of methods including

electron scattering, inelastic proton and alpha particle scattering, and photon scattering and absorption (Bertrand, 1980).

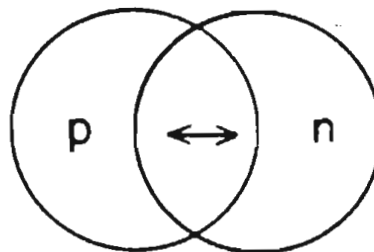
The giant resonances of a nucleus "A" can also be excited by nucleon capture into the nucleus "A-1". The principle of detail balance can be applied to infer the inverse photonuclear cross section. The capture reaction has many attractive features (Hanna, 1979). By measuring the cross sections and analyzing powers as a function of energy, complete knowledge can, in many cases, be obtained of a single decay channel. The measurements often allow the various multipoles involved in the reaction to be identified with a high degree of certainty. In addition, capture reactions are the only technique for studying giant multipole resonances built on excited states. Particle beams of high intensity and small energy spread are generally easier to produce and manipulate than  $\gamma$ -ray beams.

The modes of vibration of the nucleus for some of the lower order resonances are illustrated in Figure 1-1. In isoscalar electric modes, the nucleus as a whole vibrates. In isovector electric modes, the protons vibrate out of phase with the neutrons. In the isovector magnetic modes, protons with spin up and neutrons with spin down oscillate against protons with spin down and neutrons with spin up, respectively.

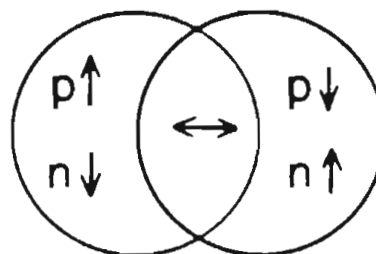
The direct-semidirect model (DSD) has been successful in describing the radiative capture process (Brown, 1964, and Clement et al., 1965). The capture reaction is separated into two components,

Figure 1-1 Schematic representations of some of the lower order modes of nuclear giant resonance oscillation.

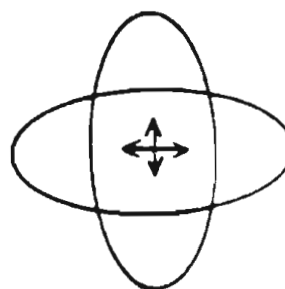
ISOVECTOR  
E1



ISOVECTOR  
M1



ISOSCALAR  
E2



the direct and the semidirect. Direct capture corresponds to the incident nucleon emitting the  $\gamma$  ray as it is captured directly to the final state of the residual nucleus. Semidirect capture corresponds to the incident nucleon exciting the nucleus into a collective state which decays to the final state through the emission of the  $\gamma$  ray. The lifetime of the collective state is longer than the time of a direct reaction but is shorter than the lifetime of a compound nuclear state. The direct capture cross section is proportional to the square of the recoil effective charge,  $\epsilon_L$  (Hayward, 1970). The effective charges for E1 and E2 radiation from proton and neutron capture are given by

$$\begin{aligned}
 1-1 \quad \epsilon_{1,p} &= \frac{N}{1 + A} \\
 \epsilon_{1,n} &= \frac{-Z}{1 + A} \\
 \epsilon_{2,p} &= \frac{(A^2 + Z)}{(1 + A)^2} \\
 \epsilon_{2,n} &= \frac{Z}{(1 + A)^2}
 \end{aligned}$$

where A and Z refer to the mass and charge of the target nucleus. For E1 radiation the effective charges are about equal, but for quadrupole radiation the neutron effective charge is less than the proton effective charge by a factor  $(A^2 + Z) / Z$ . Collective E2 strength should be much more easily observed with neutron capture than with proton capture since the direct E2 contribution to the cross section will be significantly reduced.

This work presents a continuation of the investigation of the giant resonance region of  $^{14}\text{C}$  by the radiative capture group at the Triangle Universities Nuclear Laboratory (TUNL) using the  $^{13}\text{C}(\vec{n}, \gamma_0)^{14}\text{C}$  reaction. No previous published data existed for this nucleus due to the difficulty of producing a  $^{14}\text{C}$  target for the  $(\gamma, n)$  measurements that are more commonly used to study giant resonances. The spin one half ground state of the  $^{13}\text{C}$  target along with the spin zero ground state of the  $^{14}\text{C}$  residual nucleus imply that it is possible, in principle, to perform a model-independent transition matrix analysis of the data (see chapter 6). The results of the transition matrix analysis are used to determine the multipolarity of the  $\gamma$  radiation, as discussed above. The small quadrupole recoil effective charge of the neutron means that the direct E2 radiation from neutron capture should be reduced by more than a factor of 1000 compared to proton capture. The previous TUNL data (Jensen, 1981) showed evidence for collective E2 strength at the highest energies measured but was not of sufficient quantity or statistical accuracy to unambiguously demonstrate the existence of a collective E2 resonance.



## 2 Experimental Equipment

### 2.1 Overview

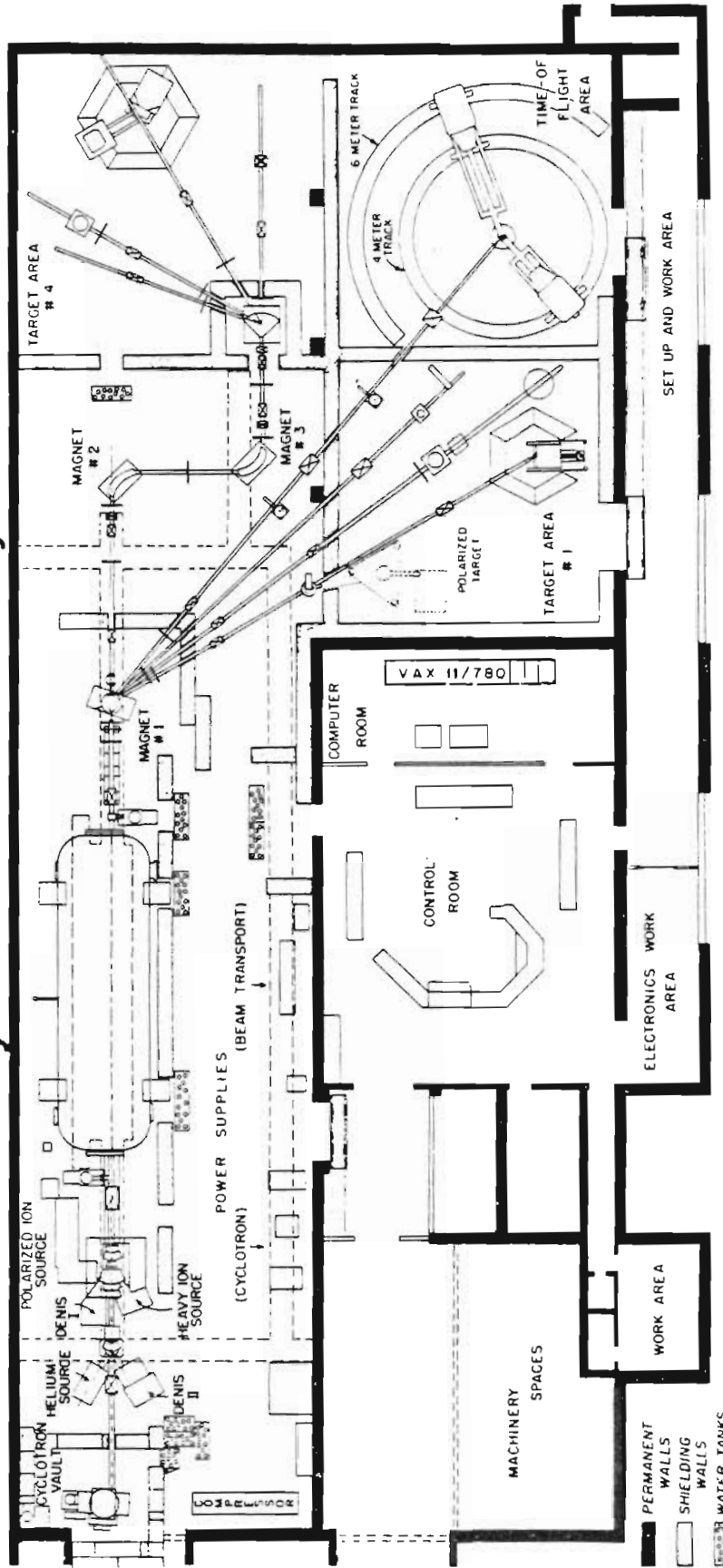
Neutrons are electrically neutral and so do not respond to the Coulomb force. This makes them useful theoretically for understanding the nuclear force but difficult to use experimentally. Neutrons cannot be produced in ion sources and accelerated directly as can charged particles but must be produced by the nuclear reaction of some charged particle with a stable nucleus. As a result, neutron beams are generally much less intense than charged particle beams and have poorer energy and spatial resolution characteristics. Because neutrons react weakly with matter, targets and detectors must be large and detectors are generally low in efficiency. Time consuming finite geometry and multiple scattering corrections must be applied to the data. Background problems arise from many sources. Despite massive shielding, neutrons scattered from walls, floors, air and anything else in the target room may enter the detector. In the case of  $\gamma$ -ray spectroscopy, neutrons scattered by the target itself also present a background problem. Target out background measurements are often required but provide only an estimate of the true background.

### 2.2 Beam

A floor plan of the TUNL Van de Graaff laboratory is shown in Figure 2-1. A direct extraction negative ion source was used to produce

Figure 2-1 TUNL Van de Graaff laboratory.

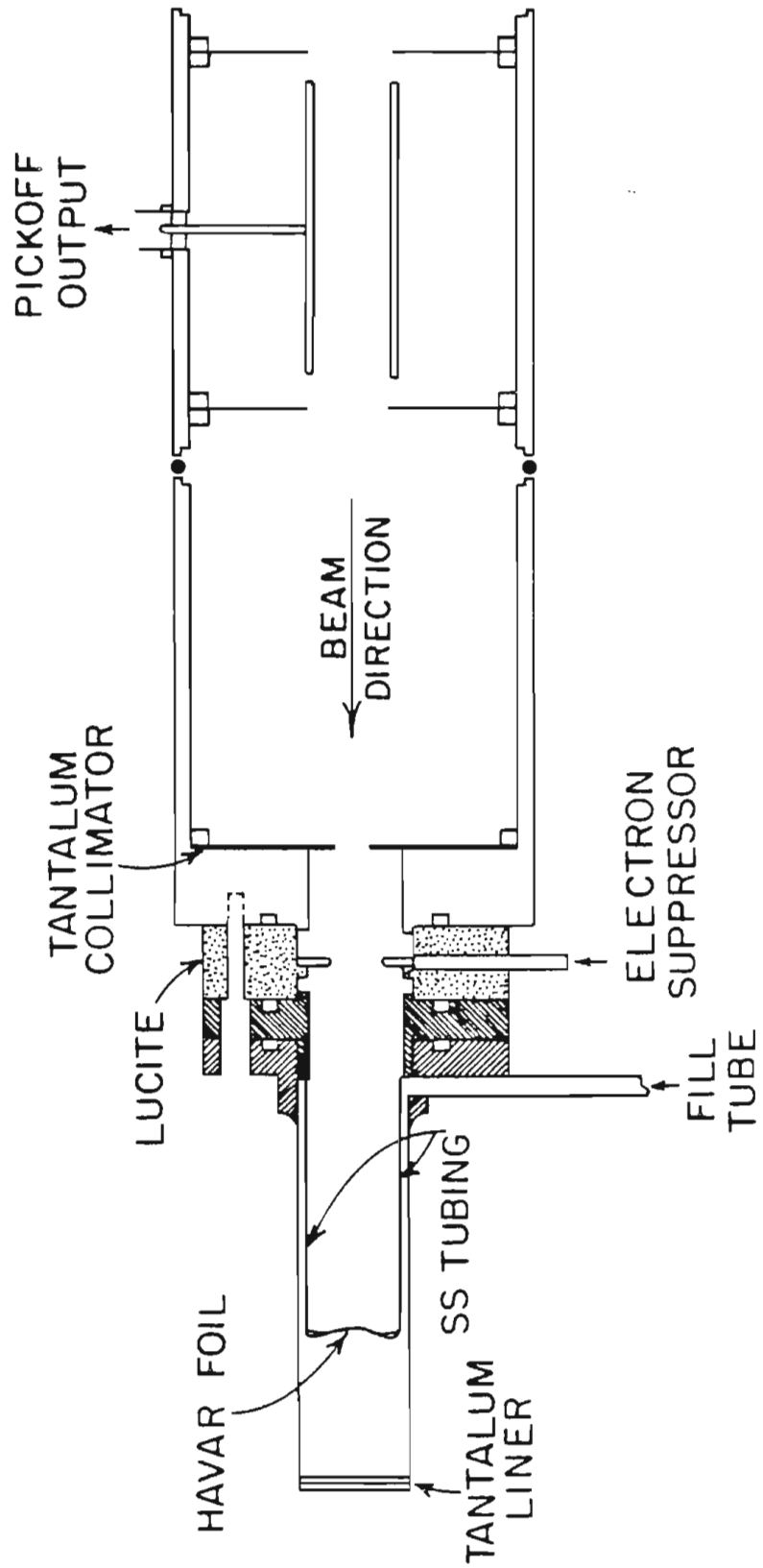
# Cyclo-Graaff Laboratory



an unpolarized deuteron beam (labeled DENIS II in Figure 2-1). The beam was passed through a radio frequency chopper and a double drift klystron buncher. The pulsing system produced beam bursts of 2 nsec on target with a repetition rate of 2 MHz. For this work, beam currents on target were typically 350 nA. The polarized beam was produced by a Lamb shift polarized ion source (Clegg et al., 1970). The beam was ramped, bunched and chopped to produce 2 nsec beam bursts with a repetition rate of 4 MHz (Wender et al., 1980). Approximately 70% of the DC beam from the source could be bunched into the pulsed beam. Typical beam currents were 90 nA. The polarization of the deuteron beam was measured using the quench ratio method (Trainor et al., 1974) and was typically 0.65. The beams from the ion sources were injected into a tandem Van de Graaff accelerator with a maximum terminal voltage of 8 MV. The beam was then momentum analyzed by two  $90^\circ$  bending magnets (see Figure 2-1).

Neutrons were produced by sending the beam through a  $5.6 \mu\text{m}$  Havar foil into a 2.5 cm gas cell filled with 6 atm of deuterium. Figure 2-2 shows a diagram of the gas cell, collimator, and time pickoff assembly. The  $^2\text{H}(d,n)$  reaction produced the neutrons. The  $^2\text{H}(d,n)$  reaction has a cross section which is forward peaked so that most of the neutrons lie in a  $20^\circ$  cone centered about the beam direction. A computer program was used to calculate the incident deuteron energy needed to produce outgoing neutrons of the desired energy at the center of the gas cell allowing for energy loss in the entrance foil and target gas. For neutron energies less than 9.2 MeV, the pressure in the gas cell was reduced to 5 atm to narrow the energy spread of the neutron beam. The

Figure 2-2 Deuterium gas cell.



energy spread of the neutrons leaving the gas cell ranged from 400 KeV at  $E_n = 7.75$  MeV to 180 KeV at  $E_n = 17.0$  MeV and is shown in Figure 2-3. The interior of the gas cell was lined with tantalum. The amount of beam used in the experiment was determined by integrating the charge deposited in the gas cell. The deuteron beam was collimated at the entrance to the gas cell by passing it through a 0.4 cm hole in a tantalum disk. Current on the collimator was kept below 1 nA. In front of the collimator was a 7.6 cm long by 1 cm diameter copper tube that served as a capacitive pickup to determine the arrival time of a beam burst at the gas cell.

Polarized neutrons were produced using a polarized deuterium beam and the excellent polarization transfer characteristics of the  ${}^2\text{H}(\vec{d}, \vec{n})$  reaction (Lisowski, 1973). The source was operated so that the vector and tensor deuteron polarizations were equal. For this case, and for the neutron energies used in this work, the neutron polarization  $P_n$  is given by

$$2-1 \quad P_n = \frac{0.95}{0.12 + P_d^{-1}}$$

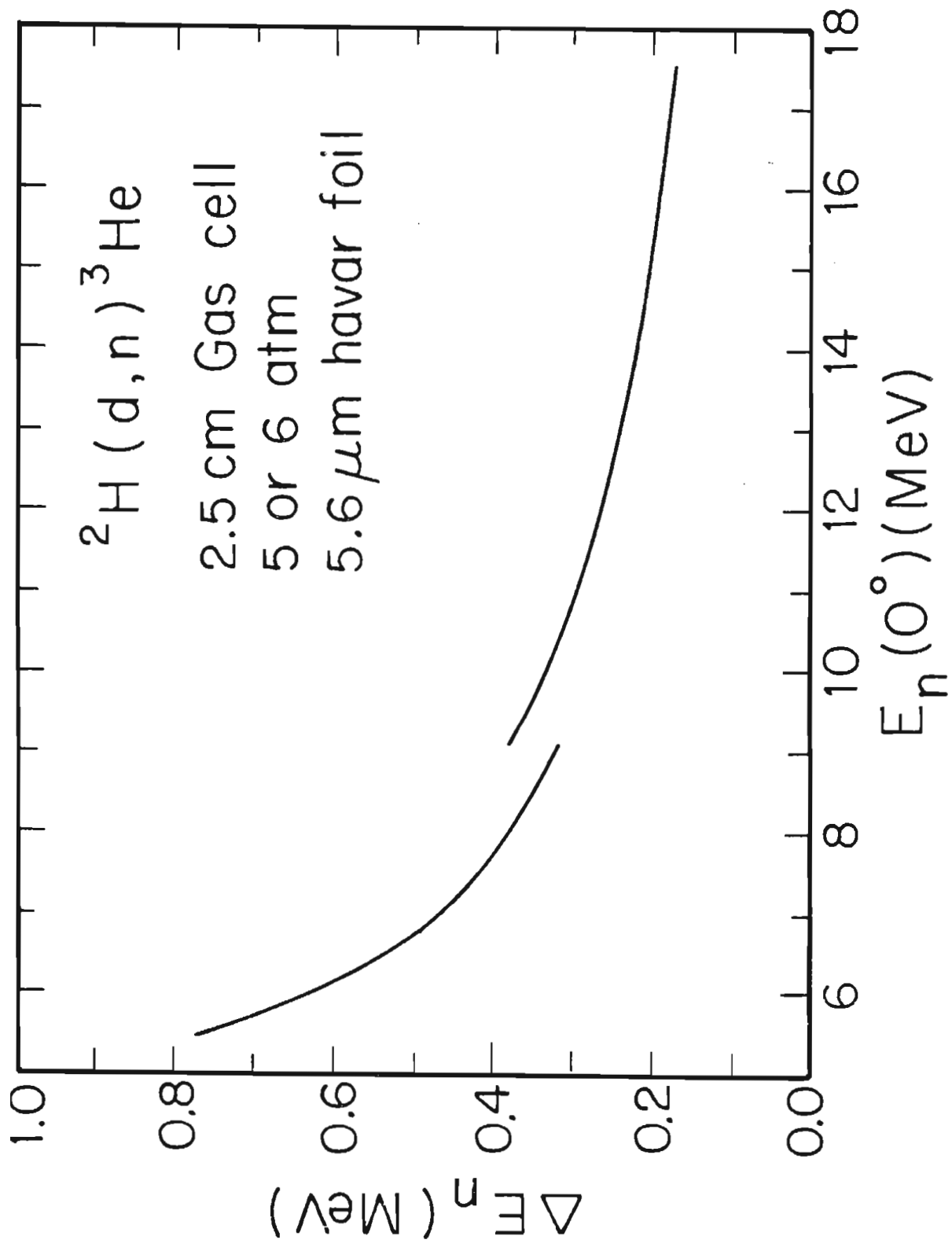
where  $P_d$  is the polarization of the deuteron beam. The cross section for production of neutrons from the  ${}^2\text{H}(\vec{d}, \vec{n})$  reaction is larger for tensor polarized deuterons than for unpolarized deuterons and is given by

$$2-2 \quad \sigma(0^0) = \sigma_u(0^0) [ 1 + 0.12 P_d ] .$$

The parameters in Equation 2-1 and Equation 2-2 were taken from Lisowski

Figure 2-3 Energy spread of the  $0^\circ$  neutron beam produced by the  ${}^2\text{H}(d, n)$  reaction in the deuterium gas cell.  $E_n$  is the neutron energy for  $0^\circ$  neutrons produced at the center of the gas cell.  $\Delta E_n$  is the difference in energy between the  $0^\circ$  neutrons produced at the front and back of the gas cell. The pressure in the gas cell was 5 atm below  $E_n = 9.1$  MeV and 6 atm above  $E_n = 9.1$  MeV.





(1973). Cross sections for the  $^2\text{H}(d,n)$  reaction were taken from Drogg (1978).

### 2.3 Target

The target consisted of 32.4 grams of 96.4% isotopically pure  $^{13}\text{C}$  in the form of a fine powder. The target was pressed into a lucite cylinder with interior dimensions of 3.8 cm height and 3.8 cm diameter. An identical empty lucite cylinder was used for performing target out measurements. The target was suspended by wires in air at a distance of 8.9 cm from the center of the target to the center of the deuterium gas cell.

### 2.4 Detectors

The  $\gamma$ -ray detection system consisted of two 25 cm by 25 cm cylindrical NaI scintillators. Each NaI detector was surrounded, except in the rear, by a 10 cm thick NE110 plastic anti-coincidence shield (Suffert et al., 1968). The shields in turn were surrounded by 10 cm of lead and 20 cm of paraffin doped with (50% by weight) lithium carbonate. The right detector had a 0.15 cm cadmium sheet between the lead and paraffin. The left detector had a 0.6 cm boron plastic sheet between the lead and paraffin. In both cases, the purpose of the additional shielding was to attenuate thermal neutrons produced in the paraffin or in the room. Each detector was collimated by a tapered lead collimator so that the rear face of the NaI detector was fully illuminated at the

standard distance of 106 cm from the center of the target to the back face of the NaI detector. Each NaI detector was shielded from neutrons produced by the gas cell using 38 kg tungsten shadow bars. Figure 2-4 shows the gas cell, target, and detector geometry.

Some of the data was taken at a target to detector distance of 145 cm. This geometry allowed much better shielding of the detector at forward angles from neutrons produced by the gas cell, and allowed the detector to move to more extreme angles without colliding with the beam line. A collimator correctly tapered for this distance was used for the fore-aft asymmetry data. The larger target to detector distance reduced the count rate by a factor of approximately 2.5 and so was used only when use of the standard distance was not possible.

An NE213 scintillator located at  $0^\circ$  at a distance of 260 cm from the target was used to monitor the neutron beam. Pulse shape discrimination was used to separate the neutrons from the  $\gamma$  rays. A time-of-flight spectrum was produced which clearly showed the neutrons from the  $^2\text{H}(d,n)$  reaction as well as the slower neutrons produced from deuteron breakup.

## 2.5 Electronics

A simplified block diagram of the electronics is presented in Figure 2-5. Each NaI detector was viewed by six gain matched RCA 8575 photo tubes. The separate outputs were summed and amplified and clipped to 350 nsec by a partially terminated coax cable clipping line. The

Figure 2-4 Gas cell, target, and  $\gamma$ -ray detector geometry.

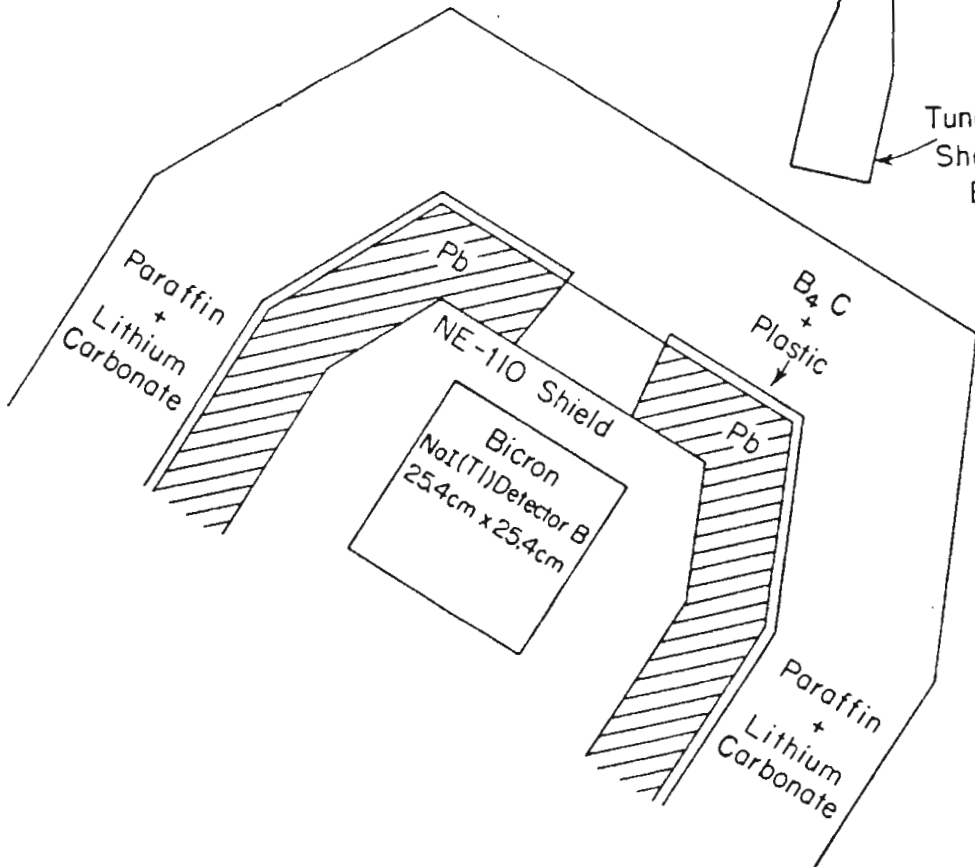
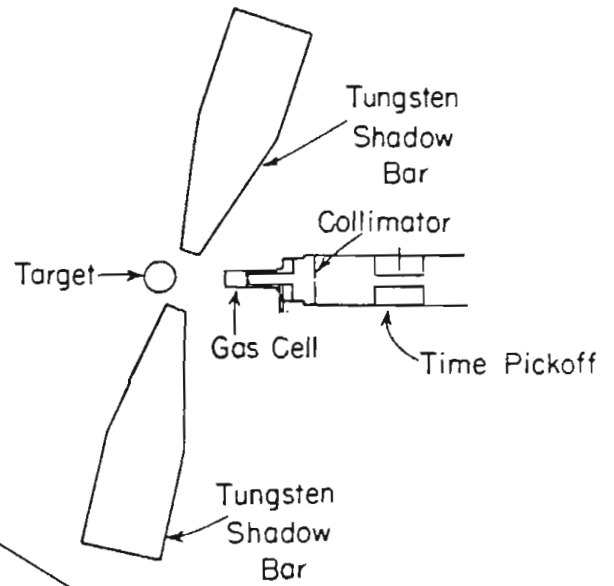
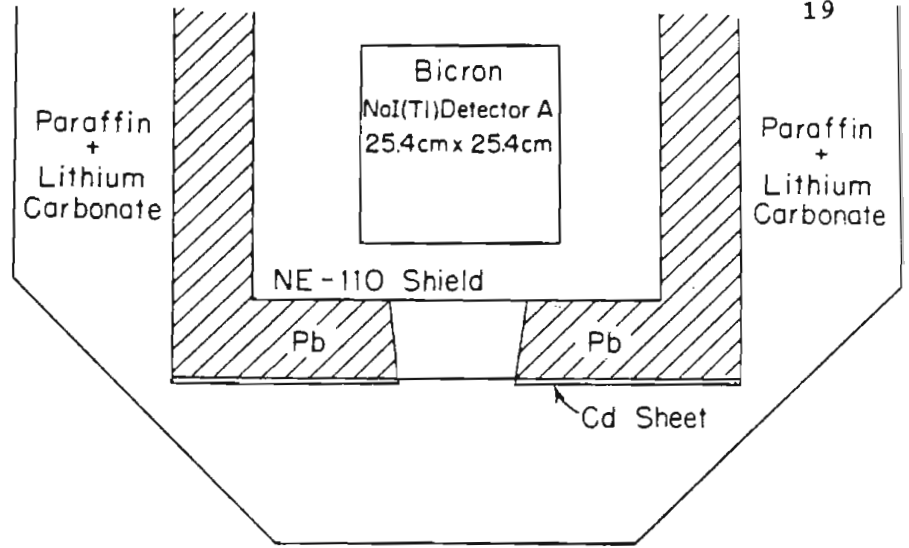
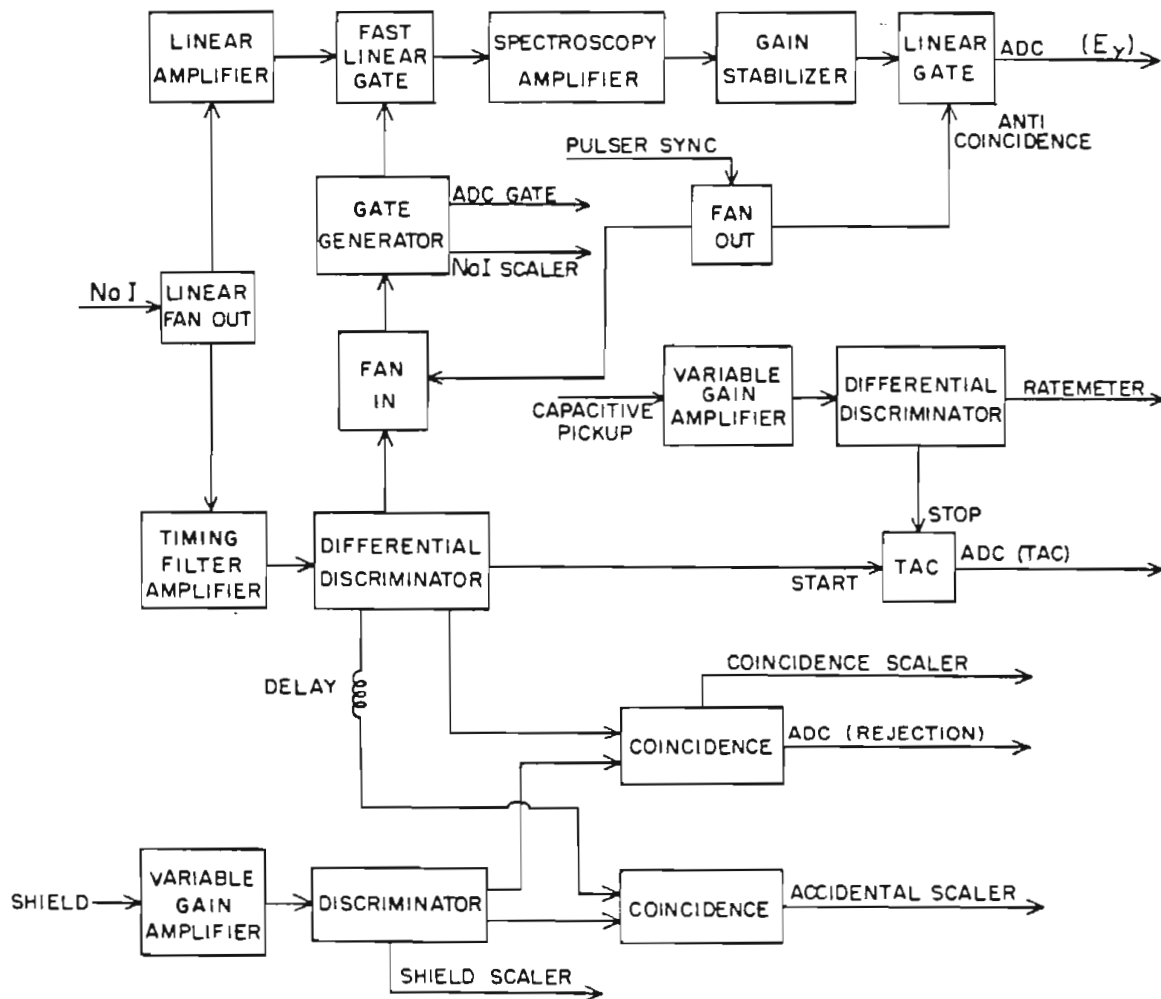


Figure 2-5 Block diagram of the  $\gamma$ -ray detection electronics for each of the NaI detectors.



signal was then sent to a 400 nsec fast linear gate, used to reduce the effects of pileup, and to a TD101 differential discriminator. The discriminator output opened the fast linear gate and was sent to two coincidence circuits. The NaI pulses were checked for coincidence with a pulse from the plastic shield. Coincident events were routed into different spectra in the computer. The peak resulting from the  $^{13}\text{C}(n, \gamma_0)^{14}\text{C}$  reaction would have been completely obscured in the spectra without the use of this active shielding. The resolving time of the coincidence system was typically 60 nsec when measured using cosmic rays. An estimate of the number of accidental coincidences between the NaI detector and the shield was provided by comparing the NaI pulses to shield pulses that were delayed by about 330 nsec. Any coincidences with the delayed shield signal must be random events. Most of the data presented in this thesis were taken in the "low rejection" mode where accidental coincidence rates are typically less than 1%. In the "high rejection" mode the beam currents occasionally were reduced in order to keep the accidental coincidence rate below 10%. Selection of rejection modes is accomplished by varying the gain on the shield. Operating in low rejection mode reduces the resolution of the detector system but increases the efficiency. Overall efficiency for the detection of the full energy of  $\gamma$  rays entering the acceptance angle of the detector system was  $27 \pm 2$  % in the low rejection mode (Weller and Roberson, 1981).

A Canberra 2050 hybrid analogue-digital gain stabilizer was used for data obtained during the latter stages of this work. A light



emitting diode inside the metal can surrounding the NaI detector was pulsed at 1 kHz to generate a signal equivalent to a 7-MeV  $\gamma$  ray in the detector. The gain stabilizer was adjusted to keep the 7-MeV pulse at a fixed voltage in the NaI linear energy signal. A synchronization signal from the electronics driving the LED was used to block the pulser signal from entering the analogue-to-digital converter (ADC) and causing pileup or dead time.

In addition to being sent to the coincidence circuitry, the signal from the NaI discriminator was sent to the start input of a time-to-amplitude converter (TAC). Stop signals were provided by the time pick-off signal from the beam. The output from the TAC was sent to an ADC and stored in the computer. Gamma-ray and neutron events could be clearly separated in the TAC spectrum. Software windows were set in the TAC spectrum and separate spectra were generated for events below, in, and above the  $\gamma$ -ray peak.

## 2.6 Data Acquisition

Three linear signals and four scaler signals were sent to the computer for each of the NaI detector systems. The three linear signals were the NaI energy, the beam burst to NaI detection time, and the shield rejection signal. The rejection signal was not a true linear signal but was the output of a gate and delay generator where the presence of a signal indicated a coincident event. The signals were fed to a LeCroy 2259A 12 input ADC. The scaler signals were NaI counts,

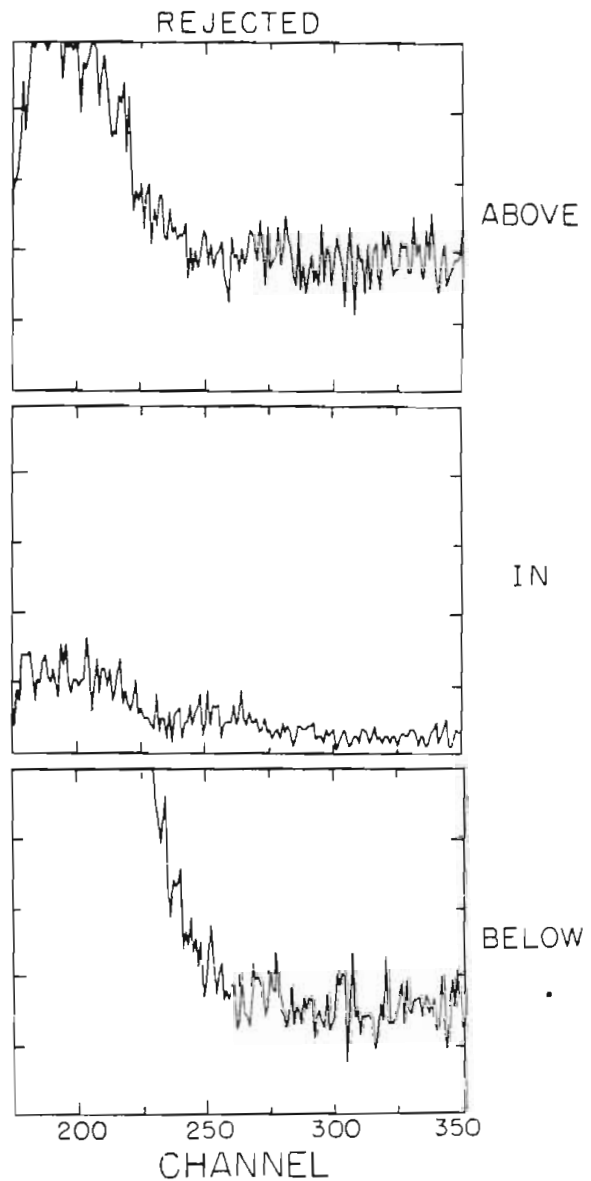
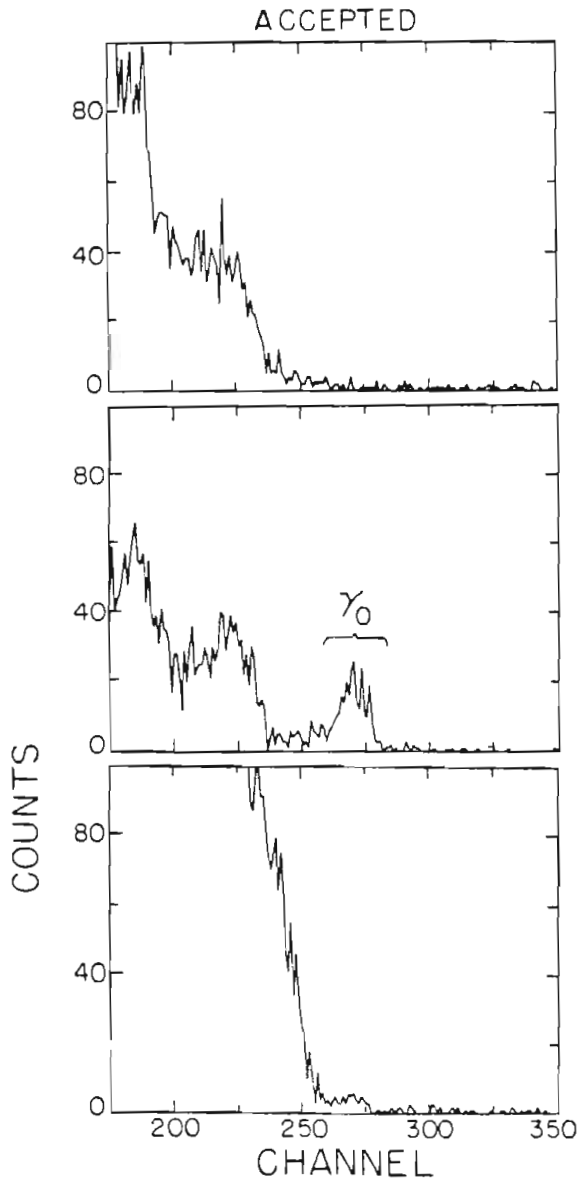
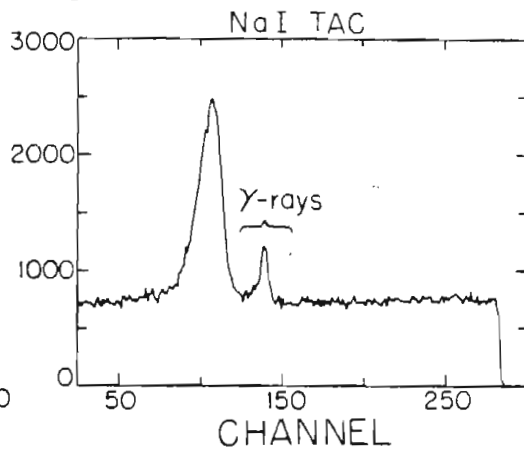
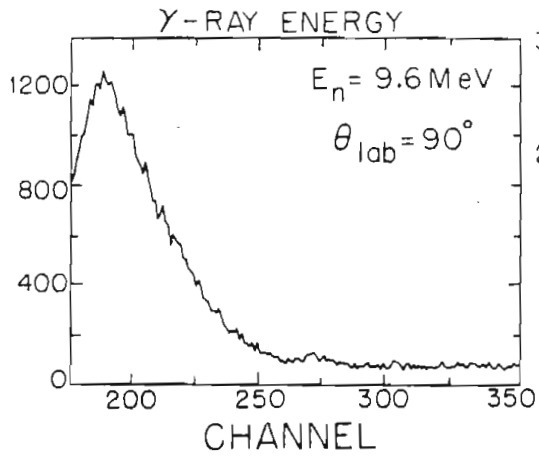
shield counts, coincidence counts, and accidental coincidence counts. Dead times for the ADC were determined by comparing the numbers of stored linear signals to the number of NaI scaler counts. Dead times were typically less than 1%. Scalers were also used to count pulses from the beam current integrator, from the beam time pick-off, and clock time.

Data taken during the early part of this work were acquired using the DDP-224 system discussed in Jensen (1981). Later data were taken using the new VAX 11/780 computer manufactured by Digital Equipment Corporation. The ADC's and scalers were resident in a CAMAC crate. The crate was interfaced to the computer system using a BiRa MBD-11 microprogrammed branch driver (Roberson and Edwards, 1981). The software used for data acquisition was the XSYS system developed at TUNL (Gould et al., 1981). Spectra were displayed on a Tektronix 4010 graphics terminal.

Thirteen spectra were accumulated for each NaI detector. The raw  $\gamma$ -ray energy spectrum was accumulated along with the six spectra generated by the time and coincidence rejection criteria. The raw TAC spectrum was accumulated along with three NaI energy gated TAC spectra. The seven  $\gamma$ -ray spectra plus the TAC spectrum are shown in Figure 2-6 for a typical data point. An additional spectrum for each NaI detector was the two valued rejection spectrum where the peak at channel 0 corresponded to accepted events and the other peak corresponded to rejected events. Since measurement of most of the data points required several hours of beam time in order to obtain an acceptable number of

Figure 2-6 Typical  $^{13}\text{C}(n, \gamma)^{14}\text{C}$  spectra. From upper left they are: accepted in window, rejected in window, accepted below window, rejected below window, accepted above window, rejected above window, all NaI events, NaI TAC.

$^{13}\text{C}(n, \gamma_0)^{14}\text{C}$



counts, the spectra were periodically dumped and cleared in order to monitor the quality of the data. The thirteenth spectrum for each detector showed the accumulation of the in-the-window, accepted  $\gamma$ -ray spectrum for all of the partial measurements. In addition a spectrum was accumulated for the  $0^\circ$  neutron monitor. During polarized beam measurement spin up and spin down spectra were both resident in memory. A total of 54 spectra were used for each polarized data point.

Scalers and other numeric data were displayed on a VT100 terminal using a software package developed by the author. Using the character graphics capabilities of the VT100 terminal, four large "scaler" boxes, thirty-two small "scaler" boxes and two large "message" boxes were drawn on the screen. Each scaler box contained room for an eight character header and an eight character value. Every two seconds the hardware scalars were read and the values written to the screen. In addition, quantities such as detector count rates, detector dead times, coincidence resolving times, accidental coincidence rates, elapsed time of current data point and time to completion of current data point were calculated and displayed. In the case of analyzing power measurements, the data peaks were summed and the current value and error of the analyzing power (defined below) was dynamically displayed on the screen. The message boxes were used to display up to ten lines of 32 character messages for communication between individuals running the experiment. A representation of the box display is shown in Figure 2-7.

Offline analysis of the spectra was performed using XSYS and the program MULFIT (King, 1980). Using standard XSYS commands, target-out

Figure 2-7 A representation of the XSYS box display after a typical run.

```

+-----+-----+-----+-----+-----+-----+-----+
| ACC1 CR | ACC2 CR | PRESET | BCI |
| 1.2 % | 0.4 % | 0 | 350000 |
+-----+-----+-----+-----+-----+
| NAI1 | SHLD1 | COIN1 | ACC1 | REM TIME | LIVETIME | TIME | RUN | NUM |
| 80174 | 622407 | 67968 | 902 | 0:00:00 | 1:41:34 | 60949 | 1559 |
+-----+-----+-----+-----+-----+
| NAI2 | SHLD2 | COIN2 | ACC2 | MONITOR | DTC | OMON |
| 71964 | 463932 | 65626 | 358 | 1015425 | 1.013778 |
+-----+-----+-----+-----+-----+
| NaI1 CR | SHLD1 CR | TACC1 CR | DTC DET1 | RSLV TM1 | T RSLV 1 | EVACTR 1 | INI | PRES |
| 14 | 101 | 1.33 | 1.012247 | 93 | 110 | 79204 | 350000 |
+-----+-----+-----+-----+-----+
| NaI2 CR | SHLD2 CR | TACC2 CR | DTC DET2 | RSLV TM2 | T RSLV 2 | EVACTR 2 | PICKOFFS |
| 12 | 76 | 0.55 | 1.021926 | 71 | 65 | 70420 | 242491 |
+-----+-----+-----+-----+-----+
| Do QR in slit mode before DU. | Total Ay = -0.064 +/- 0.054 |
| Fill trap at 9 AM and 9 PM | 0+:288. N+:255. 0-:262. N-:268. |
+-----+-----+-----+-----+-----+

```

backgrounds were normalized and subtracted from the target-in spectra. The spectra were then fit to the standard line shape (Turner, 1978) of the response function of the NaI detector using MULFIT. The number of counts in the peaks was then normalized to beam current integration, dead times, accidental coincidence rates and, for some of the data, to the  $0^\circ$  neutron monitor.



### 3 Analyzing Power and Fore-Aft Asymmetry Measurements

#### 3.1 Peak Stripping and Summing

Ninety-degree analyzing powers (see below) were measured with the two NaI detectors at 17 energies from  $E_n = 7.75$  MeV to  $E_n = 15$  MeV. Fore-aft asymmetries (see below) were measured at 7 energies from  $E_n = 10.2$  MeV to  $E_n = 17$  MeV. The response of the NaI detector to monoenergetic  $\gamma$  rays is a broadened peak that can be parameterized by a width, height, and centroid. Each spectrum was input into the MULFIT program which searched the width, height, and centroid of the standard  $\gamma$ -ray line shape to determine the best fit to the data. The widths produced by the program for the peaks did not exhibit the proper smooth increase with increasing  $\gamma$ -ray energy due to statistical fluctuations in the data. The widths for the peaks were fit to a straight line as a function of  $\gamma$ -ray energy using the method of least squares. The data were then refit by varying only the height and centroid. Due to the fluctuations in the data and to questions about the accuracy of the line shape used by MULFIT it was determined that more reliable values for the areas under the peaks could be obtained by summing the data directly rather than integrating the curve produced by the fitting procedure. The spectra were summed from 1 width below the centroid of the peak to 1.1 widths above the centroid. Fractional channels were summed at the edges of the summing region where indicated by width and centroid. The purpose of the fitting program then was to find widths for the peaks individually so that a smoothly varying width function could be

calculated, and to find the centroid of each peak so that a precise summing region could be determined.

Target-out background spectra were taken for each data point using the empty lucite shell for about 1/3 of the integrated beam current used in the target-in measurements. The target-out background spectra were summed using the same summing region for each spectrum as was used in the corresponding target-in measurement. The sums were then normalized to beam current integration, accidental coincidence rate, and electronic dead time. Since each individual background sum had only a small number of counts, the values for the sums varied from one point to the next due to statistical fluctuations but, at a given  $\gamma$ -ray angle, were essentially constant overall as a function of neutron energy. To obtain more reliable values for the background counts, the sums at each  $\gamma$ -ray angle were fit to a straight line as a function of neutron energy using the method of least squares. The fitted sums were then subtracted from the target-in sums to get the net yield for each point. The yield was then converted to the center of mass. The background ranged from 5% of the total counts where the  $^{13}\text{C}(n, \gamma_0)^{14}\text{C}$  yield was high to 25% where the yield was low.

### 3.2 Analyzing power

Analyzing power is defined as

$$3-1 \quad A_y = \frac{1}{P_n} \frac{N_+ - N_-}{N_+ + N_-}$$

where  $N_+$  is the number of counts for neutron spin up,  $N_-$  is the number of counts for neutron spin down, and  $P_n$  is the polarization of the incident neutron beam. Many experimental uncertainties can be cancelled out by doing analyzing power measurements using two detectors at the same angle on opposite sides of the beam line and flipping the spin of the beam periodically. While one detector is measuring spin up the other is simultaneously measuring spin down. Errors in beam current integration and detector efficiency are canceled out. For a two detector simultaneous measurement,  $A_y$  can be expressed by

$$3-2 \quad r = \left\langle \frac{\begin{bmatrix} L_+ & R_- \\ L_- & R_+ \end{bmatrix}}{\begin{bmatrix} L_- & R_+ \\ L_+ & R_- \end{bmatrix}} \right\rangle \frac{1}{2}$$

$$A_y = \frac{1}{P_n} \frac{r - 1}{r + 1}$$

where L represents the left detector and R represents the right detector. Following the Madison convention, for a spin "up" beam the left detector is measuring spin "up" while the right detector is measuring spin "down". The ratio r above is therefore the "true" spin up counts over the "true" spin down counts. The experimental results are shown in Figure 3-1. The data were combined, via a weighted average, with the  $90^\circ$  analyzing powers determined from the angular distribution measurements of chapter 4. The combined data are presented in Figure 3-2 and in Table A-1.

### 3.3 Fore-aft Asymmetry

Evaluation of the fore-aft asymmetry data is very similar to the

Figure 3-1 Direct two detector measurement of the  $90^\circ$  analyzing power of the  $^{13}\text{C}(\vec{n}, \gamma_0)^{14}\text{C}$  reaction.

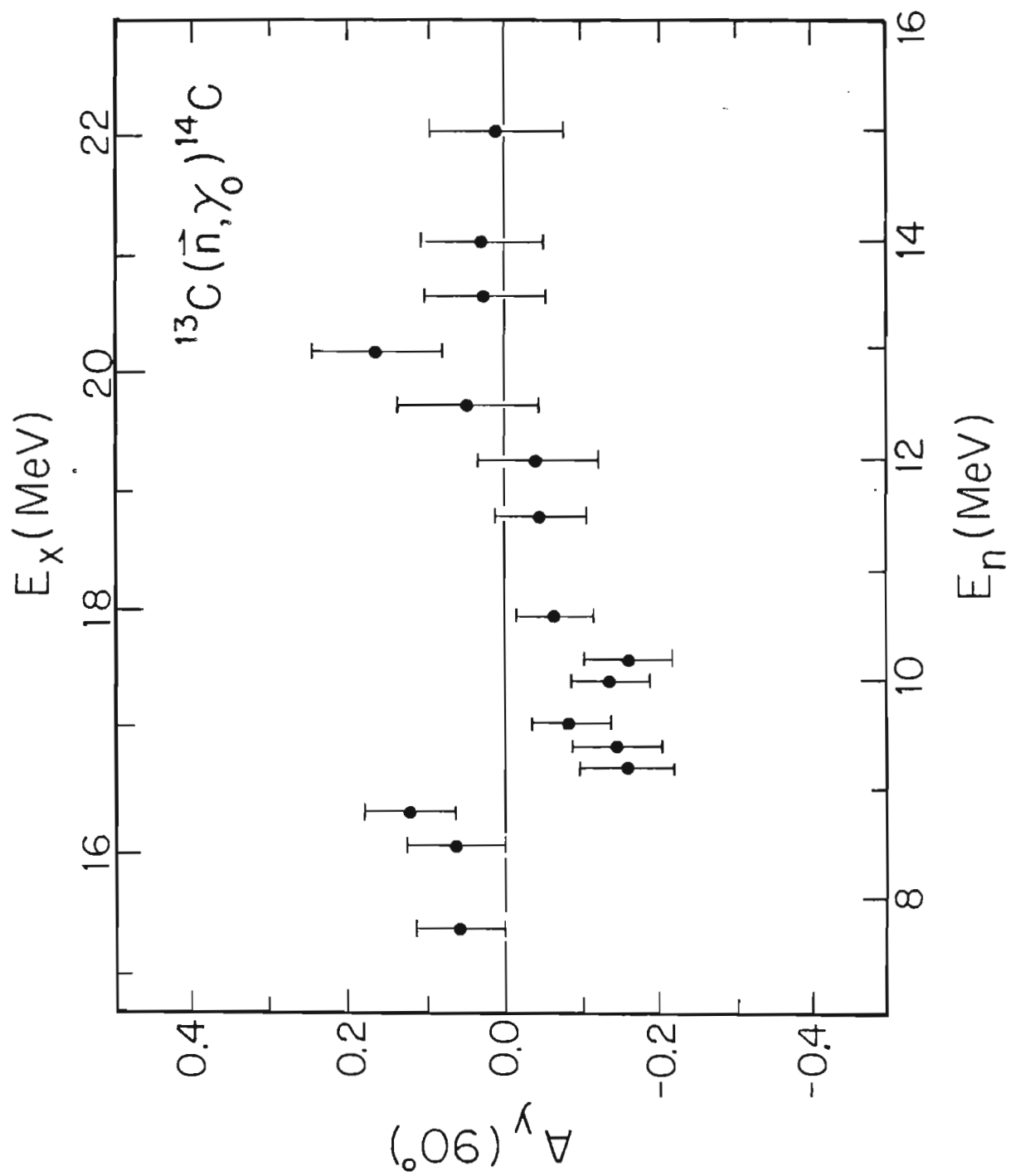
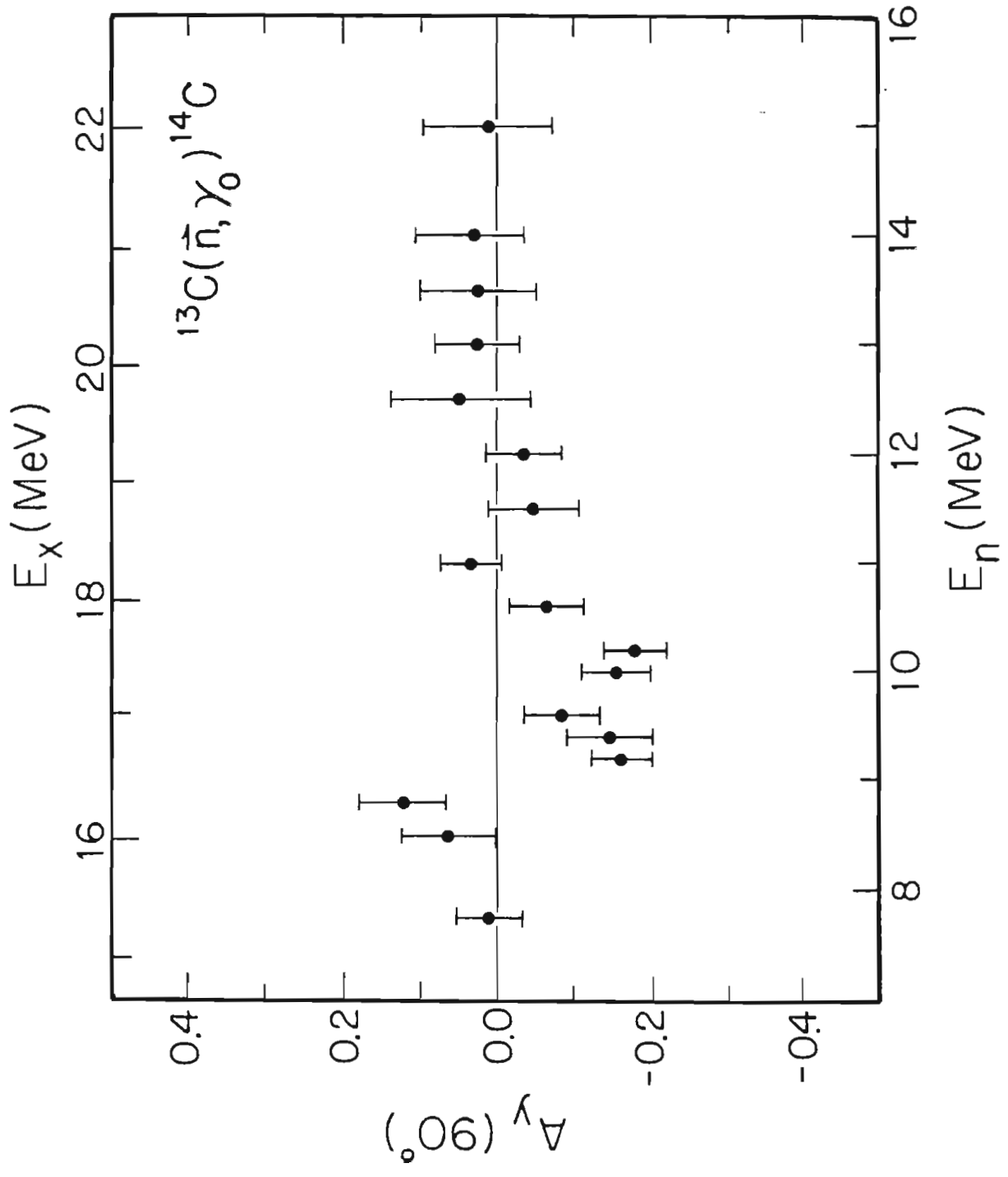


Figure 3-2 The  $90^\circ$  analyzing power of the  $^{13}\text{C}(\vec{n}, \gamma_0)^{14}\text{C}$  reaction determined by combining the direct measurements with the angular distributions.



evaluation of the analyzing power data discussed above. The fore-aft asymmetry is defined by

$$3-3 \quad a_s = \frac{N_{55} - N_{125}}{N_{55} + N_{125}}$$

where  $N_{55}$  is the number of counts observed with the  $\gamma$ -ray detector at  $55^\circ$  and  $N_{125}$  is the number of counts at  $125^\circ$ . Fore-aft asymmetry is more precisely defined at the zero's of Legendre polynomial  $P_2$  ( $54.7^\circ$  and  $125.3^\circ$ ) in the center of mass. This distinction can be neglected experimentally because of the  $10^\circ$  angular acceptance of the NaI detectors. In a manner analogous to the two detector measurement of analyzing power, we can cancel certain experimental errors in the fore-aft asymmetry measurement by placing one detector at  $55^\circ$  while the other is at  $125^\circ$  and then swapping positions and repeating the measurement. The fore-aft asymmetry can then be expressed as

$$3-4 \quad r = \left\langle \frac{\begin{bmatrix} L_{55} & R_{55} \\ L_{125} & R_{125} \end{bmatrix}}{2} \right\rangle ,$$

$$a_s = \frac{r - 1}{r + 1} .$$

The experimental results are shown in Figure 3-3. The data were combined, via a weighted average, with the fore-aft asymmetries determined from the angular distribution measurements. The combined data are presented in Figure 3-4 and in Table A-2.

### 3.4 Cross Section

The cross section at the various energies measured in the above



Figure 3-3 Direct two detector measurement of the fore-aft  
asymmetry of the  $^{13}\text{C}(n, \gamma_0)^{14}\text{C}$  reaction.

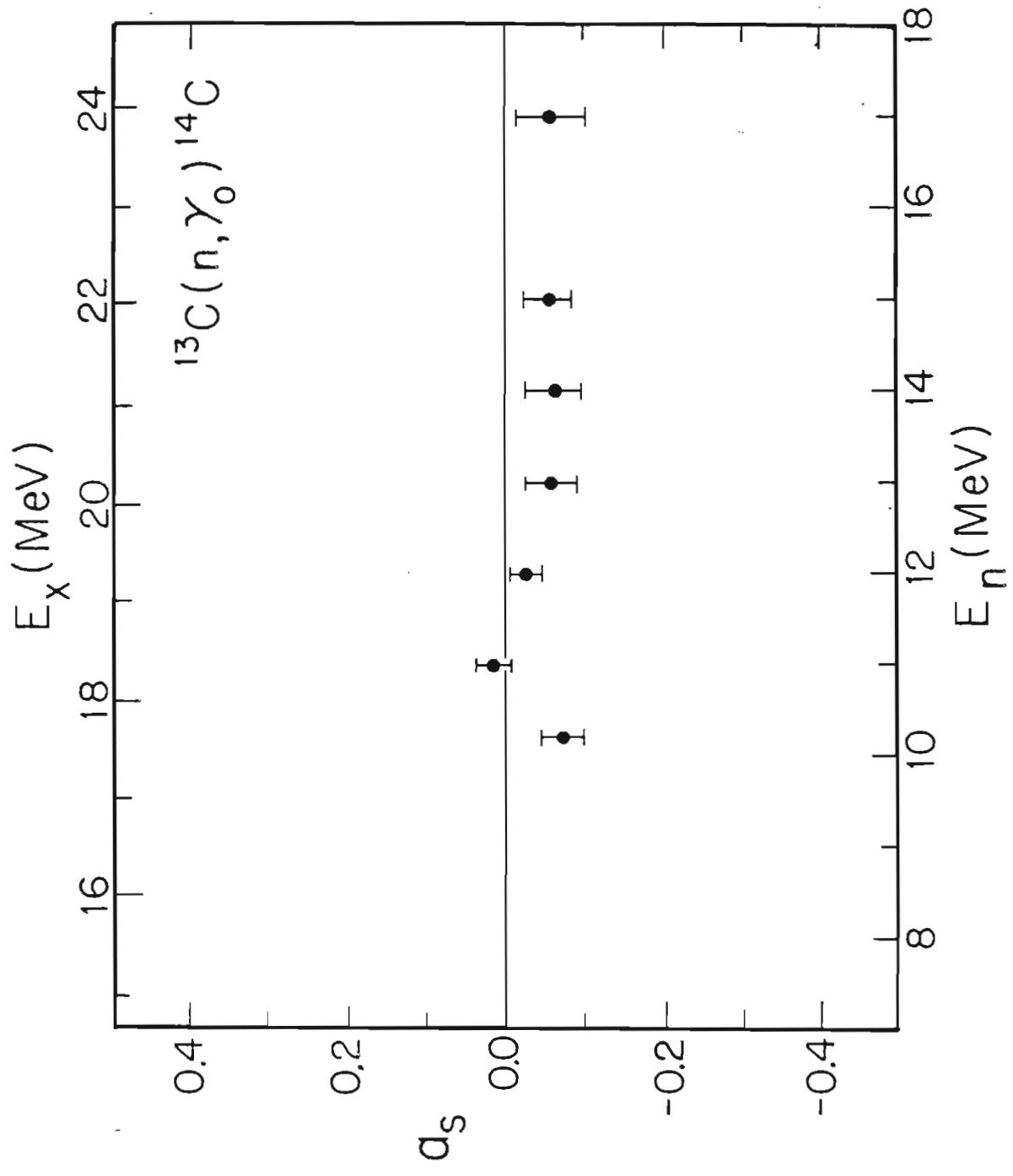
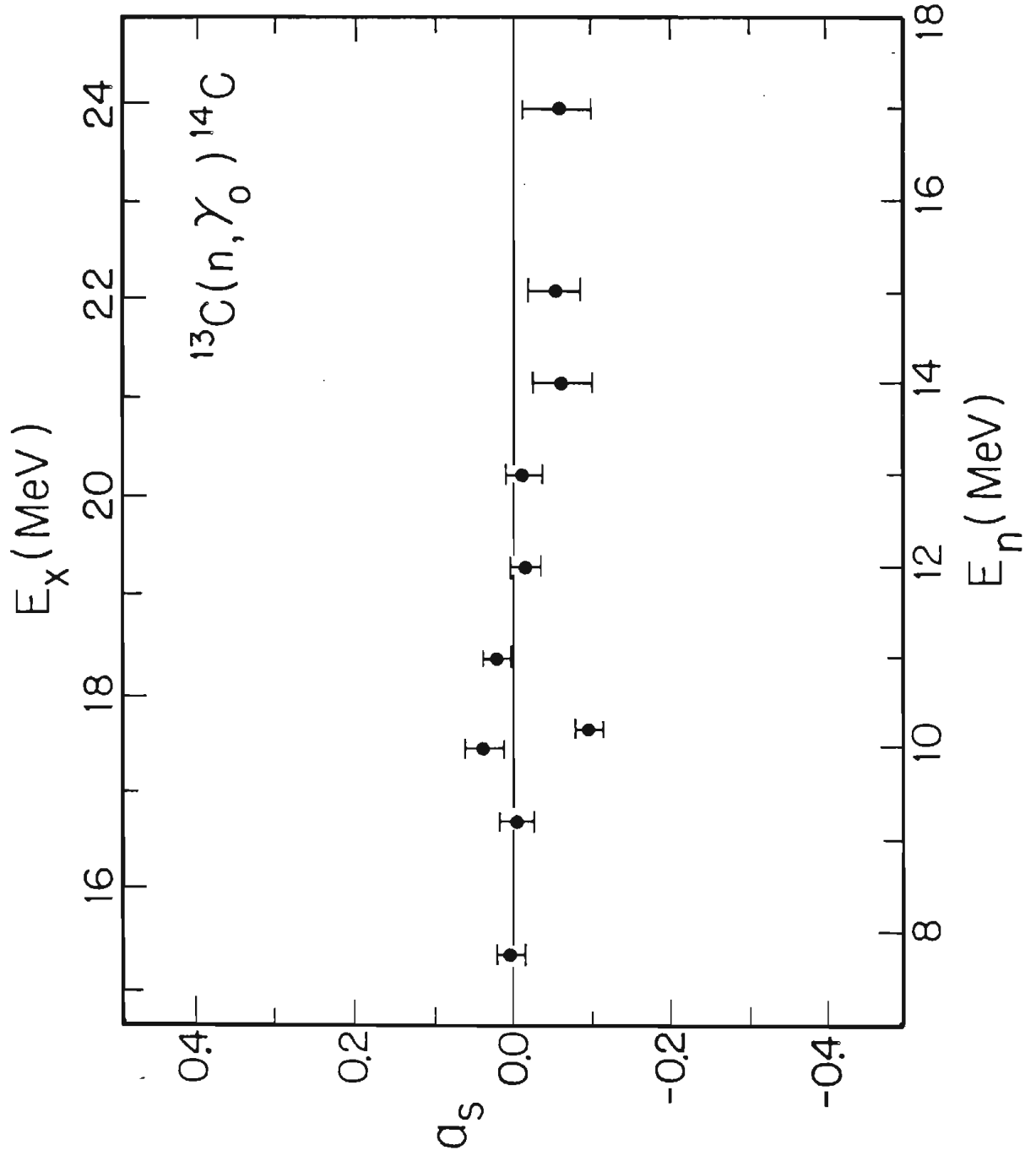


Figure 3-4 The fore-aft asymmetry of the  $^{13}\text{C}(n,\gamma_0)^{14}\text{C}$  reaction determined by combining the direct measurements with the angular distributions.



data can be calculated and compared with the  $90^\circ$  yield curve of Jensen (1981). The spin up and spin down yields from the  $90^\circ$  analyzing power measurements can be combined to form an unpolarized yield by using

$$3-5 \quad N_{\text{un}} = \frac{P_- N_+ + P_+ N_-}{P_+ + P_-}$$

where  $P_+$  is the polarization of the spin-up beam and  $P_-$  is the polarization of the spin-down beam. The unpolarized yield was corrected for the energy dependence of the  ${}^2\text{H}(\vec{d}, \vec{n})$  reaction, efficiency of the detectors, and finite geometry corrections (Jensen, 1981). Jensen's yield curve was taken at a deuterium gas cell pressure of 2 atm while the analyzing power data was taken at 5 or 6 atm. Jensen's data was converted to an equivalent yield curve for the higher gas cell pressure by performing a convolution integral for the difference in neutron energy spreads resulting from the difference in cell pressures.

The fore-aft asymmetry data was measured at  $55^\circ$  and  $125^\circ$  and therefore required conversion to equivalent  $90^\circ$  data. Including only Legendre polynomials of order up to 3, the conversion factor may be calculated by applying

$$3-6 \quad \frac{\sigma(55^\circ) + \sigma(125^\circ)}{2} = A_0 \left[ 1 - 0.0065 a_2 \right] \simeq A_0$$

and

$$\sigma(90^\circ) = A_0 \left[ 1 - 0.5 a_2 \right].$$

A value for  $a_2$  is required to complete the calculation. The conversion factor could be easily be calculated for neutron energies below

$E_n = 14$  Mev since the angular distributions of cross section had been

measured. The two-level doorway state calculations of chapter 7 were used to provide an estimate of  $a_2$  for 14, 15, and 17 MeV. The converted data was then corrected and normalized as described above.

An overall normalization factor between the two cross section data sets was determined by calculating the normalization factor for each overlapping point in the data sets separately and then performing a weighted average of the individual normalization factors. The new data were then combined with Jensen's data by a weighted average to give the final yield curve. Figure 3-5 shows the cross section from the two data sets separately while Figure 3-6 shows the combined cross section. The combined cross section is given in tabular form in Table A-3.

In order to calculate the total photoneutron cross section,  $\sigma_{\gamma, n_0}$ , we must first calculate the total radiative capture cross section,  $\sigma_{n, \gamma_0}$ , and then apply detail balance. The total capture cross section can be written (see §4-2) as

$$3-7 \quad \sigma_{n, \gamma} = 4 \pi A_0 .$$

A value for  $A_0$  is known at each energy where the angular distribution of cross section or the fore-aft asymmetry was measured. For other energies, the  $\sigma(90^\circ)/A_0$  ratio must be estimated. The two-level doorway state calculations (see §7-3) did a good job of fitting the measured  $a_2$  coefficients. The calculation represented by the dashed curve in Figure 7-4 was used to provide the  $\sigma(90^\circ)/A_0$  ratio for the entire energy range of the  $90^\circ$  cross section measurements. The total neutron capture cross section is shown in Figure 3-7 and Table A-4.

Figure 3-5  $90^\circ$  cross section of the  $^{13}\text{C}(n,\gamma_0)^{14}\text{C}$  reaction. The circles are the data of Jensen. The X's are the data of this work.

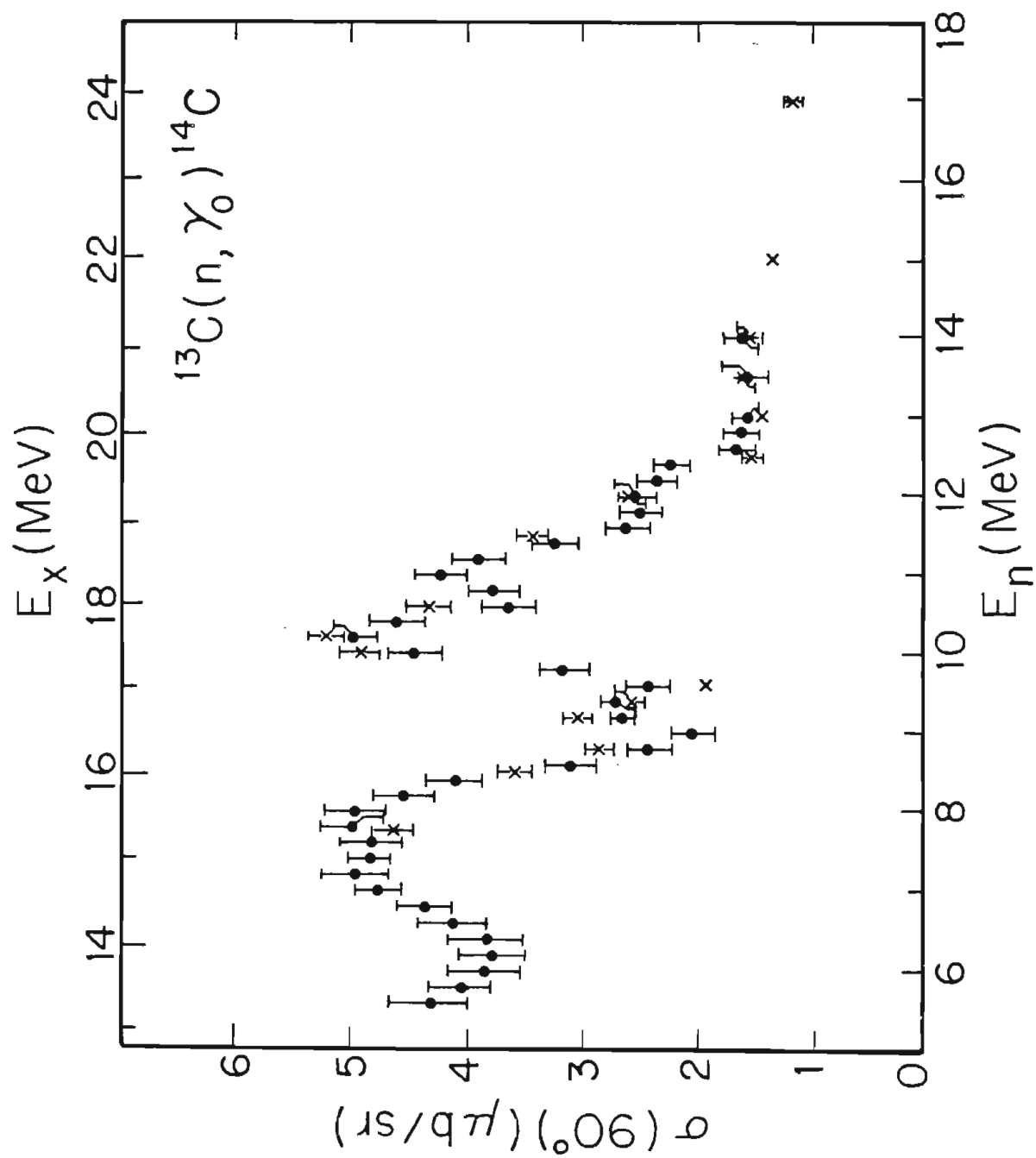




Figure 3-6  $90^\circ$  cross section of the  $^{13}\text{C}(n,\gamma_0)^{14}\text{C}$  reaction. The points represent the weighted average of the two data sets presented in Figure 3-5. The curve is the result of the direct-semidirect model calculations of chapter 7.

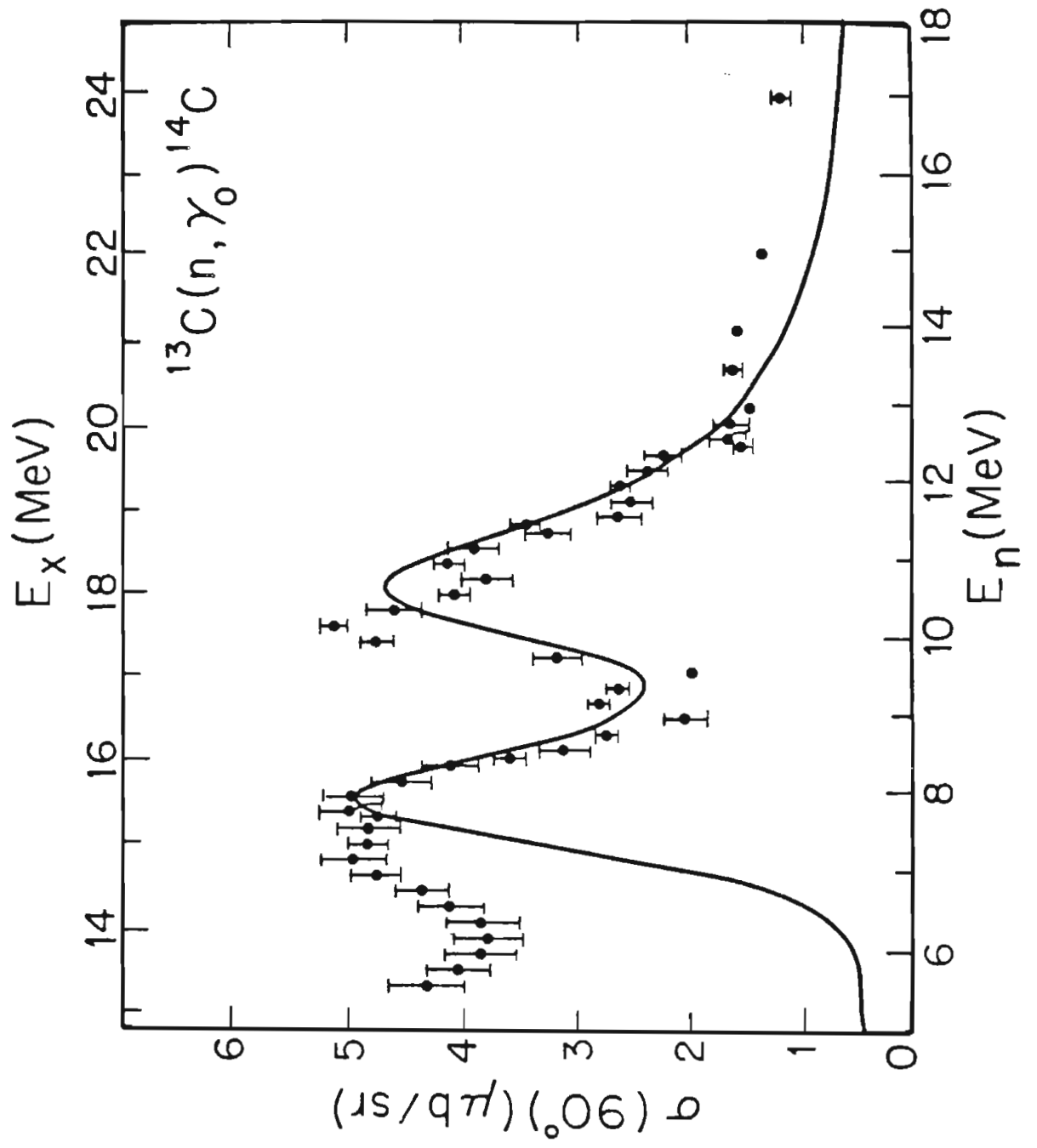
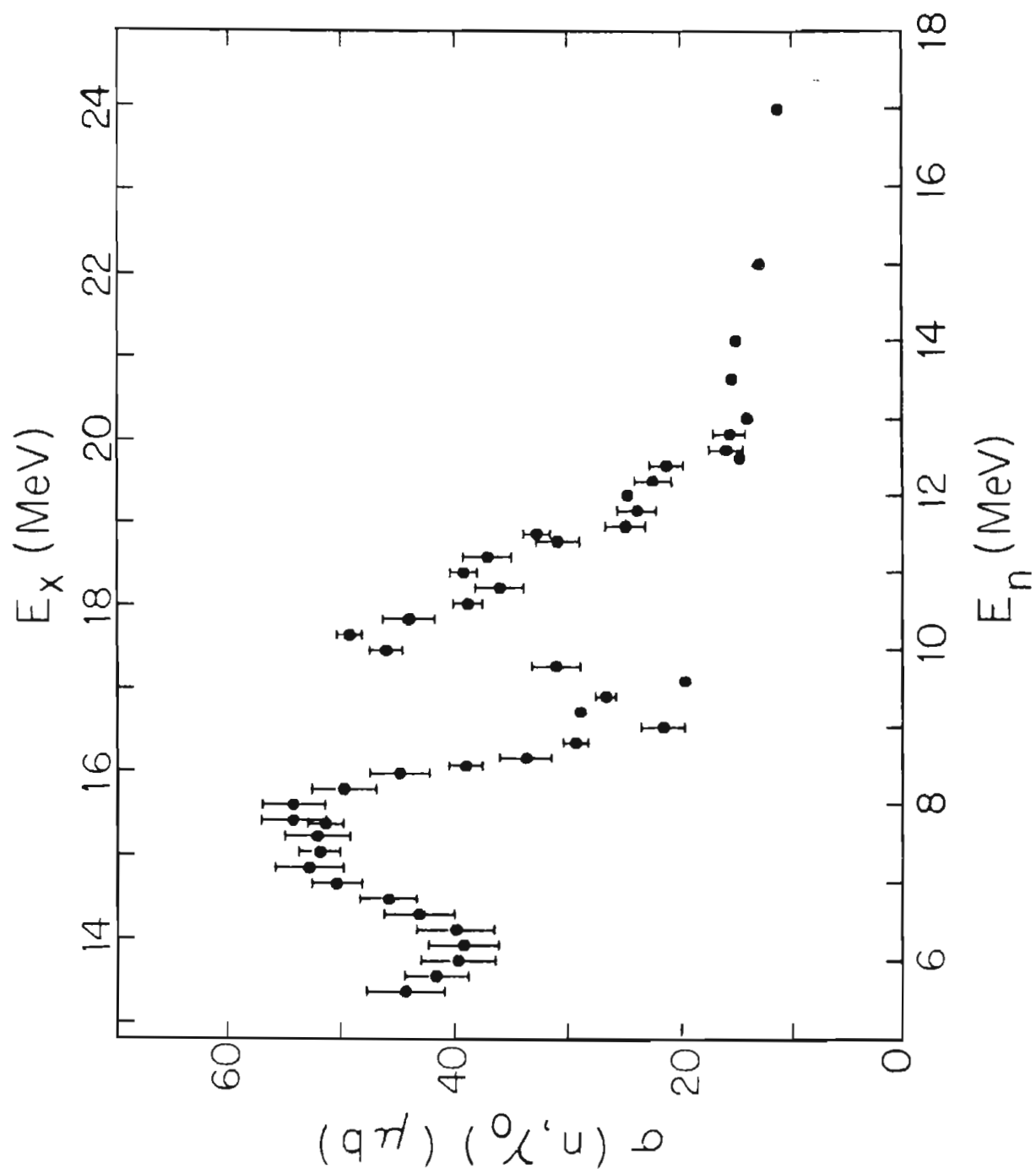


Figure 3-7 Total cross section of the  $^{13}\text{C}(n, \gamma_0)^{14}\text{C}$  reaction.

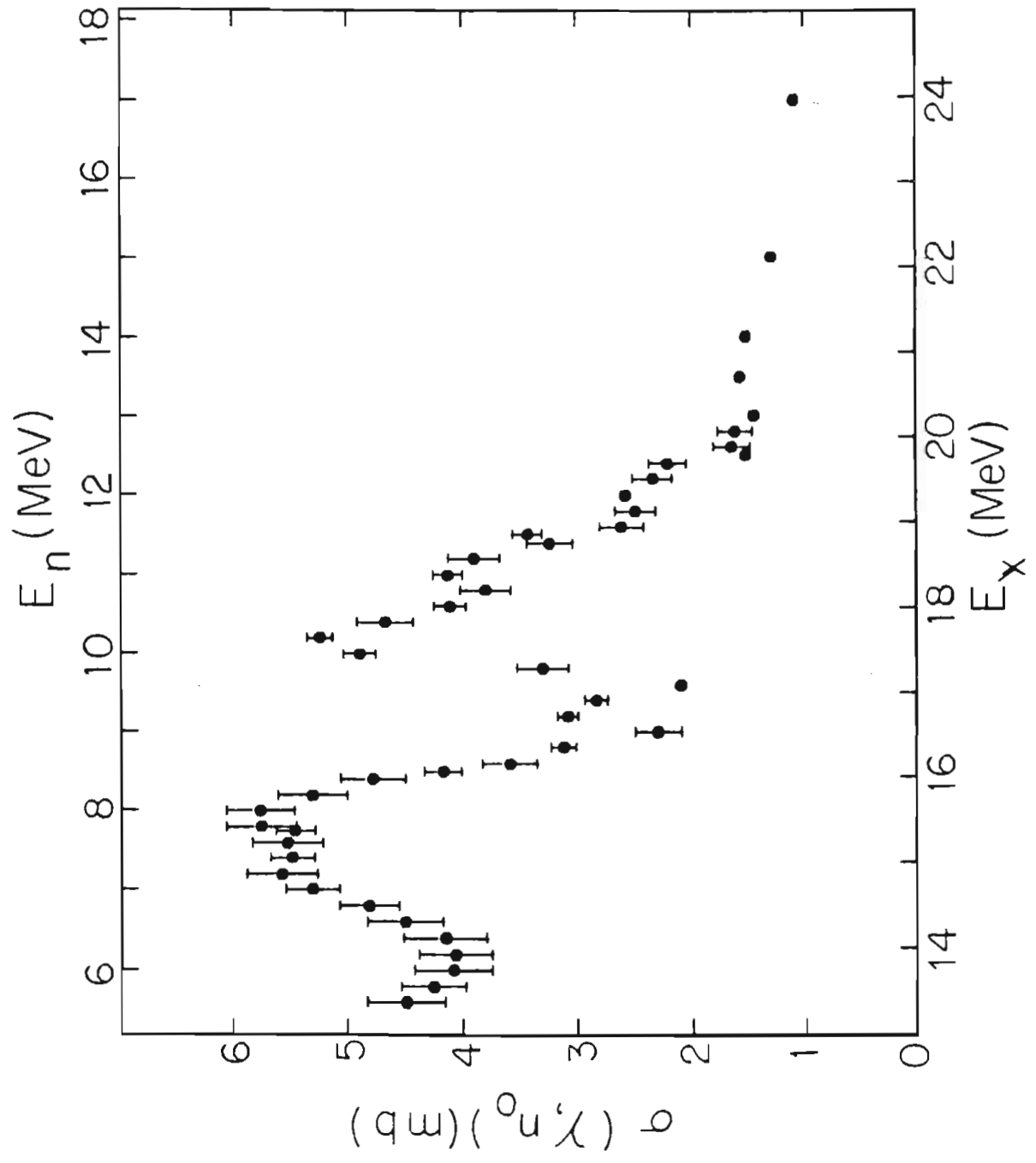


The detail balance relation between radiative capture and photonuclear emission is given by

$$3-8 \quad \sigma_{\gamma, n_0} = 2 \frac{2 J_A + 1}{2 J_{A+1} + 1} \frac{A}{A + 1} \frac{E_x - Q}{E_x^2} M c^2 \sigma_{n, \gamma_0}$$

where  $J_A$  and  $J_{A+1}$  are the spins of the neutron target and resultant nucleus,  $Q$  is the  $Q$ -value of the capture reaction, and  $M c^2$  is the energy equivalent of the rest mass of the neutron. The detail balance cross section is presented in Figure 3-8 and Table A-5.

Figure 3-8 Total cross section of the  $^{14}\text{C}(\gamma, n_0)^{13}\text{C}$  reaction  
obtained through detail balance.



## 4 Angular Distributions

### 4.1 Peak Stripping and Summing

Angular distributions of cross section were measured at neutron energies of 7.75, 12 and 13 MeV. A partial angular distribution of analyzing power was measured at  $E_n = 13$  MeV. Previously unreported angular distributions of cross section at 10 and 11 MeV and analyzing power at  $E_n = 10$  MeV were analyzed. Jensen's angular distributions of cross section and analyzing power at 7.75, 9.2, 10.2, 11, and 12 MeV were reexamined and the data at 11 and 12 MeV were completely reanalyzed.

The spectra were fit in the same manner as described in §3-1. The peaks were fit using MULFIT, the fitted peak widths were averaged for each angular distribution, and the spectra were refitted with the fixed peak widths. The spectra were then summed from 1 width below the peak to 1.1 widths above the peak. Target-out background measurements were performed for the new data sets and were analyzed as described above. Backgrounds for the older data sets were estimated by examining the number of counts per channel appearing in the spectra in the region just above the peak for all of the data sets. For data sets having target-out measurements, the target-out counts per channel in the region under the peak were about 1.5 times the counts per channel above the peak in the target-in spectra. The counts per channel above the peak were multiplied by 1.5 and summed for the proper number of channels to



give background estimates for the old data sets. The net yields were then normalized to beam current integration, accidental coincidence rate, and electronic dead time. The yields were then corrected for multiple scattering and finite geometry effects using the Monte Carlo code SPINFIX (Jensen, 1981). The data are presented in tabular form in Table B-1.

#### 4.2 Angular Distributions of Cross Section

The angular distributions of cross section can be expanded in terms of Legendre polynomials

$$4-1 \quad \sigma(\theta) = \sum_{k=0}^{k_{\max}} A_k P_k(\cos \theta)$$

where the  $A_k$  are the fitting coefficients and the  $P_k$  are the Legendre polynomials. In order to emphasize the shape of the angular distributions, the data were normalized and expanded via weighted least squares in terms of the Legendre polynomial coefficients  $a_k = A_k / A_0$  giving

$$4-2 \quad \frac{\sigma(\theta)}{A_0} = \sum_{k=0}^{k_{\max}} a_k P_k(\cos \theta) .$$

The presence of quadrupole radiation would indicate that terms up to  $k = 4$  should appear in the expansion. However, the data were of sufficient quality to justify only terms up to  $k = 3$ .

More than one measurement of the angular distribution was performed at each energy. Since the individual measurements at some

energy all describe the same physical distribution they should all be described by the same values for  $a_1$ ,  $a_2$ , and  $a_3$  and differ only in the value for  $A_0$ . The separate measurements were fit to  $A_0$  while  $a_1$  through  $a_3$  were fixed according to some initial guess. The data were normalized according to the values of  $A_0$  and the combined data were fitted to give new values for  $a_1$  through  $a_3$ . These values were used to generate new  $A_0$ 's and the procedure was iterated until the values converged. This method of normalization was particularly useful for normalizing data taken at extreme angles with the detector in the "pulled-back" position to data taken at the standard position since the extreme angle data, by itself, did not constitute a sufficiently complete angular distribution to allow expansion into Legendre polynomials. Figure 4-1 shows the angular distributions of cross section along with the Legendre polynomial fits. The coefficients for the fits are presented in Table B-2.

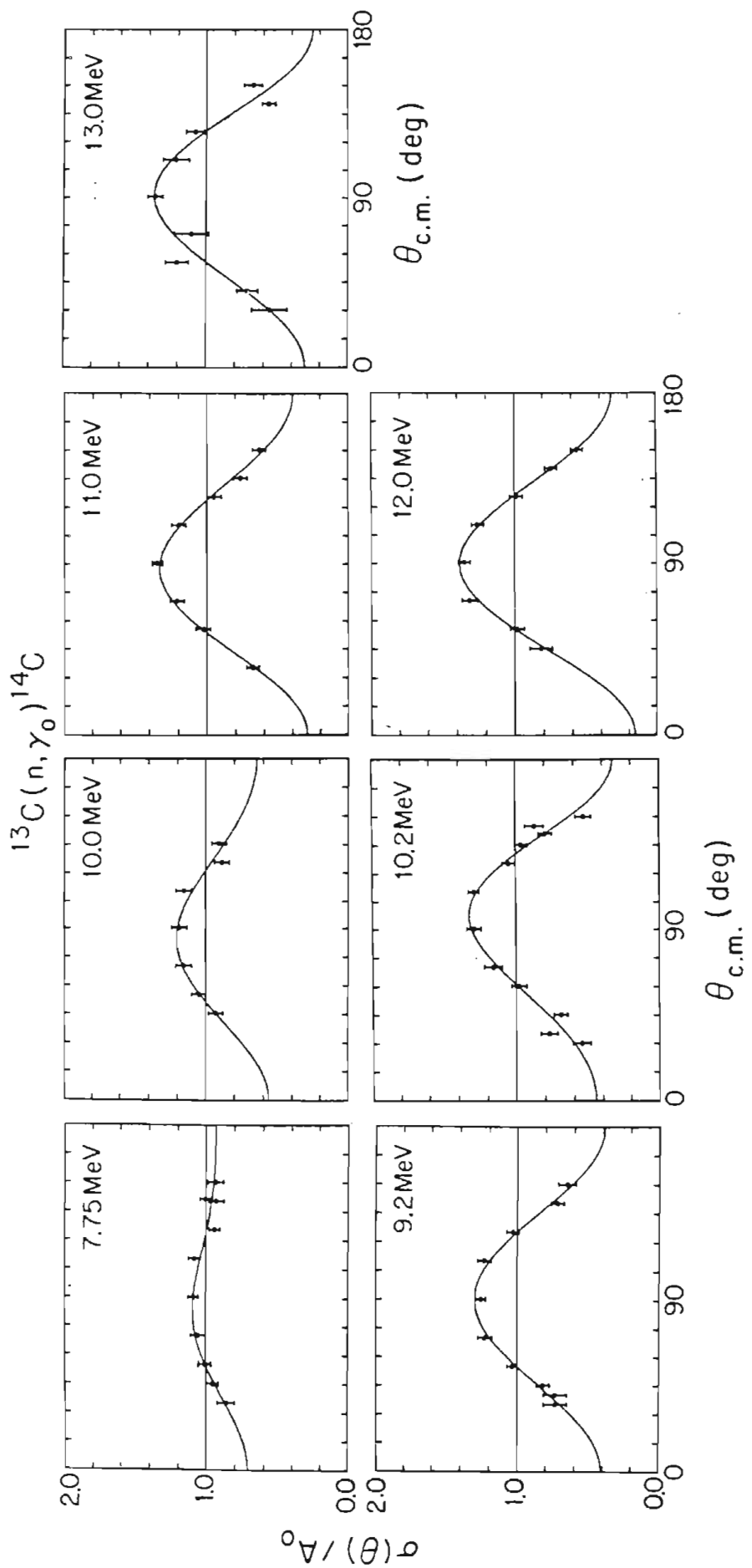
#### 4.3 Angular Distribution of Analyzing Power

The angular distributions of the cross section-analyzing power product were expanded according to

$$4-3 \quad \frac{A_y(\theta) \sigma(\theta)}{A_0} = \sum_{k=1}^{k_{\max}} b_k P_k^1(\cos \theta)$$

where the  $b_k$  are the fitting coefficients and the  $P_k^1$  are the associated Legendre polynomials of the first kind. The expansions were performed up to  $k = 3$ . The measurements of the angular distributions of analyzing power were performed before the second NaI detector was available and so

Figure 4-1 Angular distributions of cross section for the  $^{13}\text{C}(n, \gamma_0)^{14}\text{C}$  reaction at various energies. The curves are Legendre polynomial expansions through  $k = 3$ .



the formula of Equation 3-1 was used to form the analyzing power. The analyzing power was then multiplied by the cross section determined from both the polarized and unpolarized measurements to form the cross section-analyzing power product. The cross sections determined from the data taken with the polarized beam at 10, 11, and 12 MeV were inconsistent with the cross sections determined from the unpolarized data and the fore-aft asymmetry measurements at the same energies and were inconsistent with any reasonable theoretical interpretation. This behavior is partially explained by the fact that the beam produced by the polarized ion source is less intense and has poorer pulsing characteristics than the beam produced by the direct extraction source. The cross section information from the polarized beam at these three energies was not included in the final results.

#### 4.4 Constrained Fits

The angular distributions of cross section give a value for the fore-aft asymmetry according to

$$4-4 \quad a_s = 0.5773 a_1 - 0.3849 a_3 ,$$

which is derived by expanding Equation 3-3 in terms of the Legendre polynomials up to order 3. The error of the asymmetry is given by

$$4-5 \quad \Delta a_s = 0.3333 \sigma_{a_1}^2 + 0.1481 \sigma_{a_3}^2 - 0.2222 \sigma_{a_1 a_3}^2$$

where  $\sigma_{a_1 a_3}^2$  is the correlated error of  $a_1$  and  $a_3$ . The angular distributions of cross section-analyzing power product give a value for

the  $90^\circ$  analyzing power according to

$$4-6 \quad A_y = \frac{\sigma(90^\circ)}{A_0} [ b_1 - 1.5 b_3 ] ,$$

with error

$$4-7 \quad \Delta A_y = \frac{\sigma(90^\circ)}{A_0} [ \sigma_{b_1}^2 + 2.25 \sigma_{b_3}^2 - 3.0 \sigma_{b_1 b_3}^2 ] .$$

The values of  $a_s$  and  $A_y$  calculated from the angular distributions using the above equations are presented in Table B-2. They were combined by a weighted average with the direct measurements of the asymmetry and analyzing power to give the final results presented in Table B-3.

A problem now arises. The Legendre coefficients  $a_k$  are inconsistent, in the sense that Equation 4-4 is no longer obeyed, with the final fore-aft asymmetries reported in Table B-3 due to the additional fore-aft asymmetry data. Likewise, the Legendre coefficients  $b_k$  are inconsistent with the final  $90^\circ$  analyzing power data. In order to have a consistent data set, the values for the Legendre coefficients must be refined to account for the existence of the additional data. The fore-aft asymmetry data cannot simply be merged into the angular distributions of cross section since they do not represent a sufficiently complete angular distribution. Furthermore, the asymmetry measurements were performed using two detectors and the asymmetry was calculated according to Equation 3-4. The  $90^\circ$  analyzing power data could be combined with the angular distributions, but the problem with the two detector formalism still exists.

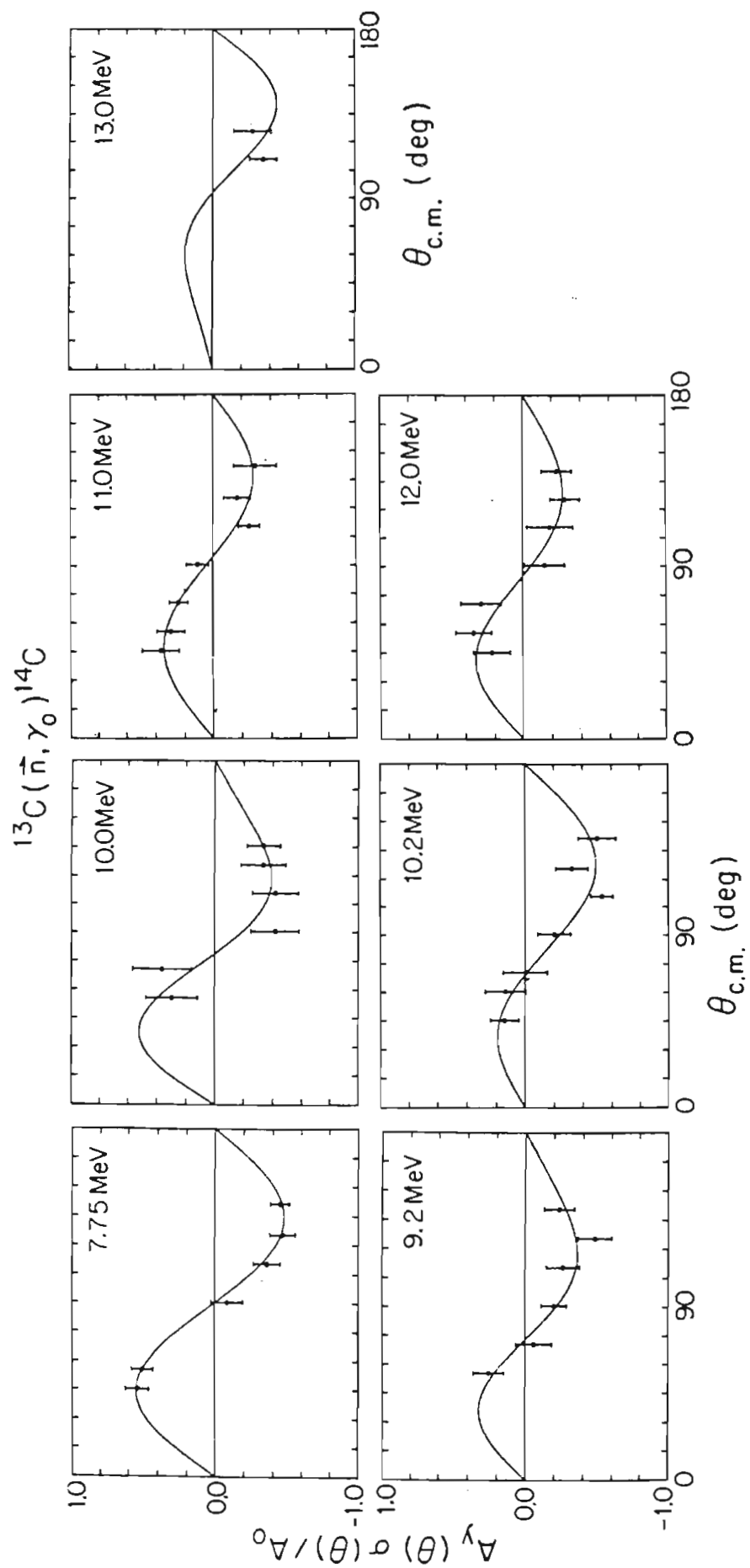
The solution was to fit the angular distributions subject to the additional constraint that the fitted coefficients generate the proper value for the asymmetry or analyzing power. In other words, the angular distributions of cross section were expanded in terms of Legendre polynomials with coefficients  $a_k$ , such that when the  $a_k$  coefficients were inserted into Equation 4-4, the desired value for the fore-aft asymmetry resulted. The constraint was required to be satisfied exactly since the value for the fore-aft asymmetry was determined using all of the available data with proper consideration being given to the various errors involved. The error of the fore-aft asymmetry was allowed to contribute to the errors on the  $a_k$  coefficients. The  $b_k$  coefficients were redetermined in the same manner. The new Legendre coefficients are presented in Table B-3. The change in the values for the Legendre coefficients was small enough that no obvious qualitative difference resulted in the appearance of the fits. The derivation of the constrained fitting procedure is presented in the next chapter and is valid for any linear least squares fitting.

The constrained fitting procedure allowed use to be made of the analyzing power measured at  $E_n = 13$  MeV at  $110^\circ$  and  $125^\circ$ . The measurement of the full angular distribution of analyzing power could not be completed due to a failure of the polarized ion source. Examination of Figure 7-1 shows that the direct-semidirect model calculations of the angular distributions of analyzing power indicate the value of  $b_2$  is constant and  $b_3$  is zero for neutron energies near 13 MeV. The data in the same energy region show similar

characteristics. The two point distribution was fit to  $b_1$  with  $b_2$  fixed at  $0.20 \pm 0.04$  and  $b_3$  fixed at  $0.01 \pm 0.03$ . The value for  $b_1$  then determined an effective value for the  $90^\circ$  analyzing power which could be averaged with the directly measured value. The final results were obtained by fixing  $b_2 = 0.20 \pm 0.04$  and fitting  $b_1$  and  $b_3$  to the  $110^\circ$  and  $125^\circ$  data subject to the  $90^\circ$  analyzing power constraint. The coefficients for the unconstrained and constrained fits are presented in Table B-2 and Table B-3, respectively. Figure 4-2 shows the angular distributions of analyzing power along with the constrained Legendre polynomial fits.



Figure 4-2 Angular distributions of analyzing power-cross section product for the  $^{13}\text{C}(\vec{n}, \gamma_0)^{14}\text{C}$  reaction at various energies. The curves are associated Legendre polynomial expansions through  $k = 3$ .



## 5 Constrained Linear Least Squares

## 5.1 Introduction

Let  $y(x)$  be any function linear in its coefficients  $a_k$ . Then  $y(x)$  can be written as

$$5-1 \quad y(x) = \sum_{k=0}^n a_k P_k(x) ,$$

where  $a_k$  is a number and  $P_k(x)$  is any function. The symbols  $a_k$  and  $P_k(x)$  are customarily used to represent the Legendre coefficients and polynomials but the discussion that follows is valid for any collection of functions and is not restricted to Legendre polynomials. Let us impose a collection of constraint equations of the form

$$5-2 \quad \sum_{k=0}^n \lambda_{kc} a_k = \tilde{\lambda}_c , \quad c=1, n$$

where  $\lambda_{kc}$  and  $\tilde{\lambda}_c$  are numbers, possibly zero, and the expression  $c=1, n$  means that  $c$  takes on all integral values from 1 to  $n$ . We can solve a constraint equation for some  $a_i$  in terms of the other coefficients appearing in the same constraint equation as

$$5-3 \quad a_i = \frac{1}{\lambda_{ic}} \left[ \tilde{\lambda}_c - \sum_{k \neq i} \lambda_{kc} a_k \right] .$$

We can use the above equation to reexpress  $y(x)$  in terms of some subset of the original  $a_k$  coefficients. We can then perform the least squares fitting to determine the values for the subset of the coefficients and substitute into Equation 5-3 to determine the remaining coefficients.

## 5.2 Reexpression of the function to be fit

The selection of which subset of the coefficients to fit and which to calculate from the constraint equations is complicated by the existence of multiple constraint equations, any of which may refer to any of the  $a_k$  coefficients. We can simplify the system of constraint equations by considering them to be a system of  $n+1$  equations in the  $n+1$  unknowns  $a_k$

$$\begin{aligned}
 5-4 \quad & \lambda_{00}a_0 + \lambda_{10}a_1 + \dots + \lambda_{n0}a_n = \tilde{\lambda}_0 \\
 & \lambda_{01}a_0 + \lambda_{11}a_1 + \dots + \lambda_{n1}a_n = \tilde{\lambda}_1 \\
 & \dots\dots\dots \\
 & \lambda_{0n}a_0 + \lambda_{1n}a_1 + \dots + \lambda_{nn}a_n = \tilde{\lambda}_n .
 \end{aligned}$$

We can then use the method of Gaussian elimination with full pivoting (Kreyszig, 1972) to reduce the the system to the form

$$\begin{aligned}
 5-5 \quad & b_0 + u_{10}b_1 + u_{20}b_2 + \dots + u_{n0}b_n = \tilde{u}_0 \\
 & b_1 + u_{21}b_2 + \dots + u_{n1}b_n = \tilde{u}_1 \\
 & \dots\dots\dots \\
 & b_r + \dots + u_{nr}b_n = \tilde{u}_r \\
 & 0 = \tilde{u}_{r+1} \\
 & \dots\dots \\
 & 0 = \tilde{u}_n
 \end{aligned}$$

where the  $a_k$  coefficients must be written as  $b_k$  coefficients since the column pivoting may rearrange the columns of the matrix. For later use,

we will define the set of functions  $G_k(x)$  to represent the same rearrangement of the  $P_k(x)$  functions of Equation 5-1. That is, we now express  $y(x)$  as

$$5-6 \quad y(x) = \sum_{k=0}^n b_k G_k(x)$$

where the set of functions  $G_k(x)$  is the same set of functions as  $P_k(x)$  except that the indices have been rearranged as a result of the Gaussian elimination, and the  $b_k$  coefficients multiply the  $G_k(x)$  functions in the same way that the  $a_k$  coefficients multiply the  $P_k(x)$  functions. We can assume the system of Equation 5-4 has more than one solution or least squares fitting would not be necessary. This implies  $0 \leq r < n$  and  $\tilde{u}_i = 0$ , for  $r < i \leq n$ . We can now solve Equation 5-5 for each  $b_i$ ,  $0 \leq i \leq r$  in terms of only  $b_j$ ,  $r+1 \leq j \leq n$ , and do the least squares fitting to determine the  $b_j$  coefficients. The solution to Equation 5-5 will be of the form

$$5-7 \quad \begin{aligned} b_0 + v_{r+1,0} b_{r+1} + \dots + v_{n0} b_n &= \tilde{v}_0 \\ b_1 + v_{r+1,1} b_{r+1} + \dots + v_{n1} b_n &= \tilde{v}_1 \\ &\dots \dots \dots \\ b_r + v_{r+1,r} b_{r+1} + \dots + v_{nr} b_n &= \tilde{v}_r . \end{aligned}$$

The  $r^{\text{th}}$  equation here is identical to the  $r^{\text{th}}$  equation in Equation 5-5 and is trivially solved giving

$$5-8 \quad b_r = \tilde{u}_r - \sum_{k=r+1}^n u_{kr} b_k = \tilde{v}_r - \sum_{k=r+1}^n v_{kr} b_k ,$$

where

$$5-9 \quad v_{rk} = u_{rk} \quad \text{and} \quad \tilde{v}_r = \tilde{u}_r \quad k=r+1, n .$$

The solution for  $b_i$ ,  $0 \leq i < r$  can be derived by

$$\begin{aligned}
 5-10 \quad b_i &= \tilde{u}_i - \sum_{j=i+1}^r u_{ji} b_j - \sum_{k=r+1}^n u_{ki} b_k, \\
 &= \tilde{u}_i - \sum_{j=i+1}^r u_{ji} \left[ \tilde{v}_j - \sum_{k=r+1}^n v_{kj} b_k \right] - \sum_{k=r+1}^n u_{ki} b_k, \\
 &= \tilde{u}_i - \sum_{j=i+1}^r u_{ji} \tilde{v}_j - \sum_{k=r+1}^n \left[ u_{ki} - \sum_{j=i+1}^r u_{ji} v_{kj} \right] b_k.
 \end{aligned}$$

This, when compared with Equation 5-7, gives the recursion relation between the  $u$ 's and  $v$ 's

$$\begin{aligned}
 5-11 \quad \tilde{v}_i &= \tilde{u}_i - \sum_{j=i+1}^r u_{ji} \tilde{v}_j, & i=0, r-1 \\
 v_{ki} &= u_{ki} - \sum_{j=i+1}^r u_{ji} v_{kj}. & i=0, r-1 \\
 & & k=r+1, n
 \end{aligned}$$

Equation 5-9 and Equation 5-11 together allow all of the  $\tilde{v}_i$ 's and  $v_{ki}$ 's to be calculated.

We can now write  $y(x)$  as a function of only a subset of the original set of  $a_k$  coefficients (now represented as  $b_k$ )

$$\begin{aligned}
 5-12 \quad y(x) &= \sum_{k=r+1}^n b_k G_k(x) + \sum_{k=0}^r b_k G_k(x), \\
 &= \sum_{k=r+1}^n b_k G_k(x) + \sum_{k=0}^r \left\langle \begin{array}{c} \tilde{v}_k \\ \left[ \tilde{v}_k - \sum_{j=r+1}^n v_{jk} b_j \right] \end{array} \right\rangle G_k(x),
 \end{aligned}$$

$$= \sum_{k=r+1}^n b_k G_k(x) + \sum_{k=0}^r \tilde{v}_k G_k(x) - \sum_{j=r+1}^n b_j \left[ \sum_{k=0}^r v_{jk} G_k(x) \right].$$

The above expression can be simplified by defining

$$5-13 \quad F_k(x) \equiv G_k(x) - \sum_{f=0}^r v_{kf} G_f(x).$$

Finally we can write

$$5-14 \quad y(x) = \sum_{k=r+1}^n b_k F_k(x) + \sum_{k=0}^r \tilde{v}_k G_k(x).$$

### 5.3 Determination of fitting coefficients

We will now follow the method of Bevington (1969) to determine the fitting coefficients. The data set to be fitted consists of a set of  $N$  measurements  $y_i$  with error  $\sigma_i$  at the points  $x_i$ . We define the function  $\chi^2$  as a measure of the goodness of fit by

$$5-15 \quad \chi^2 \equiv \sum_{i=1}^N \frac{1}{\sigma_i} \left[ y_i - y(x_i) \right]^2.$$

We can now minimize  $\chi^2$  by taking its derivative with respect to each of the fitting coefficients  $b_k$  and setting each derivative to zero.

$$5-16 \quad \frac{\partial \chi^2}{\partial b_k} = \frac{\partial}{\partial b_k} \sum_{i=1}^N \frac{1}{\sigma_i} \left[ y_i - \sum_{f=r+1}^n b_f F_f(x_i) - \sum_{f=0}^r \tilde{v}_f G_f(x_i) \right]^2 = 0. \quad k=r+1, n$$

The derivative can be evaluated and the expression rearranged to give

$$5-17 \quad \sum_{i=1}^N \frac{F_k(x_i)}{\sigma_i} \left[ y_i - \sum_{f=0}^r \tilde{v}_f G_f(x_i) \right] = \sum_{f=r+1}^n b_f \sum_{i=1}^N \frac{F_k(x_i) F_f(x_i)}{\sigma_i}. \quad k=r+1, n$$

The above equation can be reexpressed as a matrix equation by defining

$$5-18 \quad \beta_k \equiv \sum_{i=1}^N \frac{F_k(x_i)}{\sigma_i^2} \left[ y_i - \sum_{l=0}^r \tilde{v}_l G_l(x_i) \right], \quad k=r+1, n$$

$$a_{lk} \equiv \sum_{i=1}^N \frac{F_k(x_i) F_l(x_i)}{\sigma_i^2}. \quad k=r+1, n$$

Equation 5-17 becomes

$$5-19 \quad \beta_k = \sum_{l=r+1}^n a_{lk} b_l \quad \text{or} \quad \vec{\beta} = \overset{\leftrightarrow}{\alpha} \vec{b}.$$

We can invert the curvature matrix  $\overset{\leftrightarrow}{\alpha}$  to produce an inverse matrix  $\overset{\leftrightarrow}{\varepsilon}$ , customarily referred to as the error matrix. Note that the indices for these matrices run from  $r+1$  to  $n$ . Then

$$5-20 \quad \vec{b} = \vec{\beta} \overset{\leftrightarrow}{\varepsilon}.$$

The expressions for the  $b_k$  coefficients become

$$5-21 \quad b_k = \sum_{l=r+1}^n \varepsilon_{kl} \left[ \sum_{i=1}^N \frac{F_l(x_i)}{\sigma_i^2} \left[ y_i - \sum_{j=0}^r \tilde{v}_j G_j(x_i) \right] \right], \quad k=r+1, n$$

$$b_k = \tilde{v}_k - \sum_{l=r+1}^n v_{lk} b_l. \quad k=0, r$$

The  $b_k$  coefficients can then be rearranged to produce the  $a_k$  coefficients originally desired.

#### 5.4 Error on fitted coefficients

We need to calculate the error on the  $b_k$  coefficients due to the error on the data points. We can also allow a somewhat restrictive error condition on the constraint equations. Namely let



$$5-22 \quad \sum_{k=0}^n \lambda_{kc} a_k = \tilde{\lambda}_c \pm \Delta \tilde{\lambda}_c \quad c = 1, n$$

be the constraint equations and assume that the errors on the  $\tilde{\lambda}_c$ 's are uncorrelated. Note that the  $\lambda_{kc}$ 's have no error associated with them. After the Gaussian elimination of §5-2, the system of constraint equations is reduced to Equation 5-7 so that  $\Delta \tilde{\lambda}_c \rightarrow \Delta \tilde{v}_c$ .

The error, or variance, on a  $b_k$  coefficient is the root sum square of the errors on the quantities used to determine the coefficient times the effect that quantity has on the value of the coefficient. That is, for the  $b_k$  coefficients determined from the  $\chi^2$ -fit,

$$5-23 \quad \sigma_{b_k}^2 = \sum_{d=1}^N \sigma_d^2 \left[ \frac{\partial b_k}{\partial y_d} \right]^2 + \sum_{m=0}^r \Delta \tilde{v}_m^2 \left[ \frac{\partial b_k}{\partial \tilde{v}_m} \right]^2 \quad k=r+1, n$$

Taking the partial derivatives,

$$5-24 \quad \frac{\partial b_k}{\partial y_d} = \sum_{l=r+1}^n \varepsilon_{kl} \frac{F_l(x_d)}{\sigma_d^2} \quad k=r+1, n$$

$$\frac{\partial b_k}{\partial \tilde{v}_m} = \sum_{l=r+1}^n \varepsilon_{kl} \left\langle \left[ \sum_{d=1}^N \frac{F_l(x_d)}{\sigma_d^2} (-G_m(x_d)) \right] \right\rangle \equiv \sum_{l=r+1}^n \varepsilon_{kl} \mu_{lm} \quad k=r+1, n$$

where we have defined  $\mu_{lm}$  as the term in the braces in order to simplify the expressions that follow. Instead of evaluating the variance,  $\sigma_{b_k}^2$ , we will want evaluate the covariance,  $\sigma_{b_k b_l}^2$ , so that we will determine the correlated errors of the coefficients.

$$5-25 \quad \sigma_{b_k b_l}^2 = \sum_{d=1}^N \sigma_d^2 \frac{\partial b_k}{\partial y_d} \frac{\partial b_l}{\partial y_d} + \sum_{m=0}^r \Delta \tilde{v}_m^2 \frac{\partial b_k}{\partial \tilde{v}_m} \frac{\partial b_l}{\partial \tilde{v}_m} \quad k, l=r+1, n$$

$$\begin{aligned}
&= \sum_{d=1}^N \sigma_d^2 \left\langle \left[ \sum_{i=r+1}^n \varepsilon_{ki} \frac{F_i(x_d)}{\sigma_d} \right] \left[ \sum_{j=r+1}^n \varepsilon_{lj} \frac{F_j(x_d)}{\sigma_d} \right] \right\rangle \\
&\quad + \sum_{m=0}^r \Delta \tilde{v}_m^2 \left\langle \left[ \sum_{i=r+1}^n \varepsilon_{ki} \mu_{im} \right] \left[ \sum_{j=r+1}^n \varepsilon_{lj} \mu_{jm} \right] \right\rangle, \\
&= \sum_{i=r+1}^n \sum_{j=r+1}^n \varepsilon_{ki} \varepsilon_{lj} \left\langle \left[ \sum_{d=1}^N \frac{F_i(x_d) F_j(x_d)}{\sigma_d} \right] \right\rangle \\
&\quad + \sum_{i=r+1}^n \sum_{j=r+1}^n \varepsilon_{ki} \varepsilon_{lj} \left\langle \left[ \sum_{m=0}^r \Delta \tilde{v}_m^2 \mu_{im} \mu_{jm} \right] \right\rangle, \\
&= \sum_{i=r+1}^n \sum_{j=r+1}^n \varepsilon_{ki} \varepsilon_{lj} \alpha_{ij} \\
&\quad + \sum_{i=r+1}^n \sum_{j=r+1}^n \varepsilon_{ki} \varepsilon_{lj} \left\langle \left[ \sum_{m=0}^r \Delta \tilde{v}_m^2 \mu_{im} \mu_{jm} \right] \right\rangle,
\end{aligned}$$

$$5-26 \quad \sigma_{b_k b_l}^2 = \varepsilon_{kl} + \sum_{i=r+1}^n \sum_{j=r+1}^n \varepsilon_{ki} \varepsilon_{lj} \left\langle \left[ \sum_{m=0}^r \Delta \tilde{v}_m^2 \mu_{im} \mu_{jm} \right] \right\rangle. \quad k, l = r+1, n$$

We thus have the usual result for unconstrained fits,  $\varepsilon_{kl}$ , plus a term due to the error on the  $\tilde{v}_m$ . We will define the quantity on the right hand side of the above equation to be the total error matrix,  $\tilde{\varepsilon}_{kl}$ , that is

$$5-27 \quad \tilde{\varepsilon}_{kl} \equiv \varepsilon_{kl} + \sum_{i=r+1}^n \sum_{j=r+1}^n \varepsilon_{ki} \varepsilon_{lj} \left\langle \left[ \sum_{m=0}^r \Delta \tilde{v}_m^2 \mu_{im} \mu_{jm} \right] \right\rangle. \quad k, l = r+1, n$$

## 5.5 Error on all coefficients

The error on any function  $H(a_0, a_1, \dots, a_n)$  of the fitting coefficients, for example, the fore-aft asymmetry in Equation 4-4, is given by

$$5-28 \quad \sigma_H^2 = \sum_{i=0}^n \sum_{j=0}^n \sigma_{a_i a_j}^2 \frac{\partial H}{\partial a_i} \frac{\partial H}{\partial a_j} .$$

What we have calculated so far (Equation 5-26) is only the covariance between some of the coefficients, namely  $b_{r+1}, \dots, b_n$ . In order to find the error on  $H$  we must first reexpress  $H$  as a function  $H'(b_{r+1}, \dots, b_n)$  and apply the formula

$$5-29 \quad \sigma_{H'}^2 = \sum_{i=r+1}^n \sum_{j=r+1}^n \sigma_{b_i b_j}^2 \frac{\partial H'}{\partial b_i} \frac{\partial H'}{\partial b_j} .$$

It clearly will be more convenient to evaluate the covariance between all of the coefficients; both those that were fitted and those that were determined from the constraint equations. The covariances can then be relabeled to give  $\sigma_{a_i a_j}^2$  and Equation 5-28 can be used directly. Recall from Equation 5-21 we have

$$5-30 \quad b_k = \tilde{v}_k - \sum_{i=r+1}^n v_{ik} b_i . \quad k=0, r$$

Taking derivatives,

$$5-31 \quad \frac{\partial b_k}{\partial y_d} = - \sum_{i=r+1}^n v_{ik} \frac{\partial b_i}{\partial y_d} , \quad k=0, r$$

$$\frac{\partial b_k}{\partial \tilde{v}_m} = \delta_{mk} - \sum_{i=r+1}^n v_{ik} \frac{\partial b_i}{\partial \tilde{v}_m} \quad k=0, r$$

where  $\delta_{mk}$  is zero if  $m \neq k$  and is 1 if  $m=k$ . Then for  $k, l \leq r$  we can write

$$5-32 \quad \sigma_{b_k b_l}^2 = \sum_{d=1}^N \sigma_d^2 \frac{\partial b_k}{\partial y_d} \frac{\partial b_l}{\partial y_d} + \sum_{m=0}^r \Delta \tilde{v}_m^2 \frac{\partial b_k}{\partial \tilde{v}_m} \frac{\partial b_l}{\partial \tilde{v}_m}, \quad k, l=0, r$$

$$= \sum_{i=r+1}^n \sum_{j=r+1}^n v_{ik} v_{jl} \left[ \sum_{d=1}^N \sigma_d^2 \frac{\partial b_i}{\partial y_d} \frac{\partial b_i}{\partial y_d} \right]$$

$$+ \sum_{m=0}^r \Delta \tilde{v}_m^2 \delta_{mk} \delta_{ml}$$

$$- \sum_{m=0}^r \Delta \tilde{v}_m^2 \delta_{mk} \left[ \sum_{j=r+1}^n v_{jl} \frac{\partial b_j}{\partial \tilde{v}_m} \right]$$

$$- \sum_{m=0}^r \Delta \tilde{v}_m^2 \delta_{ml} \left[ \sum_{i=r+1}^n v_{ik} \frac{\partial b_i}{\partial \tilde{v}_m} \right]$$

$$+ \sum_{i=r+1}^n \sum_{j=r+1}^n v_{ik} v_{jl} \left[ \sum_{m=0}^r \Delta \tilde{v}_m^2 \frac{\partial b_i}{\partial \tilde{v}_m} \frac{\partial b_j}{\partial \tilde{v}_m} \right],$$

$$5-33 \quad \sigma_{b_k b_l}^2 = \sum_{i=r+1}^n \sum_{j=r+1}^n v_{ik} v_{jl} \tilde{\varepsilon}_{ij} + \Delta \tilde{v}_k^2 \delta_{kl}$$

$$- \Delta \tilde{v}_k^2 \sum_{j=r+1}^n \sum_{i=r+1}^n v_{jl} \varepsilon_{ji} \mu_{ik} - \Delta \tilde{v}_l^2 \sum_{i=r+1}^n \sum_{j=r+1}^n v_{ik} \varepsilon_{ij} \mu_{jl}.$$

$k, l=0, r$

We now calculate  $\sigma_{b_k b_l}^2$  for  $k=0, r$  and  $l=r+1, n$ , and by symmetry, for  $k=r+1, n$  and  $l=0, r$ .

$$\begin{aligned}
5-34 \quad \sigma_{b_k b_l}^2 &= \sum_{d=1}^N \sigma_d^2 \frac{\partial b_l}{\partial y_d} \left\langle - \sum_{i=r+1}^n v_{ik} \frac{\partial b_i}{\partial y_d} \right\rangle \\
&+ \sum_{m=0}^r \Delta \tilde{v}_m \frac{\partial b_l}{\partial \tilde{v}_m} \left\langle \delta_{mk} - \sum_{i=r+1}^n v_{ik} \frac{\partial b_i}{\partial y_d} \right\rangle \quad \begin{array}{l} k=0, r \\ l=r+1, n \end{array} \\
&= - \sum_{i=r+1}^n v_{ik} \left\langle \sum_{d=1}^N \sigma_d^2 \frac{\partial b_l}{\partial y_d} \frac{\partial b_i}{\partial y_d} \right\rangle + \sum_{m=0}^r \Delta \tilde{v}_m^2 \delta_{mk} \frac{\partial b_l}{\partial \tilde{v}_m} \\
&- \sum_{i=r+1}^n v_{ik} \left\langle \sum_{m=0}^r \Delta \tilde{v}_m^2 \frac{\partial b_l}{\partial \tilde{v}_m} \frac{\partial b_i}{\partial y_d} \right\rangle,
\end{aligned}$$

$$5-35 \quad \sigma_{b_k b_l}^2 = - \sum_{i=r+1}^n v_{ik} \tilde{\varepsilon}_{il} + \Delta \tilde{v}_k^2 \sum_{j=r+1}^n \varepsilon_{l j \mu j k} \cdot \quad \begin{array}{l} k=0, r \\ l=r+1, n \end{array}$$

## 6 Transition Matrix Analysis

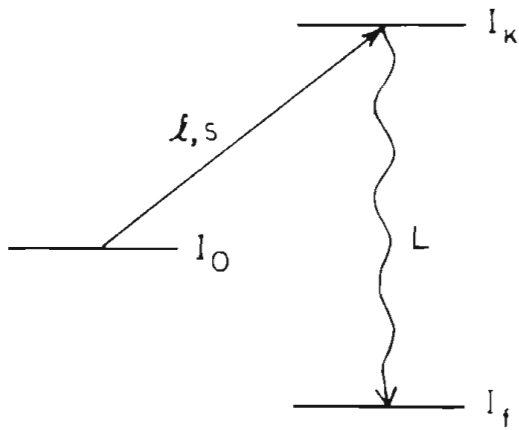
### 6.1 Introduction

Non-zero odd terms in the Legendre polynomial expansions of the angular distributions of cross section and analyzing power indicate the presence of non-E1 radiation. The Legendre coefficients do not, however, indicate the magnitude of the non-E1 radiation. We can reexpress the Legendre coefficients in terms of the transition matrix elements described by Seyler and Weller (1979). The transition matrix elements will be written in the j-j coupling scheme (Hayward, 1970). The incident particle with spin  $\vec{s}$  and orbital angular momentum  $\vec{l}$  is captured by a nucleus with spin  $\vec{I}_0$ . The angular momenta  $\vec{l}$  and  $\vec{s}$  couple to form  $\vec{j}$  and then  $\vec{j}$  and  $\vec{I}_0$  couple to form the spin of the excited state,  $\vec{I}_k$ . The excited state decays to the final state, with spin  $\vec{I}_f$ , by the emission of a  $\gamma$  ray of multipolarity L. The angular momenta must obey the triangle selection rule

$$6-1 \quad | I_k - I_f | \leq L \leq I_k + I_f .$$

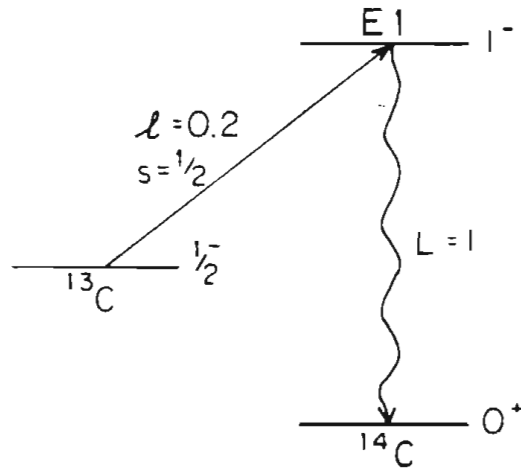
A schematic diagram of the allowed E1, E2, and M1 transition matrix elements for the  $^{13}\text{C}(\vec{n}, \gamma_0)^{14}\text{C}$  reaction is shown in Figure 6-1. The transition matrix elements associated with a given multipolarity  $\gamma$  ray can be denoted by the the incident neutron's orbital and total angular momenta. Each matrix element is complex and can be written as a real amplitude and phase. Equations 6-2, 6-3, and 6-4 in the following sections give the relationships between the Legendre coefficients and

Figure 6-1 Schematic representation of radiative capture in the j-j coupling scheme and the E1, E2, and M1 transition j-j coupling schemes for the  $^{13}\text{C}(n,\gamma_0)^{14}\text{C}$  reaction.



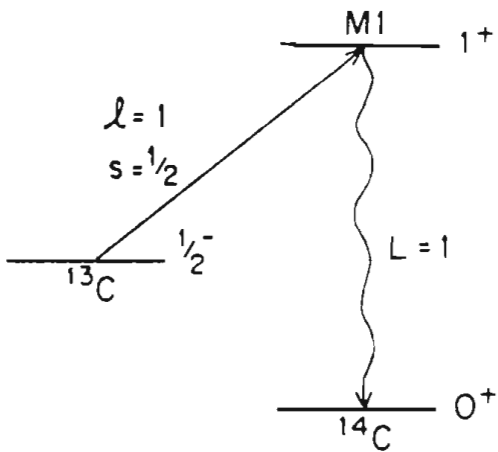
$$\vec{l} + \vec{s} = \vec{j}$$

$$\vec{j} + \vec{I}_0 = \vec{I}_k$$



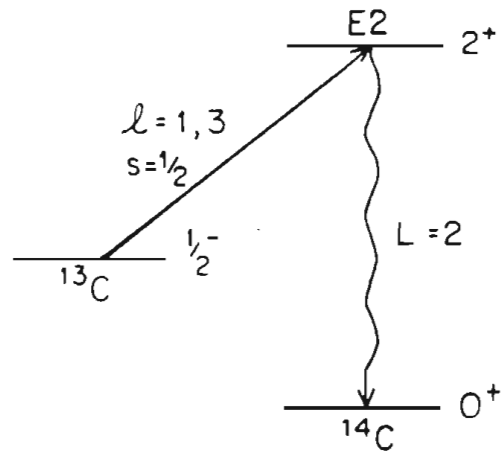
$$l = 0, j = 1/2: s_{1/2}$$

$$l = 2, j = 3/2: d_{3/2}$$



$$l = 1, j = 1/2: p_{1/2}$$

$$l = 1, j = 3/2: p_{3/2}$$



$$l = 1, j = 3/2: p_{3/2}$$

$$l = 3, j = 5/2: f_{5/2}$$



the transition matrix elements.

Two methods can be used to determine the transition matrix elements. The data can first be fit with Legendre polynomials, yielding the Legendre coefficients, and then the matrix elements can be calculated from the coefficients using the systems of equations given below. Problems can arise when the Legendre coefficients describe an unphysical distribution, for example, one where the cross section is negative at extreme angles. In addition, to fully describe the error in the original angular distribution it would be necessary to use the entire error matrix produced by the Legendre polynomial fitting procedure and not just the error on each of the coefficients separately. These problems can be avoided by fitting the transition matrix elements directly to the data using non-linear least squares. An initial guess for the values of the matrix elements is made, then Legendre coefficients are calculated from the matrix elements and used to generate an angular distribution which is compared to the observed distribution. The matrix elements are varied to produce the best fit, using chi-squared criteria, between the observed and calculated distributions. The errors in the transition matrix elements obtained with this procedure are directly related to the errors in the data.

As was discussed in chapter 4, the Legendre coefficients determined from the fits to the angular distributions were constrained to be consistent with the independent measurements of fore-aft asymmetry and  $90^\circ$  analyzing power. Unfortunately, there is no easy way to include these constraints when fitting the matrix elements directly to the data.

Therefore for the non-E1 analysis reported in the following sections, the values for the amplitudes and phases were taken from the fits to the coefficients while the errors on the amplitudes and phases were taken from the fits to the data. In all cases, except 13 MeV, the difference in the values for the matrix elements generated by the two methods was less than 1/2 of the corresponding error bar. It was essential to fit the matrix elements for the 13 MeV data to the constrained coefficients because the angular distribution of analyzing power at that energy contained only two data points.

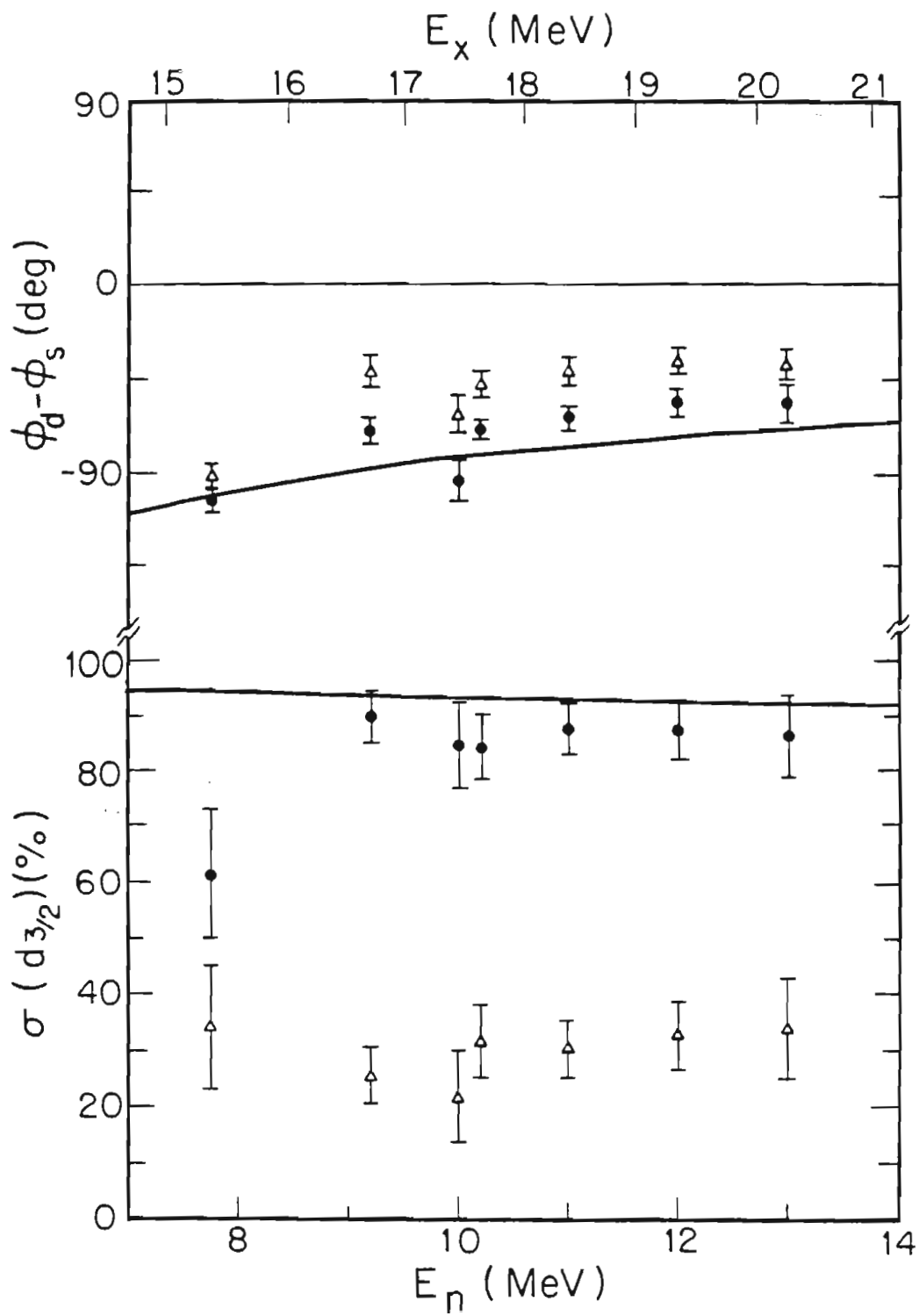
## 6.2 E1 Analysis

For E1 radiation resulting from the  $^{13}\text{C}(n,\gamma_0)^{14}\text{C}$  reaction, there are two complex valued transition matrix elements,  $s_{1/2} \exp[i\varphi_{s_{1/2}}]$  and  $d_{3/2} \exp[i\varphi_{d_{3/2}}]$ . The two amplitudes and their relative phase,  $\varphi_{d_{3/2}} - \varphi_{s_{1/2}}$ , can be determined from the angular distribution of cross section and analyzing power by

$$\begin{aligned}
 6-2 \quad a_0 &= s_{1/2}^2 + 2 d_{3/2}^2 \\
 a_2 &= -2 s_{1/2} d_{3/2} \cos[\varphi_{d_{3/2}} - \varphi_{s_{1/2}}] - d_{3/2}^2 \\
 b_2 &= -s_{1/2} d_{3/2} \sin[\varphi_{d_{3/2}} - \varphi_{s_{1/2}}].
 \end{aligned}$$

The quadratic nature of the above equations results in two solutions. One solution has a dominant  $s_{1/2}$  matrix element and the other has a dominant  $d_{3/2}$  matrix element. The two solutions are presented in Table C-1 and Figure 6-2. The curves in Figure 6-2 are the result of

Figure 6-2 E1 solutions for the  $^{13}\text{C}(\vec{n}, \gamma_0)^{14}\text{C}$  reaction. The quadratic nature of the E1 equations resulted in two solutions for each energy. The  $d_{3/2}$  cross section and relative phase are plotted for the two solutions. The solid lines are the result of a direct-semidirect model calculation and indicate the physical solution.



the direct-semidirect model calculation presented in the next chapter. The calculation clearly indicates that the dominant  $d_{3/2}$  solution is the physical one. The remainder of the transition matrix analysis will be performed using only the dominant  $d_{3/2}$  solution.

### 6.3 E1-E2 Analysis

The maximum order of the Legendre expansion needed to describe radiation of multipolarity  $L_{\max}$  is  $2 * L_{\max}$ . Quadrupole radiation can therefore give rise to non-zero values for Legendre coefficients up to  $a_4$  and  $b_4$ . For this reaction, E2 radiation is due to two transition matrix elements,  $p_{3/2} \exp[ i \varphi_{p_{3/2}} ]$  and  $f_{5/2} \exp[ i \varphi_{f_{5/2}} ]$ . The resulting angular distribution equations are given by

$$\begin{aligned}
 6-3 \quad a_0 &= s_{1/2}^2 + 2 d_{3/2}^2 + 2 p_{3/2}^2 + 3 f_{5/2}^2 \\
 a_1 &= 3.464 s_{1/2} p_{3/2} \cos[ \varphi_{p_{3/2}} - \varphi_{s_{1/2}} ] \\
 &\quad + 0.6928 d_{3/2} p_{3/2} \cos[ \varphi_{p_{3/2}} - \varphi_{d_{3/2}} ] \\
 &\quad + 6.235 d_{3/2} f_{5/2} \cos[ \varphi_{f_{5/2}} - \varphi_{d_{3/2}} ] \\
 a_2 &= - d_{3/2}^2 + p_{3/2}^2 + 1.714 f_{5/2}^2 \\
 &\quad - 2 s_{1/2} d_{3/2} \cos[ \varphi_{d_{3/2}} - \varphi_{s_{1/2}} ] \\
 &\quad + 0.8571 p_{3/2} f_{5/2} \cos[ \varphi_{f_{5/2}} - \varphi_{p_{3/2}} ]
 \end{aligned}$$

$$\begin{aligned}
a_3 &= - 3.464 s_{1/2} f_{5/2} \cos[ \varphi_{f_{5/2}} - \varphi_{s_{1/2}} ] \\
&\quad - 4.157 d_{3/2} p_{3/2} \cos[ \varphi_{p_{3/2}} - \varphi_{d_{3/2}} ] \\
&\quad - 2.771 d_{3/2} f_{5/2} \cos[ \varphi_{f_{5/2}} - \varphi_{d_{3/2}} ] \\
a_4 &= - 1.714 f_{5/2}^2 \\
&\quad - 6.857 p_{3/2} f_{5/2} \cos[ \varphi_{f_{5/2}} - \varphi_{p_{3/2}} ] \\
b_1 &= - 1.732 s_{1/2} p_{3/2} \sin[ \varphi_{p_{3/2}} - \varphi_{s_{1/2}} ] \\
&\quad - 1.386 d_{3/2} p_{3/2} \sin[ \varphi_{p_{3/2}} - \varphi_{d_{3/2}} ] \\
&\quad + 3.118 d_{3/2} f_{5/2} \sin[ \varphi_{f_{5/2}} - \varphi_{d_{3/2}} ] \\
b_2 &= - s_{1/2} d_{3/2} \sin[ \varphi_{d_{3/2}} - \varphi_{s_{1/2}} ] \\
&\quad + 0.7143 p_{3/2} f_{5/2} \sin[ \varphi_{f_{5/2}} - \varphi_{p_{3/2}} ] \\
b_3 &= - 1.155 s_{1/2} f_{5/2} \sin[ \varphi_{f_{5/2}} - \varphi_{s_{1/2}} ] \\
&\quad + 1.386 d_{3/2} p_{3/2} \sin[ \varphi_{p_{3/2}} - \varphi_{d_{3/2}} ] \\
&\quad - 0.2309 d_{3/2} f_{5/2} \sin[ \varphi_{f_{5/2}} - \varphi_{d_{3/2}} ] \\
b_4 &= - 1.714 p_{3/2} f_{5/2} \sin[ \varphi_{f_{5/2}} - \varphi_{p_{3/2}} ] .
\end{aligned}$$

The above system of equations represents 9 equations in 7 unknowns; 4 amplitudes and 3 relative phases. However, the experimental data were not of sufficient quantity and statistical accuracy to allow extraction of  $a_4$  and  $b_4$ . This means we now have 7 equations in 7 unknowns. A solution can still be found but will not result in a value for

chi-square. It is desirable to drop one of the E2 matrix elements from the analysis so that we have 7 equations in 5 unknowns and can determine a chi-square. The DSD calculations, discussed in the next chapter, were used as a guide and indicated that the  $p_{3/2}$  matrix element will be smaller than the  $f_{5/2}$  element by at least a factor of 10 in the energy region being considered. The  $p_{3/2}$  matrix element was set to zero and the analysis was performed using the  $f_{5/2}$  element only.

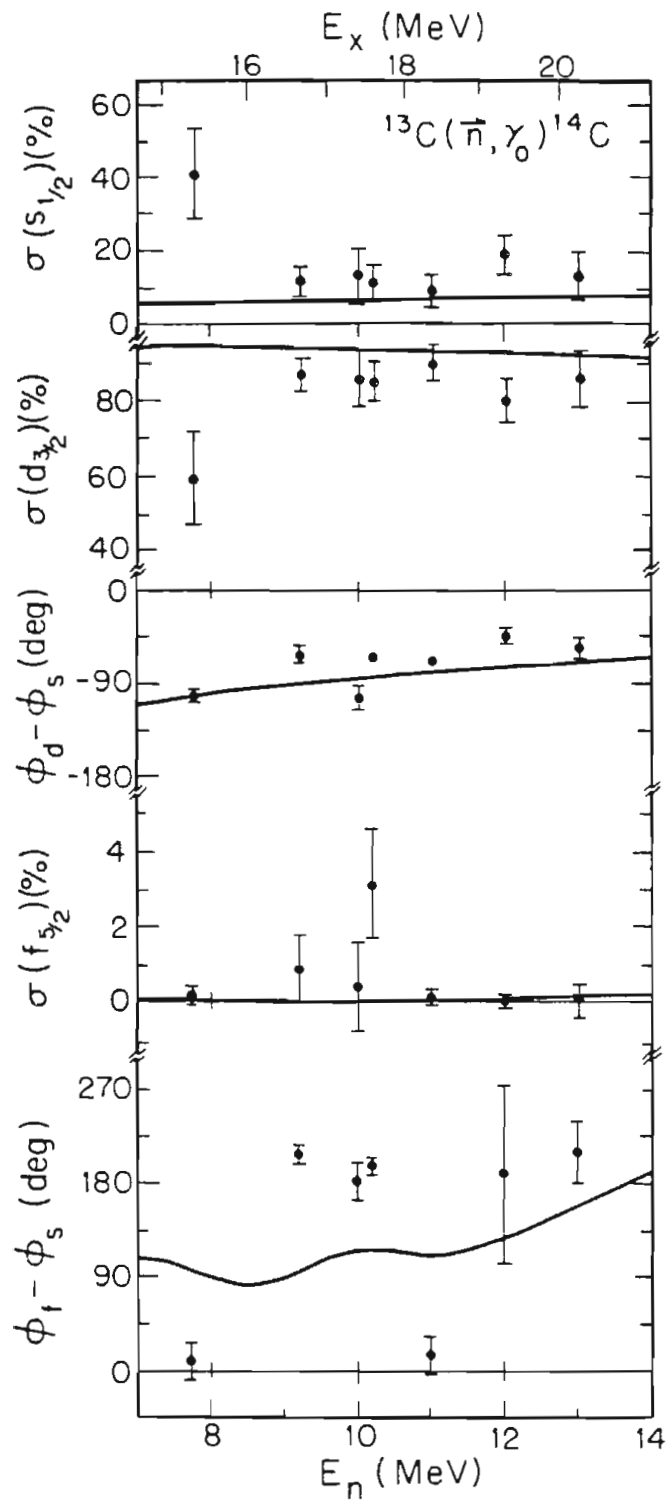
The results are presented in Table C-2 and Figure 6-3. The  $f_{5/2}$  amplitude is small and consistent with zero at 4 of the energies measured. The apparent E2 strength seen between 9.2 MeV and 10.2 MeV will be seen in the next chapter to be more likely due to M1 radiation than E2 radiation. The  $f_{5/2}$  relative phases were not well determined from the analysis due to the small values for the  $f_{5/2}$  amplitudes. The solid lines in Figure 6-3 are the result of an E1-E2 direct-semidirect model calculation using an E2 resonance whose parameters are typical for E2 resonances in this mass region (see Table D-1).

#### 6.4 E1-E2-M1 Analysis

Structure in the  $a_1$  and  $b_1$  coefficients without corresponding structure in the  $a_3$  and  $b_3$  coefficients can arise from the presence of M1 radiation. For M1 radiation there exists two possible transition matrix elements,  $p_{1/2} \exp[ i \phi_{p_{1/2}} ]$  and  $p'_{3/2} \exp[ i \phi'_{p'_{3/2}} ]$ . The  $p_{1/2}$  matrix element describes the transition between two wave functions which differ only in their principle quantum number. Since the M1 operator

Figure 6-3 E1-E2 solutions for the  $^{13}\text{C}(\vec{n},\gamma_0)^{14}\text{C}$  reaction. Two E1 amplitudes, the  $f_{5/2}$  E2 amplitude and two relative phases were fit. The solid lines are the result of a direct-semidirect model calculation.





has no radial dependence, this matrix element is identically zero. The  $f_{5/2}$  E2 matrix element will also be included in the analysis but the  $p_{3/2}$  E2 element will not be used, as in the case of the E2 analysis. The angular distribution equations are

$$6-4 \quad a_0 = s_{1/2}^2 + 2 d_{3/2}^2 + 2 p_{3/2}'^2 + 3 f_{5/2}^2$$

$$a_1 = 2 s_{1/2} p_{3/2}' \cos[\varphi_{p_{3/2}'} - \varphi_{s_{1/2}}] \\ - 2 d_{3/2} p_{3/2}' \cos[\varphi_{p_{3/2}'} - \varphi_{d_{3/2}}] \\ + 6.235 d_{3/2} f_{5/2} \cos[\varphi_{f_{5/2}} - \varphi_{d_{3/2}}]$$

$$a_2 = - d_{3/2}^2 - p_{3/2}'^2 + 1.714 f_{5/2}^2 \\ - 2 s_{1/2} d_{3/2} \cos[\varphi_{d_{3/2}} - \varphi_{s_{1/2}}] \\ - 3.464 p_{3/2}' f_{5/2} \cos[\varphi_{p_{3/2}'} - \varphi_{f_{5/2}}]$$

$$a_3 = - 3.464 s_{1/2} f_{5/2} \cos[\varphi_{f_{5/2}} - \varphi_{s_{1/2}}] \\ - 2.771 d_{3/2} f_{5/2} \cos[\varphi_{f_{5/2}} - \varphi_{d_{3/2}}]$$

$$a_4 = - 1.714 f_{5/2}^2$$

$$b_1 = - s_{1/2} p_{3/2}' \sin[\varphi_{p_{3/2}'} - \varphi_{s_{1/2}}] \\ + 4 d_{3/2} p_{3/2}' \sin[\varphi_{p_{3/2}'} - \varphi_{d_{3/2}}] \\ + 3.118 d_{3/2} f_{5/2} \sin[\varphi_{f_{5/2}} - \varphi_{d_{3/2}}]$$

$$\begin{aligned}
b_2 &= - s_{1/2} d_{3/2} \sin[ \varphi_{d_{3/2}} - \varphi_{s_{1/2}} ] \\
&\quad + 2.887 p'_{3/2} f_{5/2} \sin[ \varphi_{p'_{3/2}} - \varphi_{f_{5/2}} ] \\
b_3 &= - 1.155 s_{1/2} f_{5/2} \sin[ \varphi_{f_{5/2}} - \varphi_{s_{1/2}} ] \\
&\quad - 0.2309 d_{3/2} f_{5/2} \sin[ \varphi_{f_{5/2}} - \varphi_{d_{3/2}} ] \\
b_4 &= 0 .
\end{aligned}$$

The chi-square as a function of M1 and E2 cross section was calculated for each of the seven angular distributions. The value of  $\sigma(p'_{3/2})$  was varied in 24 steps of varying size between 0% and 20% of the total cross section. The value of  $\sigma(f_{5/2})$  was varied in 24 steps of varying size between 0% and 10% of the total. The two E1 amplitudes and the three relative phases were searched by the fitting code to produce the minimum chi-square at each of the 576 points of E2 and M1 cross section. Figure 6-4 and Figure 6-5 show, as examples, contour plots of reduced chi-square for the 10.2 and 12 MeV angular distributions. The contour interval is 0.25 chi-square in each plot. The 10.2 MeV plot shows a broad valley of low chi-square in the region of one percent E2 and from one to over twenty percent M1 cross section. The surface rises quickly for E2 cross sections above two percent. The 12 MeV plot shows a valley of from zero to two percent E2 and zero to six percent M1 and another with less than one percent E2 and zero to over twenty percent M1 cross section. The 12 MeV chi-square surface is clearly very shallow and serves mainly to indicate that the E2 cross section is less than five percent of the total.

Figure 6-4 Contours of reduced chi-square as a function of M1 and E2 cross section for the  $E_n = 10.2$  MeV polarized angular distribution. The two E1 amplitudes and the three relative phases were searched to yield the minimum chi-square while the M1 and E2 cross section were held constant.

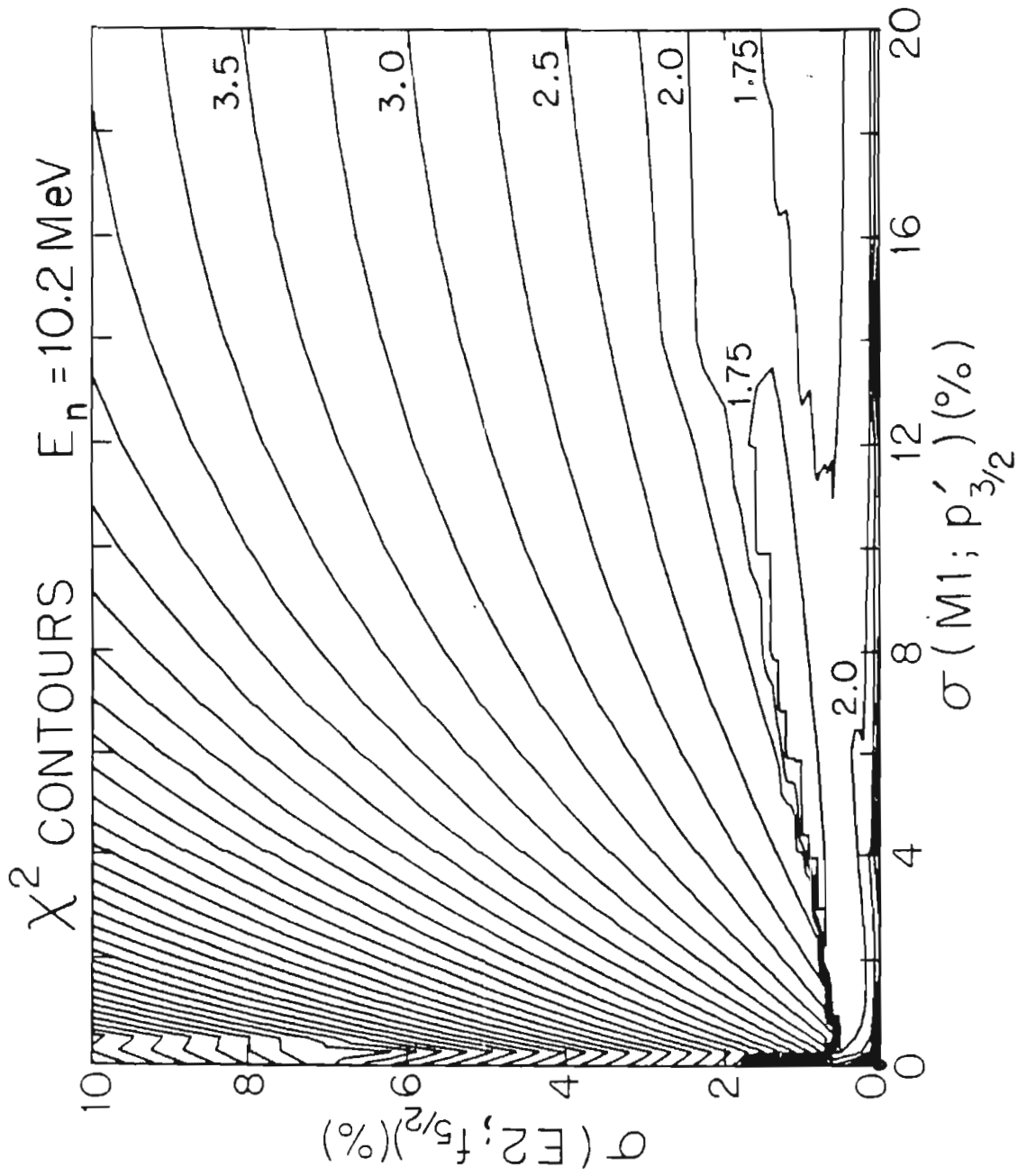
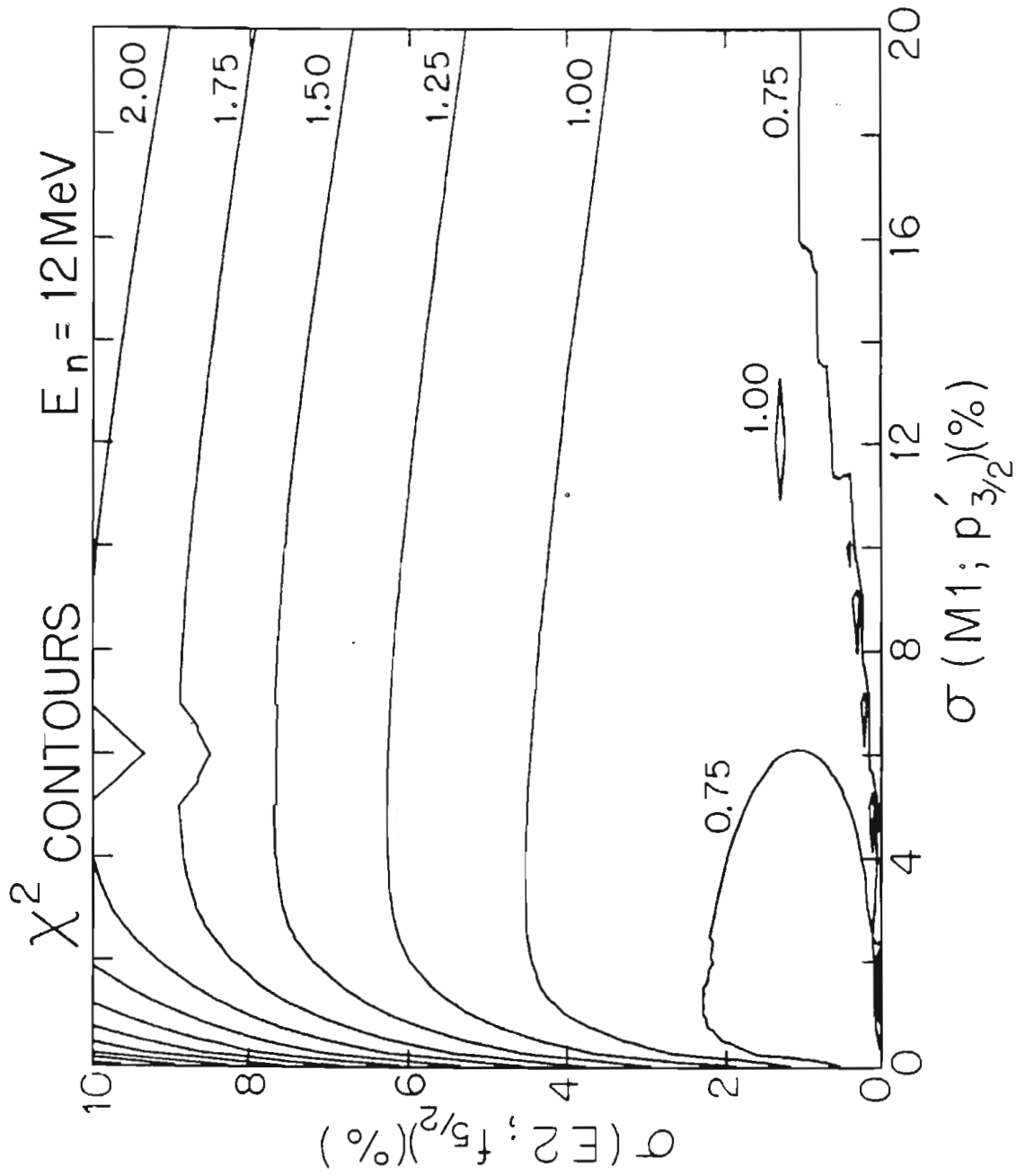


Figure 6-5 Same as Figure 6-4 for  $E_n = 12$  MeV.



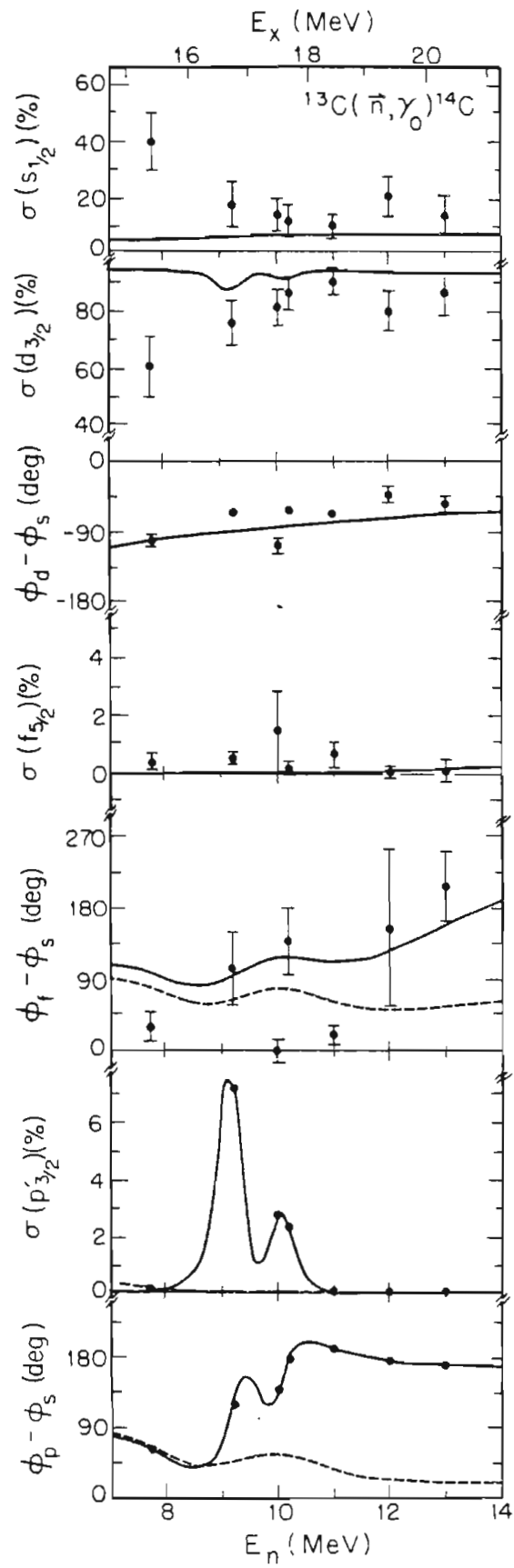
The behavior of the chi-square surfaces show that it will not be possible to extract a unique value for the M1 cross section from the data since the data are consistent with almost any value for the M1 cross section. The DSD calculations of the next chapter were therefore used to calculate the  $p'_{3/2}$  transition matrix element, and thus the M1 cross section, as a function of energy. At each energy, the complex M1 transition matrix element was fixed at the calculated value and the E2 and E1 matrix elements were determined by the fitting code. The results are presented in Table C-3 and Figure 6-6.

The large E2 amplitude seen at  $E_n = 10.2$  MeV in the calculation of the previous section is now essentially zero. The E2 cross section is less than one percent at all energies except 10.0 MeV where the value has a large error bar. The  $f_{5/2}$  relative phases are still not well determined from the data. The solid lines in Figure 6-6 are the result of an E1-E2 direct-semidirect model calculation using an E2 resonance whose parameters are typical for E2 resonances in this mass region (see Table D-1). The dashed lines on the same plots result from inclusion of direct E2 only. The solid lines for the  $\sigma(p'_{3/2})$  and  $(\varphi_{p'_{3/2}} - \varphi_{s_{1/2}})$  plots are the result of the DSD calculation and are the values used in the fitting procedure. The dashed lines represent the  $p'_{3/2}$  matrix element resulting from direct M1 only. In conclusion, the data are consistent with zero to twenty percent M1 and with one or two percent E2.



Figure 6-6 E1-E2-M1 solutions for the  $^{13}\text{C}(n,\gamma_0)^{14}\text{C}$  reaction.

Two E1 amplitudes, the  $f_{5/2}$  E2 amplitude and the two relative phases were fit. The  $p'_{3/2}$  M1 complex matrix element was held constant to the value determined at each energy by the direct-semidirect model calculation of Chapter 7 including two M1 resonances. The solid lines are the result of the DSD calculation; the dashed lines are the result of a DSD calculation including only direct E2 and M1.



## 7 Comparison to Theory

## 7.1 Sum Rules

The sum rules are a measure of the photonuclear absorptive strength (Hayward, 1970). For E1 absorption, the classical dipole sum rule is given by

$$7-1 \quad \int \sigma_{\gamma}(E1) dE_{\gamma} = 60 \frac{NZ}{A} \text{ mb} \cdot \text{MeV} .$$

For  $^{14}\text{C}$ , the dipole absorptive strength is 206 mb·MeV. For isoscalar E2 radiation, the strength is given by the isoscalar energy weighted sum rule (Gell-Mann and Telegdi, 1953)

$$7-2 \quad \int \frac{\sigma_{\gamma}(E2)}{E_{\gamma}^2} = \frac{\pi^2}{137} \frac{A}{12} \frac{\langle r_0^2 \rangle}{938} \text{ fm}^2/\text{MeV} .$$

Using the value  $\langle r_0^2 \rangle = 6.66 \text{ fm}^2$  for the nuclear radius determined from electron scattering (deJager *et al.*, 1974), the E2 absorptive strength for  $^{14}\text{C}$  is  $5.97 \cdot 10^{-4} \text{ fm}^2/\text{MeV} = 5.97 \text{ } \mu\text{b}/\text{MeV}$ . The fraction of the sum rule strengths measured in the  $(\gamma, n_0)$  channel was calculated by separating the detail balance  $(\gamma, n_0)$  total cross section of Table A-5 into an E1 and an E2 component according to the results of the transition matrix analysis of Table C-3 and integrating using a weighted histogram rule. The E1 integral yielded a result of  $29.1 \pm 0.2 \text{ mb} \cdot \text{MeV}$  and therefore the  $(\gamma, n_0)$  channel exhausted  $14.1 \pm 0.1 \%$  of the classical dipole sum. The E2 integral gave a result of  $0.17 \pm 0.03 \text{ } \mu\text{b}/\text{MeV}$  exhausting  $2.8 \pm 0.6 \%$  of the isoscalar E2 energy weighted sum.

## 7.2 Direct-Semidirect Model

The direct-semidirect model code HIKARI (Kitazawa, 1980) was used to fit the  $^{13}\text{C}(n, \gamma_0)^{14}\text{C}$  experimental data. The continuum wave functions for the unbound neutron were calculated with the optical model using the parameter set of Watson *et al.* (1969). This set uses an energy dependent real well potential and an imaginary surface potential. The spin orbit potential strength and the radius and diffuseness parameters are not functions of energy. The bound state wave functions were calculated using a Wood-Saxon well whose depth was modified until the binding energy of the neutron was correct. The radius and diffuseness parameters and the spin orbit well depth were the same as the Watson real well potential parameters. The spectroscopic factor was taken from Cohen and Kurath (1967). The recoil effective charges were calculated using Equation 1-1. The parameters used in the DSD model calculations are presented in Table D-1.

Two E1 resonances were included in the calculation of the  $90^\circ$  cross section, and the positions, widths, and strengths of these resonances were varied to produce the best fit to the data. The fine structure is, of course, not reproduced by the calculation. The deviation of the fit from the data at lower energies is assumed to be due to compound nuclear effects not included in the DSD model.

In order to fit the odd terms in the Legendre expansions of cross sections and analyzing power, an isoscalar E2 resonance was included in

the calculation using parameters typical for E2 resonances in this mass region (Weller and Roberson, 1980). Included in the DSD calculation was a convolution integral to account for the energy spread of the incident neutron beam (see Figure 2-3). The results of the calculation of the angular distributions are shown in Figure 7-1 while the  $90^\circ$  cross section calculation is shown in Figure 3-6. The E2 cross section was small enough compared to the E1 cross section that the E2 resonance had no effect on the appearance of the cross section curve in Figure 3-6 or the  $a_2$  and  $b_2$  curves in Figure 7-1. The calculation is in general agreement with the data for the odd Legendre coefficients except for  $b_1$  in the region of 17 MeV excitation energy. The structure seen below  $E_x = 18$  MeV in the calculated curves is the result of direct M1 and E2 capture. In the region above  $E_x = 18$  MeV where the effect of the E2 resonance becomes more significant, we see a disagreement between the calculation and the fore-aft asymmetry and  $90^\circ$  analyzing power data. The transition matrix elements resulting from the calculation can be compared with the transition matrix analysis of the preceding chapter (see Figure 6-3 and Figure 6-6). The data show little evidence for the existence of E2 radiation in the  $(\gamma, n_0)$  channel.

The structure seen in  $b_1$  and  $A_y(90^\circ)$  can arise from the presence of M1 radiation. The results of a DSD calculation including two narrow M1 resonances at  $E_x = 16.7$  and 17.5 MeV are presented in Figure 7-2 and Figure 7-3. The widths used for both resonances in the calculation were 200 keV. The calculated curves also have the approximately 300 keV energy spread of the incident neutron beam folded into them. The

Figure 7-1 Legendre expansion coefficients, fore-aft symmetry, and  $90^\circ$  analyzing power for the  $^{13}\text{C}(\vec{n}, \gamma_0)^{14}\text{C}$  reaction. The solid lines are the result of a direct-semidirect calculation including an isoscalar E2 resonance whose parameters are typical for this mass region.

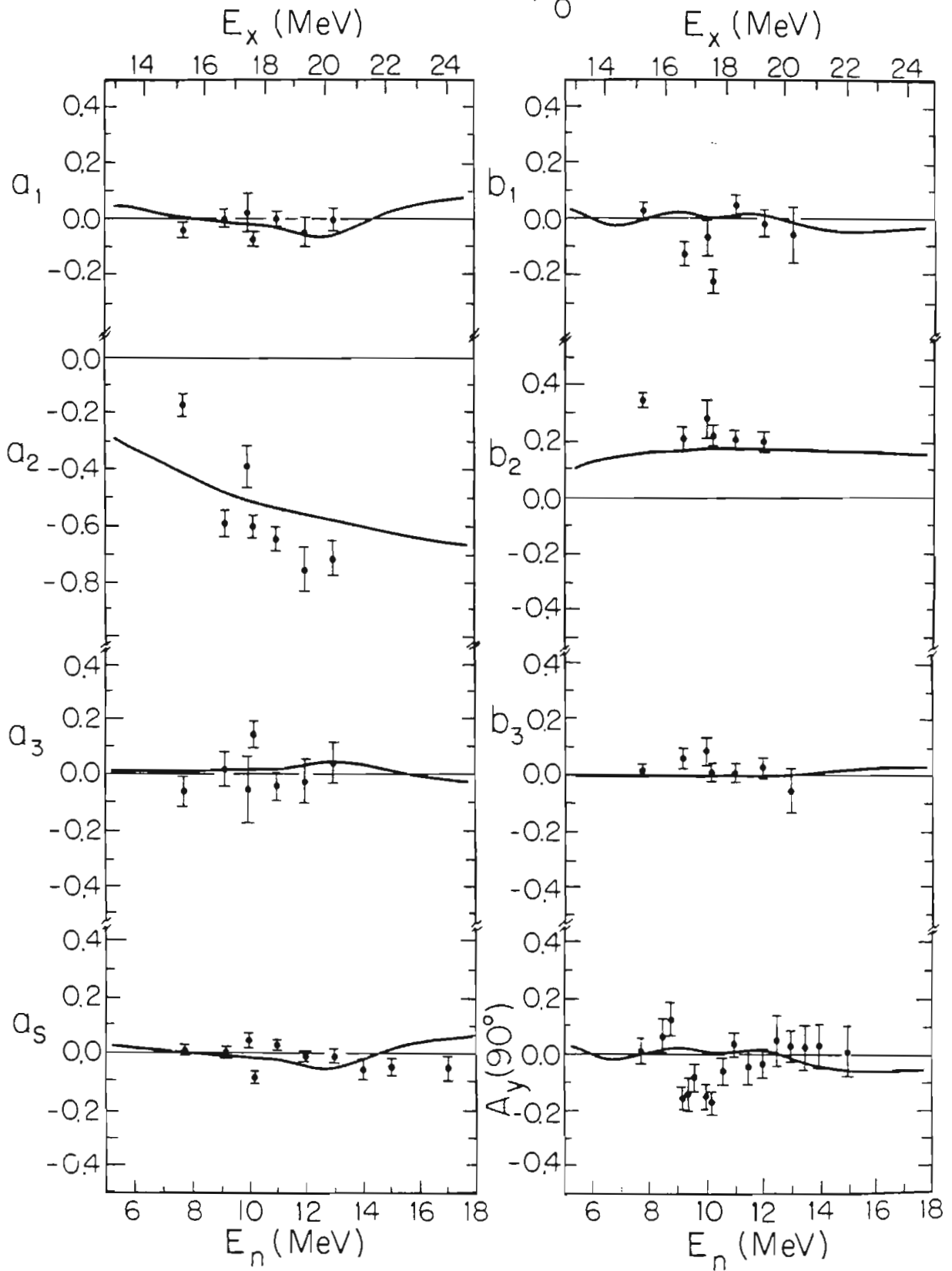


Figure 7-2 Legendre expansion coefficients, fore-aft asymmetry, and  $90^\circ$  analyzing power for the  $^{13}\text{C}(n, \gamma_0)^{14}\text{C}$  reaction. The solid lines are the result of a direct-semidirect calculation including two isovector M1 resonances whose parameters were optimized to fit the  $A_y(90^\circ)$  data.



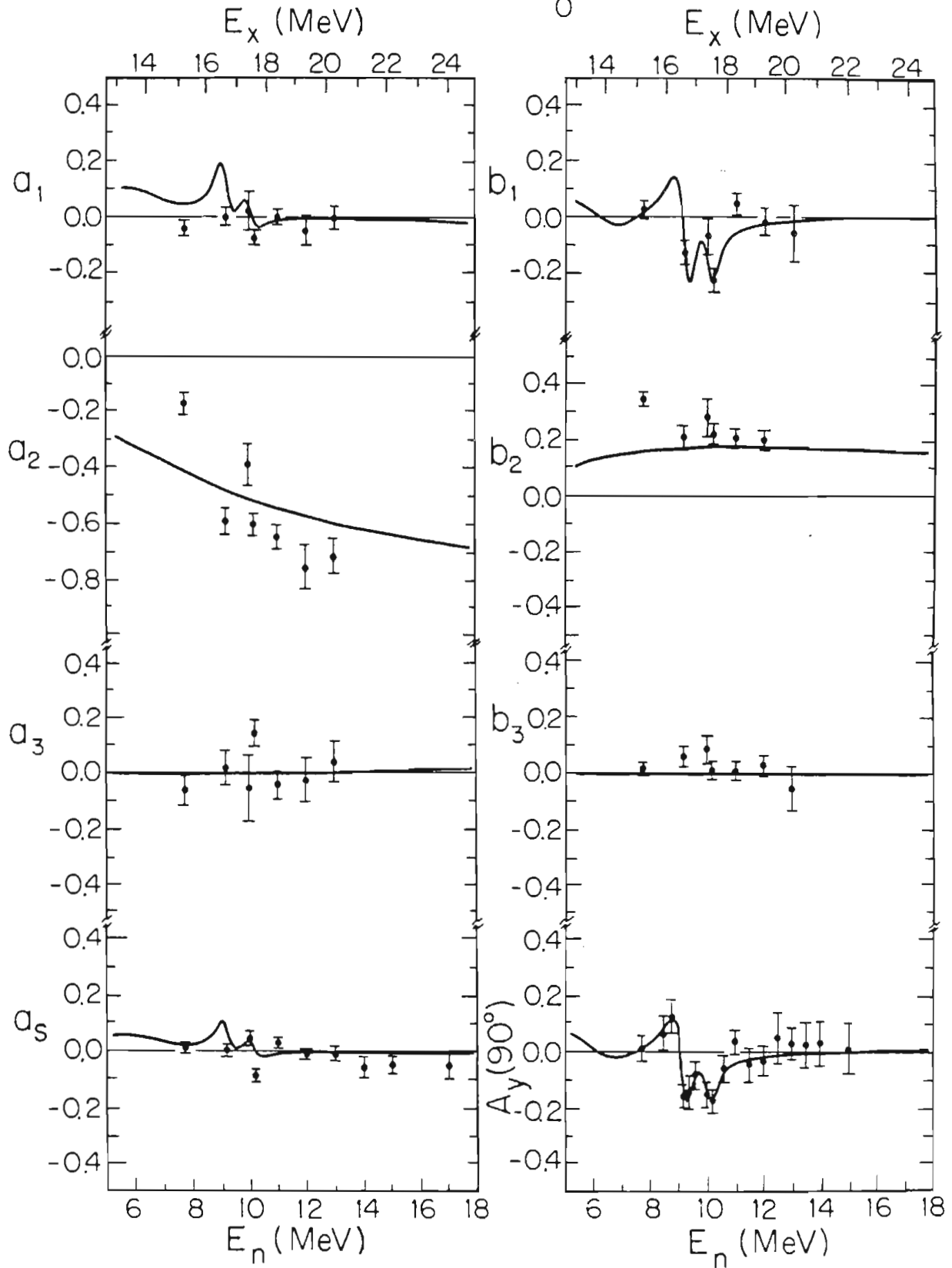
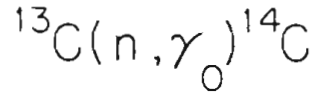
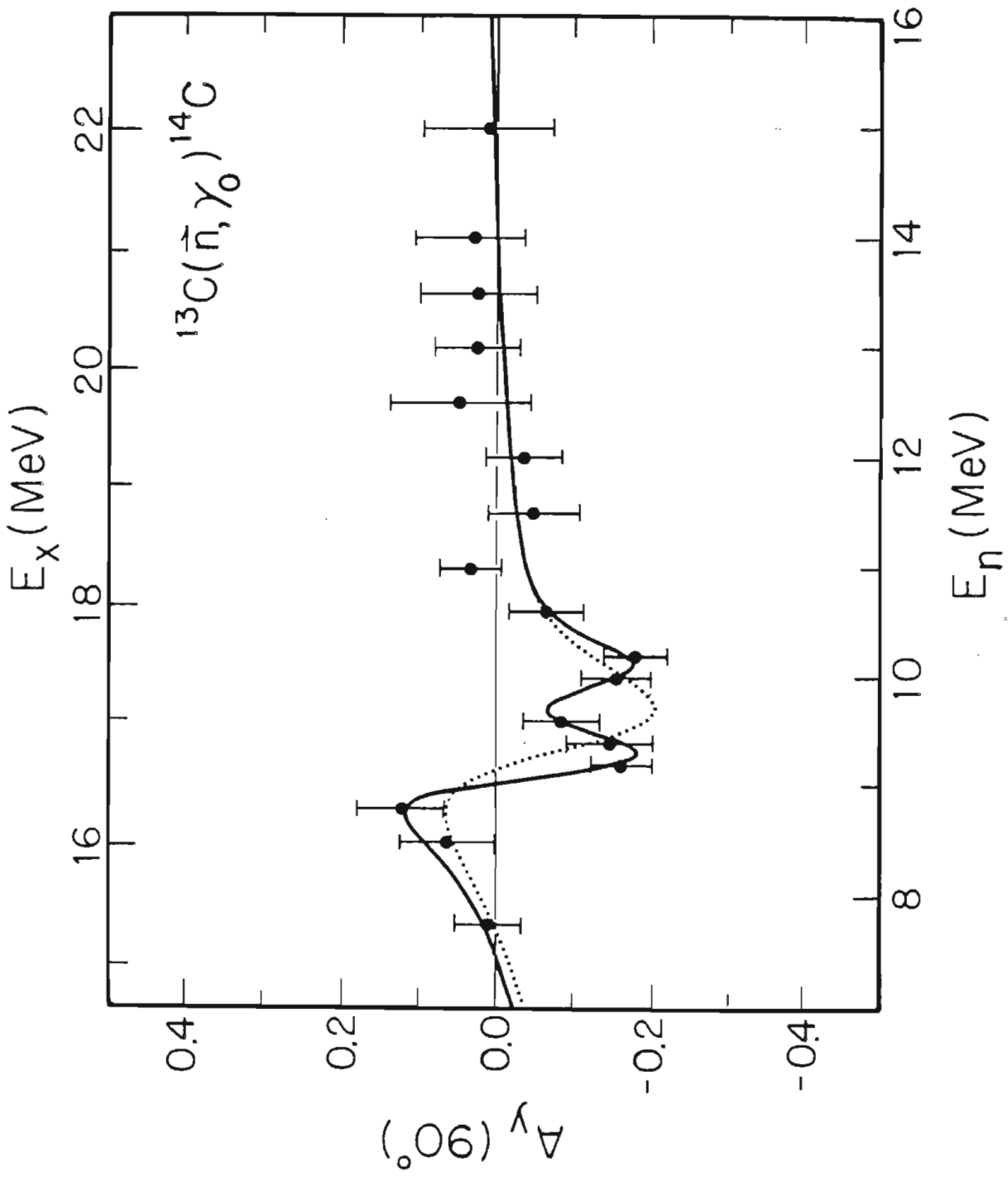


Figure 7-3 The  $A_y(90^\circ)$  data for the  $^{13}\text{C}(n, \gamma_0)^{14}\text{C}$  reaction. The solid line is the result of a direct-semidirect calculation including two isovector M1 resonances. The dotted line is the result of a DSD calculation including only one isovector M1 resonance.



resonance parameters were optimized to fit the  $A_y(90^\circ)$  data, and the agreement between the  $A_y(90^\circ)$  data and the calculation is excellent throughout the energy region measured. The qualitative features of the fore-aft asymmetry data are also reproduced. As in the case of the E2 calculation, the M1 cross section was small enough that no effect was seen in the  $90^\circ$  cross section or the  $a_2$  and  $b_2$  coefficients. The M1 strengths determined from the fits were  $0.24 \mu_0^2$  for the 16.7 MeV resonance and  $0.17 \mu_0^2$  for the 17.5 MeV resonance.

Similar M1 resonances have been seen by Snover *et al.* (1979) in  $^{15}\text{N}(p, \gamma_0)^{16}\text{O}$  at 16.22, 17.14, and 18.8 MeV excitation energy with widths of 18, 36, and  $\sim 250$  keV, respectively. The total M1 strength in  $^{16}\text{O}$  was  $\sim 0.24 \mu_0^2$ , which is similar in magnitude to the value of  $\sim 0.41 \mu_0^2$  seen in  $^{14}\text{C}$  in this work. The values of  $B(\text{M1})$  reported here for  $^{14}\text{C}$  should be considered as only approximate values since the M1 states may have large single particle components and thus are not strictly described by the DSD model. The dotted curve in Figure 7-3 represents a DSD calculation including only one M1 resonance at  $E_x = 17.0$  MeV with a width of 800 keV and a strength  $B(\text{M1}) = 0.50 \mu_0^2$ . The calculation does not describe the data nearly as well as the calculation involving 2 M1 resonances.

The large energy spread of the incident neutron beam limits the number of points of  $90^\circ$  analyzing power that can be measured. Conclusive results await the availability of a higher flux polarized deuteron beam allowing a lower pressure in the deuterium gas cell and therefore a smaller neutron energy spread.

## 7.3 Two-Level Doorway State Calculations

The DSD calculations do not reproduce the structure seen in  $a_2$  and  $b_2$  at  $E_n = 7.75$  MeV. Another approach is to perform a two-level doorway state calculation (Calarco *et al.*, 1977) to obtain the transition matrix elements as a function of energy, and from them calculate the Legendre coefficients  $A_0$ ,  $a_2$ , and  $b_2$ . For a given neutron channel  $l, j$ , the transition matrix element  $T_{l, j}$  can be written as

$$7-3 \quad T_{l, j} = \frac{\left\langle \begin{matrix} g_A^{l, j} g_A^\gamma [E - E_A + i \frac{\Gamma_A}{2}] + g_A^{l, j} g_B^\gamma V_{AB} \\ g_A^{l, j} g_A^\gamma [E - E_A + i \frac{\Gamma_A}{2}] \end{matrix} \right\rangle e^{i\varphi_A^l}}{\left[ E - E_A + i \frac{\Gamma_A}{2} \right] \left[ E - E_B + i \frac{\Gamma_B}{2} \right] - |V|^2} + \frac{\left\langle \begin{matrix} g_B^{l, j} g_B^\gamma [E - E_B + i \frac{\Gamma_B}{2}] + g_B^{l, j} g_A^\gamma V_{BA} \\ g_B^{l, j} g_B^\gamma [E - E_B + i \frac{\Gamma_B}{2}] \end{matrix} \right\rangle e^{i\varphi_B^l}}{\left[ E - E_A + i \frac{\Gamma_A}{2} \right] \left[ E - E_B + i \frac{\Gamma_B}{2} \right] - |V|^2}$$

where  $g^{l, j}$  and  $g^\gamma$  are the square roots of the particle and  $\gamma$  decay widths, and  $\varphi^l$  is the phase, of partial wave  $l$ , and where  $V$  is the interaction strength between the levels A and B. The energies and widths for the two E1 resonances were taken from the DSD calculations of the preceding section (see Table D-1). The values for  $g^{l, j}$  and  $\varphi^l$  were taken from the  $s_{1/2}$  and  $d_{3/2}$  amplitudes and phases extracted from the data at the energies corresponding to the peaks of the two E1 resonances (see Table C-1). The  $\gamma$  decay widths,  $g^\gamma$ , and the interaction strength,  $V$ , were varied to produce the best fit to the data. Also included in the calculation was a noninterfering constant background of  $0.89 \mu\text{b}$ . The results of the calculations are presented as the solid line in

Figure 7-4 The  $90^\circ$  cross section,  $a_2$  and  $b_2$  Legendre coefficients, and  $s_{1/2}$  and  $d_{3/2}$  transition matrix elements for the  $^{13}\text{C}(n, \gamma_0)^{14}\text{C}$  reaction. The solid lines are the result of a two-level doorway state calculation using parameters taken from the DSD calculations and the transition matrix element analysis. The dashed lines are the result of a two-level doorway state calculation where the transition matrix element parameters were varied to produce the best fit to the data. The dotted lines are the result of a direct-semidirect model calculation.

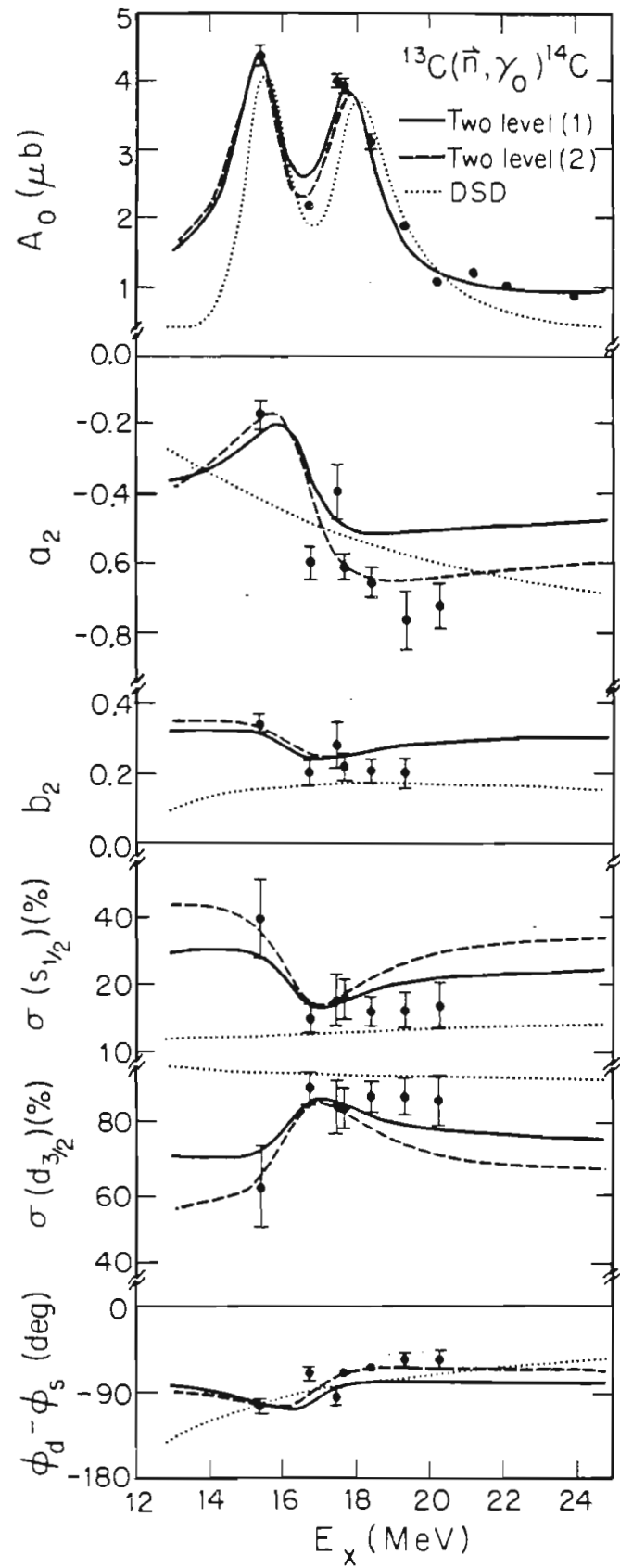


Figure 7-4 while the dotted line in the same figure represents the result of the DSD calculations of the preceding section. The energy dependence of the data is well reproduced by the calculation. The angular distribution at  $E_n = 10.0$  MeV suffered from large backgrounds at extreme angles so that the value for  $a_2$  at 10.0 MeV should lie alongside the values at neighboring energies. If the intrinsic values for the  $s_{1/2}$  to  $d_{3/2}$  ratio and phase of the two resonances are adjusted so that the two-level calculation gives the observed values at the peaks of the two resonances then the calculation gives better quantitative agreement for  $a_2$  and  $b_2$  throughout the energy region measured, as seen by the dashed line in Figure 7-4. The two-level calculation indicates that the parameterization of the giant dipole resonance as the two resonances used in the DSD calculations is a reasonable one.

If the interaction strength between two nearby levels of the same spin and parity is not zero then the cross section between the two resonances can have two minima and one maximum which is not itself a resonance (Lane and Thomas, 1958). This effect could be used to explain the small peak observed in the  $90^\circ$  cross section minimum at  $E_n = 9.2$  MeV. The effect arises due to the interference of the two resonances with all other resonances on both sides. The lack of information about other possible resonances in this energy region makes calculations of the effect difficult. A calculation using a coherent background with a constant amplitude and phase did produce a small cross section bump between the two resonances but did not result in an acceptable overall fit to the data. The best fits to the data occurred



when the interaction strength  $V$  between the two resonances was set to zero.

#### 7.4 Summary

The giant dipole resonance in  $^{14}\text{C}$  was found to be split into two components at excitation energies of 15.45 and 17.85 MeV and with widths of 1.5 and 1.75 MeV, respectively. Two-level doorway state calculations agree well with the measured  $a_2$  and  $b_2$  coefficients and indicate that it is reasonable to parameterize the giant dipole resonance as two different levels of the same spin and parity. After detail balance conversion to photoneutron cross section, the integrated E1 yield exhausted 14 % of the classical dipole sum rule in the  $(\gamma, n_0)$  channel in the region of 13.4 to 24 MeV excitation energy. A model independent E1 transition matrix analysis of the data yielded two solutions, one where the  $d_{3/2}$  matrix element accounted for about 85 % of the E1 cross section, the other where the  $d_{3/2}$  element accounted for about 30 % of the E1 cross section. Direct-semidirect model calculations indicate the dominant  $d_{3/2}$  solution to be the physical one.

The E1-E2-M1 transition matrix element analysis showed that the E2 strength was less than 2 % of the total cross section and that the M1 strength could not be determined by examination of a single angular distribution. The observed E2 strength exhausts  $2.8 \pm 0.6$  % of the isoscalar E2 energy weighted sum rule. The data show little evidence for collective E2 strength in the  $(\gamma, n_0)$  channel.

Structure in the  $90^\circ$  analyzing power and in the Legendre coefficient  $b_1$  near 9.2 and 10.2 MeV neutron energy suggests the existence of narrow M1 resonances at these energies. A direct-semidirect model calculation was in good overall agreement with all of the experimental data when it included two M1 resonances at excitation energies 16.7 and 17.5 MeV, with strengths 0.24 and  $0.17 \mu_0^2$ , and widths less than the 300 keV energy spread of the neutron beam.

## 8 References

H. H. Barschall and W. Haeberli, Editors

Polarization Phenomena in Nuclear Reactions

Wisconsin Press, Madison, 1970

Fred E. Bertrand, Editor

Giant Multipole Resonances

Harwood Academic, New York, 1980

Philip R. Bevington

Data Reduction and Error Analysis for the Physical Sciences.

McGraw-Hill, New York, 1969.

G. E. Brown

Direct and Semi-Direct  $(p, \gamma)$  and  $(n, \gamma)$  Reactions

Nucl. Phys. 57 (1964) 339

J. R. Calarco, S. W. Wissink, M. Sasao, K. Wienhard, and S. S. Hanna

Structure in the Giant Dipole Resonance of  $^{16}\text{O}$ : Evidence  
for a Secondary Doorway State from Polarized-Proton  
Capture

Phys. Rev. Lett. 39 15 (1977) 925

T.B. Clegg, G.A. Bissenger, W. Haeberli, and P.A. Owen

Lamb-Shift Polarized Ion Sources for Tandem Accelerators  
at Wisconsin and Triangle Universities Nuclear Laboratory  
in Barschall, 1970, p. 835

C.F. Clement, A.M. Lane, and J.A. Rook

Radiative Capture by Excitation of Collective Vibrations:  
(I) Theory  
Nucl. Phys. 66 (1965) 273

C.F. Clement, A.M. Lane, and J.A. Rook

Radiative Capture by Excitation of Collective Vibrations:  
(II) Calculation  
Nucl. Phys. 66 (1965) 293

S. Cohen and D. Kurath

Spectroscopic Factors for the 1p Shell  
Nucl. Phys. A101 (1967) 1

C.W. de Jager, L.H. de Vries, and L.C. de Vries

Nuclear Charge- and Magnetization-Density-Distributions  
Parameters from Elastic Electron Scattering  
At. Data and Nucl. Data Tab. 14 (1974) 479

M. Drosg

Unified Absolute Differential Cross Section for Neutron  
Production by the Hydrogen Isotopes for Charged-Particle  
Energies Between 6 and 7 MeV  
Nucl. Sci. Engr. 67 (1978) 190

E.G. Fuller

Giant Resonances  
in Encyclopedia of Physics, Edited by R.G. Lerner and  
G.L. Trigg, Addison-Wesley Publishing Co., Reading,  
Massachusetts, 1981, p. 882

M. Gell-Mann and V.L. Telegdi

Consequences of Charge Independence for Nuclear Reactions  
Involving Photons  
Phys. Rev. 91 (1953) 169

C.R. Gould, L.G. Holzweig, S.E. King, Y.C. Lau, R.V. Poore,

N.R. Roberson, and S.A. Wender  
The XSYS Data Acquisition System at Triangle Universities  
Nuclear Laboratory  
IEEE Trans. on Nucl. Sci. NS-28 , No. 5 (1981) 3708

S. S. Hanna

Study of the Giant Resonances with Capture Reactions  
in Nuclear Physics with Electromagnetic Interactions.  
Proceedings, Mainz 1979, Edited by H. Arenhövel and  
D. Drechsel, (Institut für Kernphysik, Universität Mainz,  
1979) p. 288

E. Hayward

Photonuclear Reactions  
U.S. Natl. Bur. Stand. Monograph No. 118  
Washington, DC, 1970

Mark Jay Jensen

Fast Neutron Capture by  $^{13}\text{C}$   
Ph.D. Dissertation, North Carolina State University,  
1981.

S. E. King

Private Communication, 1980

H. Kitazawa

Private Communication, 1980

Erwin Kreyszig

Advanced Engineering Mathematics, Third Edition  
John Wiley and Sons, Inc., New York, 1972

A. M. Lane and R. G. Thomas

R-Matrix Theory of Nuclear Reactions

Rev. Mod. Phys. 30 2 (1958) 257

P. W. Lisowski

The Transfer Polarization of the  ${}^2\text{H}(\vec{d}, \vec{n}){}^3\text{He}$  Reaction and  
the Scattering of Polarized Neutrons from  ${}^4\text{He}$  and  ${}^3\text{He}$

Ph.D. Dissertation, Duke University, 1973

N. R. Roberson and S. E. Edwards

Interface for the TUNL VAX Data Acquisition Facility

IEEE Trans. on Nucl. Sci. NS-28, No. 5 (1981) 3834

R. G. Seyler and H. R. Weller

Angular Distribution Theory for Particle-Capture-Gamma  
Reactions

Phys. Rev. C 20 2 (1979) 453

K. A. Snover, P. G. Ikossi, and T. A. Trainor

Observation of Magnetic Dipole Strength in  ${}^{16}\text{O}$

Phys. Rev. Lett. 43 2 (1979) 117

M. Suffert, W. Feldman, J. Mahieux, and S. S. Hanna

One-Crystal NaI Spectrometer

Nucl. Inst. Meth. 63 (1968) 1

T.A. Trainor, T.B. Clegg, and P.W. Lisowski

The Tensor Analyzing Power  $A_{zz}$  at  $\theta = 0^\circ$  for the  
 ${}^3\text{He}(\vec{d}, p){}^4\text{He}$  Reaction

Nucl. Phys. A220 (1974) 533

James David Turner

The Giant Dipole Resonance Region of  ${}^{14}\text{N}$ : Polarized and  
Unpolarized Proton Capture Measurements

Ph.D. Dissertation, Duke University, 1978

B.A. Watson, P.P. Singh, and R.E. Segel

Optical-Model Analysis of Nucleon Scattering from  
1p-Shell Nuclei between 10 and 50 MeV

Phys. Rev. 182 4 (1969) 977

H.R. Weller and N.R. Roberson

Capture Reactions with Protons, Neutrons, and Alpha  
Particles

Rev. Mod. Phys. 52 4 (1980) 699

H.R. Weller and N.R. Roberson

Proton and Neutron Radiative Capture

IEEE Trans. Nucl. Sci. NS-28 4 (1981) 1268

S.A. Wender, C.E. Floyd, T.B. Clegg, and W.R. Wylie

A High Efficiency Bunching System for Polarized Beams

Nucl. Inst. Meth. 174 (1980) 341



## A Excitation Functions

Table A-1 The  $90^\circ$  analyzing power of the  $^{13}\text{C}(\vec{n}, \gamma_0)^{14}\text{C}$  reaction. The uncertainties represent one standard deviation of the statistical error.

$E_n$ (MeV)	$90^\circ$ analyzing power
7.75	$0.009 \pm 0.045$
8.50	$0.062 \pm 0.062$
8.80	$0.120 \pm 0.057$
9.20	$-0.161 \pm 0.040$
9.40	$-0.146 \pm 0.057$
9.60	$-0.085 \pm 0.049$
10.00	$-0.154 \pm 0.044$
10.20	$-0.178 \pm 0.040$
10.60	$-0.065 \pm 0.048$
11.00	$0.033 \pm 0.041$
11.50	$-0.047 \pm 0.059$
12.00	$-0.036 \pm 0.051$
12.50	$0.046 \pm 0.091$
13.00	$0.025 \pm 0.056$
13.50	$0.023 \pm 0.078$
14.00	$0.027 \pm 0.078$
15.00	$0.008 \pm 0.086$

Table A-2 The fore-aft asymmetry of the  $^{13}\text{C}(n,\gamma_0)^{14}\text{C}$  reaction. The uncertainties represent one standard deviation of the statistical error.

$E_n$ (MeV)	Fore-aft asymmetry
7.75	$0.003 \pm 0.017$
9.20	$-0.006 \pm 0.020$
10.00	$0.036 \pm 0.024$
10.20	$-0.095 \pm 0.017$
11.00	$0.020 \pm 0.016$
12.00	$-0.017 \pm 0.016$
13.00	$-0.015 \pm 0.024$
14.00	$-0.063 \pm 0.036$
15.00	$-0.055 \pm 0.033$
17.00	$-0.059 \pm 0.044$

Table A-3 The  $90^\circ$  cross section of the  $^{13}\text{C}(n,\gamma_0)^{14}\text{C}$  reaction. The uncertainties represent one standard deviation of the statistical error.

$E_n$ (MeV)	$\sigma(90^\circ)$ ( $\mu\text{b}/\text{sr}$ )	$E_n$ (MeV)	$\sigma(90^\circ)$ ( $\mu\text{b}/\text{sr}$ )	$E_n$ (MeV)	$\sigma(90^\circ)$ ( $\mu\text{b}/\text{sr}$ )
5.60	$4.33 \pm 0.33$	8.50	$3.59 \pm 0.14$	11.50	$3.44 \pm 0.13$
5.80	$4.05 \pm 0.27$	8.60	$3.11 \pm 0.21$	11.60	$2.62 \pm 0.19$
6.00	$3.85 \pm 0.32$	8.80	$2.74 \pm 0.10$	11.80	$2.51 \pm 0.18$
6.20	$3.79 \pm 0.30$	9.00	$2.06 \pm 0.18$	12.00	$2.60 \pm 0.07$
6.40	$3.84 \pm 0.33$	9.20	$2.81 \pm 0.08$	12.20	$2.37 \pm 0.17$
6.60	$4.13 \pm 0.30$	9.40	$2.64 \pm 0.09$	12.40	$2.24 \pm 0.16$
6.80	$4.37 \pm 0.24$	9.60	$1.99 \pm 0.06$	12.50	$1.55 \pm 0.08$
7.00	$4.77 \pm 0.21$	9.80	$3.17 \pm 0.21$	12.60	$1.68 \pm 0.16$
7.20	$4.96 \pm 0.28$	10.00	$4.75 \pm 0.14$	12.80	$1.65 \pm 0.15$
7.40	$4.84 \pm 0.17$	10.20	$5.12 \pm 0.11$	13.00	$1.48 \pm 0.05$
7.60	$4.83 \pm 0.27$	10.40	$4.60 \pm 0.24$	13.50	$1.62 \pm 0.07$
7.75	$4.74 \pm 0.15$	10.60	$4.07 \pm 0.14$	14.00	$1.58 \pm 0.05$
7.80	$4.99 \pm 0.27$	10.80	$3.78 \pm 0.22$	15.00	$1.36 \pm 0.06$
8.00	$4.96 \pm 0.26$	11.00	$4.12 \pm 0.13$	17.00	$1.18 \pm 0.08$
8.20	$4.55 \pm 0.26$	11.20	$3.90 \pm 0.22$		
8.40	$4.11 \pm 0.24$	11.40	$3.25 \pm 0.20$		

Table A-4 The total cross section of the  $^{13}\text{C}(n,\gamma_0)^{14}\text{C}$  reaction. The uncertainties represent one standard deviation of the statistical error.

$E_n$ (MeV)	$\sigma_{n,\gamma_0}$ ( $\mu\text{b}$ )	$E_n$ (MeV)	$\sigma_{n,\gamma_0}$ ( $\mu\text{b}$ )	$E_n$ (MeV)	$\sigma_{n,\gamma_0}$ ( $\mu\text{b}$ )
5.60	44.3 $\pm$ 3.4	8.50	39.0 $\pm$ 1.5	11.50	32.7 $\pm$ 1.2
5.80	41.6 $\pm$ 2.8	8.60	33.7 $\pm$ 2.3	11.60	24.9 $\pm$ 1.8
6.00	39.7 $\pm$ 3.3	8.80	29.3 $\pm$ 1.1	11.80	23.9 $\pm$ 1.7
6.20	39.2 $\pm$ 3.1	9.00	21.6 $\pm$ 1.9	12.00	24.7 $\pm$ 0.7
6.40	39.9 $\pm$ 3.4	9.20	28.9 $\pm$ 0.8	12.20	22.5 $\pm$ 1.6
6.60	43.1 $\pm$ 3.1	9.40	26.6 $\pm$ 0.9	12.40	21.3 $\pm$ 1.5
6.80	45.8 $\pm$ 2.5	9.60	19.7 $\pm$ 0.6	12.50	14.8 $\pm$ 0.8
7.00	50.3 $\pm$ 2.2	9.80	31.0 $\pm$ 2.1	12.60	16.0 $\pm$ 1.5
7.20	52.7 $\pm$ 3.0	10.00	46.0 $\pm$ 1.4	12.80	15.7 $\pm$ 1.4
7.40	51.8 $\pm$ 1.8	10.20	49.2 $\pm$ 1.1	13.00	14.1 $\pm$ 0.5
7.60	52.0 $\pm$ 2.9	10.40	44.0 $\pm$ 2.3	13.50	15.5 $\pm$ 0.7
7.75	51.3 $\pm$ 1.6	10.60	38.8 $\pm$ 1.3	14.00	15.1 $\pm$ 0.5
7.80	54.1 $\pm$ 2.9	10.80	36.0 $\pm$ 2.1	15.00	13.0 $\pm$ 0.6
8.00	54.1 $\pm$ 2.8	11.00	39.2 $\pm$ 1.2	17.00	11.3 $\pm$ 0.8
8.20	49.7 $\pm$ 2.8	11.20	37.1 $\pm$ 2.1		
8.40	44.8 $\pm$ 2.6	11.40	30.9 $\pm$ 1.9		

Table A-5 The total cross section of the  $^{14}\text{C}(\gamma, n_0)^{13}\text{C}$  reaction from detail balance. The uncertainties represent one standard deviation of the statistical error.

$E_n$ (MeV)	$\sigma_{\gamma, n_0}$ (mb)	$E_n$ (MeV)	$\sigma_{\gamma, n_0}$ (mb)	$E_n$ (MeV)	$\sigma_{\gamma, n_0}$ (mb)
13.38	$4.49 \pm 0.34$	16.07	$4.17 \pm 0.16$	18.86	$3.43 \pm 0.13$
13.56	$4.25 \pm 0.28$	16.16	$3.59 \pm 0.24$	18.95	$2.61 \pm 0.19$
13.75	$4.08 \pm 0.34$	16.35	$3.12 \pm 0.11$	19.13	$2.49 \pm 0.18$
13.93	$4.06 \pm 0.32$	16.53	$2.30 \pm 0.20$	19.32	$2.58 \pm 0.07$
14.12	$4.15 \pm 0.36$	16.72	$3.08 \pm 0.09$	19.51	$2.34 \pm 0.17$
14.31	$4.50 \pm 0.33$	16.91	$2.83 \pm 0.10$	19.69	$2.21 \pm 0.16$
14.49	$4.81 \pm 0.26$	17.09	$2.10 \pm 0.06$	19.78	$1.53 \pm 0.08$
14.68	$5.30 \pm 0.23$	17.28	$3.30 \pm 0.22$	19.88	$1.65 \pm 0.16$
14.86	$5.57 \pm 0.31$	17.46	$4.89 \pm 0.14$	20.06	$1.62 \pm 0.15$
15.05	$5.48 \pm 0.19$	17.65	$5.23 \pm 0.11$	20.25	$1.45 \pm 0.05$
15.23	$5.52 \pm 0.31$	17.83	$4.67 \pm 0.24$	20.71	$1.58 \pm 0.07$
15.37	$5.45 \pm 0.17$	18.02	$4.11 \pm 0.14$	21.18	$1.53 \pm 0.05$
15.42	$5.75 \pm 0.31$	18.21	$3.80 \pm 0.22$	22.11	$1.30 \pm 0.06$
15.61	$5.76 \pm 0.30$	18.39	$4.13 \pm 0.13$	23.96	$1.09 \pm 0.07$
15.79	$5.30 \pm 0.30$	18.58	$3.90 \pm 0.22$		
15.98	$4.78 \pm 0.28$	18.76	$3.24 \pm 0.20$		

## B Angular Distributions

Table B-1 Observed cross section and analyzing power angular distributions for the  $^{13}\text{C}(\vec{n}, \gamma_0)^{14}\text{C}$  reaction at neutron energies of 7.75, 9.2, 10.0, 10.2, 11, 12, and 13 MeV. The uncertainties represent one standard deviation of the statistical error.

$E_n$	$\theta$	$\sigma(\theta)/A_0$	$A_y(\theta)$	$A_y(\theta)\sigma(\theta)/A_0$
7.75	35	$0.861 \pm 0.061$		
	45	$0.956 \pm 0.042$	$0.564 \pm 0.080$	$0.539 \pm 0.080$
	55	$1.004 \pm 0.025$	$0.500 \pm 0.073$	$0.502 \pm 0.075$
	70	$1.055 \pm 0.051$		
	90	$1.090 \pm 0.034$	$-0.075 \pm 0.100$	$-0.082 \pm 0.109$
	110	$1.083 \pm 0.039$	$-0.329 \pm 0.083$	$-0.357 \pm 0.091$
	125	$0.942 \pm 0.038$	$-0.493 \pm 0.091$	$-0.464 \pm 0.088$
	140	$0.928 \pm 0.052$		
	141	$1.005 \pm 0.038$	$-0.445 \pm 0.063$	$-0.447 \pm 0.066$
	150	$0.933 \pm 0.054$		

Table B-1 Continued.

$E_n$	$\theta$	$\sigma(\theta)/A_0$	$A_y(\theta)$	$A_y(\theta)\sigma(\theta)/A_0$
9.2	35	$0.735 \pm 0.081$		
	40	$0.737 \pm 0.081$		
	45	$0.820 \pm 0.045$		
	55	$1.035 \pm 0.038$	$0.248 \pm 0.101$	$0.257 \pm 0.105$
	70	$1.227 \pm 0.049$	$-0.046 \pm 0.102$	$-0.056 \pm 0.125$
	90	$1.257 \pm 0.034$	$-0.157 \pm 0.069$	$-0.197 \pm 0.087$
	110	$1.233 \pm 0.046$	$-0.210 \pm 0.092$	$-0.259 \pm 0.115$
	125	$1.032 \pm 0.042$	$-0.465 \pm 0.113$	$-0.480 \pm 0.117$
	140	$0.722 \pm 0.043$	$-0.327 \pm 0.139$	$-0.236 \pm 0.103$
	150	$0.655 \pm 0.061$		
10.0	45	$0.932 \pm 0.049$		
	55	$1.051 \pm 0.049$	$0.283 \pm 0.168$	$0.297 \pm 0.177$
	70	$1.155 \pm 0.054$	$0.315 \pm 0.174$	$0.364 \pm 0.202$
	90	$1.186 \pm 0.055$	$-0.351 \pm 0.138$	$-0.417 \pm 0.165$
	110	$1.154 \pm 0.055$	$-0.363 \pm 0.137$	$-0.419 \pm 0.159$
	125	$0.888 \pm 0.051$	$-0.377 \pm 0.173$	$-0.335 \pm 0.155$
	135	$0.909 \pm 0.051$	$-0.371 \pm 0.122$	$-0.338 \pm 0.113$

Table B-1 Continued.

$E_n$	$\theta$	$\sigma(\theta)/A_0$	$A_y(\theta)$	$A_y(\theta)\sigma(\theta)/A_0$
10.2	30	$0.549 \pm 0.062$		
	35	$0.772 \pm 0.058$		
	45	$0.691 \pm 0.045$	$0.206 \pm 0.136$	$0.143 \pm 0.097$
	60	$0.979 \pm 0.053$	$0.139 \pm 0.093$	$0.136 \pm 0.140$
	70	$1.157 \pm 0.062$	$0.000 \pm 0.090$	$0.000 \pm 0.153$
	90	$1.290 \pm 0.049$	$-0.154 \pm 0.086$	$-0.199 \pm 0.112$
	110	$1.291 \pm 0.037$	$-0.410 \pm 0.060$	$-0.530 \pm 0.078$
	125	$1.051 \pm 0.045$	$-0.306 \pm 0.105$	$-0.322 \pm 0.111$
	135	$0.964 \pm 0.042$		
	141	$0.797 \pm 0.048$	$-0.622 \pm 0.094$	$-0.496 \pm 0.131$
	145	$0.871 \pm 0.065$		
	150	$0.533 \pm 0.054$		
	11.	35	$0.680 \pm 0.044$	
45			$0.416 \pm 0.075$	$0.362 \pm 0.128$
55		$1.027 \pm 0.052$	$0.285 \pm 0.091$	$0.292 \pm 0.095$
70		$1.209 \pm 0.049$	$0.197 \pm 0.053$	$0.238 \pm 0.065$
90		$1.347 \pm 0.033$	$0.079 \pm 0.057$	$0.106 \pm 0.076$
110		$1.197 \pm 0.049$	$-0.208 \pm 0.060$	$-0.250 \pm 0.072$
125		$0.952 \pm 0.053$	$-0.176 \pm 0.095$	$-0.167 \pm 0.091$
135		$0.767 \pm 0.048$		



Table B-1 Continued.

$E_n$	$\theta$	$\sigma(\theta)/A_0$	$A_y(\theta)$	$A_y(\theta)\sigma(\theta)/A_0$
11.	Continued.			
	142		$-0.411 \pm 0.099$	$-0.294 \pm 0.148$
	150	$0.635 \pm 0.044$		
12.	45	$0.821 \pm 0.079$	$0.266 \pm 0.152$	$0.218 \pm 0.127$
	55	$0.986 \pm 0.049$	$0.348 \pm 0.124$	$0.343 \pm 0.123$
	70	$1.314 \pm 0.053$	$0.222 \pm 0.105$	$0.292 \pm 0.138$
	90	$1.350 \pm 0.040$	$-0.111 \pm 0.101$	$-0.149 \pm 0.137$
	110	$1.259 \pm 0.041$	$-0.148 \pm 0.126$	$-0.186 \pm 0.159$
	125	$0.989 \pm 0.045$	$-0.295 \pm 0.101$	$-0.292 \pm 0.101$
	140	$0.747 \pm 0.042$	$-0.313 \pm 0.138$	$-0.233 \pm 0.104$
	150	$0.566 \pm 0.042$		
13.	30	$0.559 \pm 0.123$		
	40	$0.713 \pm 0.074$		
	55	$1.204 \pm 0.080$		
	70	$1.103 \pm 0.121$		
	90	$1.354 \pm 0.050$		
	110	$1.213 \pm 0.090$	$-0.287 \pm 0.073$	$-0.348 \pm 0.093$
	125	$1.080 \pm 0.062$	$-0.253 \pm 0.118$	$-0.274 \pm 0.129$
	140	$0.566 \pm 0.048$		
	150	$0.675 \pm 0.062$		

Table B-2 Unconstrained cross section and analyzing power angular distribution coefficients for the  $^{13}\text{C}(n,\gamma_0)^{14}\text{C}$  reaction, with  $k_{\text{max}} = 3$ . Also shown are the fore-aft asymmetry and the  $90^\circ$  analyzing power determined from the Legendre coefficients. The uncertainties represent one standard deviation of the statistical error.

$E_n$ (MeV)	Legendre Coefficients		$\chi_n^2$
7.75	$a_1$	$-0.041 \pm 0.027$	0.90
	$a_2$	$-0.179 \pm 0.041$	
	$a_3$	$-0.069 \pm 0.054$	
	$b_1$	$-0.012 \pm 0.048$	0.02
	$b_2$	$0.340 \pm 0.025$	
	$b_3$	$0.031 \pm 0.028$	
	$a_s$	$0.003 \pm 0.017$	
	$A_y(90^\circ)$	$-0.062 \pm 0.071$	

Table B-2 Continued.

$E_n$ (MeV)	Legendre Coefficients	$\chi_n^2$	
9.2	$a_1$	$-0.001 \pm 0.031$	1.04
	$a_2$	$-0.598 \pm 0.045$	
	$a_3$	$0.012 \pm 0.062$	
	$b_1$	$-0.127 \pm 0.051$	0.93
	$b_2$	$0.203 \pm 0.042$	
	$b_3$	$0.052 \pm 0.039$	
	$a_s$	$-0.006 \pm 0.020$	
	$A_y (90^\circ)$	$-0.163 \pm 0.055$	
10.0	$a_1$	$0.020 \pm 0.069$	1.35
	$a_2$	$-0.396 \pm 0.075$	
	$a_3$	$-0.062 \pm 0.117$	
	$b_1$	$-0.103 \pm 0.082$	0.97
	$b_2$	$0.284 \pm 0.065$	
	$b_3$	$0.113 \pm 0.063$	
	$a_s$	$0.036 \pm 0.024$	
	$A_y (90^\circ)$	$-0.234 \pm 0.102$	

Table B-2 Continued.

$E_n$ (MeV)	Legendre Coefficients	$\chi_n^2$	
10.2	$a_1$	$-0.082 \pm 0.024$	2.40
	$a_2$	$-0.610 \pm 0.038$	
	$a_3$	$0.167 \pm 0.052$	
	$b_1$	$-0.233 \pm 0.049$	1.10
	$b_2$	$0.217 \pm 0.036$	
	$b_3$	$0.013 \pm 0.036$	
	$a_s$	$-0.112 \pm 0.022$	
	$A_y(90^\circ)$	$-0.198 \pm 0.057$	
11.	$a_1$	$0.003 \pm 0.029$	0.72
	$a_2$	$-0.654 \pm 0.042$	
	$a_3$	$-0.058 \pm 0.057$	
	$b_1$	$0.047 \pm 0.038$	0.85
	$b_2$	$0.206 \pm 0.030$	
	$b_3$	$-0.002 \pm 0.033$	
	$a_s$	$0.024 \pm 0.024$	
	$A_y(90^\circ)$	$0.033 \pm 0.041$	

Table B-2 Continued.

$E_n$ (MeV)	Legendre Coefficients	$\chi_n^2$	
12.	$a_1$	$-0.039 \pm 0.055$	0.62
	$a_2$	$-0.756 \pm 0.082$	
	$a_3$	$-0.043 \pm 0.079$	
	$b_1$	$-0.007 \pm 0.060$	0.61
	$b_2$	$0.198 \pm 0.037$	
	$b_3$	$0.018 \pm 0.040$	
	$a_s$	$-0.006 \pm 0.024$	
		$A_y(90^\circ)$	$-0.030 \pm 0.070$
13.	$a_1$	$0.025 \pm 0.041$	4.38
	$a_2$	$-0.723 \pm 0.061$	
	$a_3$	$-0.089 \pm 0.091$	
	$b_1$	$-0.107 \pm 0.097$	0.71
	$b_2^*$	$0.200 \pm 0.040$	
	$b_3^*$	$0.010 \pm 0.025$	
	$a_s$	$0.048 \pm 0.038$	
		$A_y(90^\circ)$	

\* fixed - see text.

Table B-3 Constrained cross section and analyzing power angular distribution coefficients for the  $^{13}\text{C}(n, \gamma_0)^{14}\text{C}$  reaction, with  $k_{\text{max}} = 3$ . Also shown are the fore-aft asymmetry and the  $90^\circ$  analyzing power determined from the Legendre coefficients. The uncertainties represent one standard deviation of the statistical error. The method of constraint is discussed in §4-3.

$E_n$ (MeV)	Legendre Coefficients	$\chi^2_n$	
7.75	$a_1$	$-0.041 \pm 0.027$	0.90
	$a_2$	$-0.179 \pm 0.041$	
	$a_3$	$-0.069 \pm 0.054$	
	$b_1$	$0.025 \pm 0.035$	0.21
	$b_2$	$0.340 \pm 0.025$	
	$b_3$	$0.010 \pm 0.021$	
	$a_s$	$0.003 \pm 0.017$	
	$A_y(90^\circ)$	$0.009 \pm 0.045$	

Table B-3 Continued.

$E_n$ (MeV)	Legendre Coefficients		$\chi_n^2$
9.2	$a_1$	$-0.001 \pm 0.031$	1.04
	$a_2$	$-0.598 \pm 0.045$	
	$a_3$	$0.012 \pm 0.062$	
	$b_1$	$-0.128 \pm 0.047$	0.70
	$b_2$	$0.203 \pm 0.042$	
	$b_3$	$0.054 \pm 0.034$	
	$a_s$	$-0.006 \pm 0.020$	
	$A_y(90^\circ)$	$-0.161 \pm 0.040$	
10.0	$a_1$	$0.020 \pm 0.069$	1.35
	$a_2$	$-0.396 \pm 0.075$	
	$a_3$	$-0.062 \pm 0.117$	
	$b_1$	$-0.066 \pm 0.067$	0.85
	$b_2$	$0.278 \pm 0.065$	
	$b_3$	$0.079 \pm 0.047$	
	$a_s$	$0.036 \pm 0.024$	
	$A_y(90^\circ)$	$-0.154 \pm 0.044$	

Table B-3 Continued.

$E_n$ (MeV)	Legendre Coefficients		$\chi_n^2$
10.2	$a_1$	$-0.074 \pm 0.023$	2.19
	$a_2$	$-0.611 \pm 0.038$	
	$a_3$	$0.135 \pm 0.046$	
	$b_1$	$-0.224 \pm 0.042$	0.89
	$b_2$	$0.218 \pm 0.036$	
	$b_3$	$0.006 \pm 0.030$	
	$a_s$	$-0.095 \pm 0.017$	
	$A_y(90^\circ)$	$-0.178 \pm 0.040$	
11.	$a_1$	$0.001 \pm 0.027$	0.58
	$a_2$	$-0.654 \pm 0.042$	
	$a_3$	$-0.051 \pm 0.047$	
	$b_1$	$0.047 \pm 0.038$	0.85
	$b_2$	$0.206 \pm 0.030$	
	$b_3$	$0.002 \pm 0.033$	
	$a_s$	$0.020 \pm 0.016$	
	$A_y(90^\circ)$	$0.038 \pm 0.040$	



Table B-3 Continued.

$E_n$ (MeV)	Legendre Coefficients		$\chi_n^2$
12.	$a_1$	$-0.050 \pm 0.053$	0.54
	$a_2$	$-0.763 \pm 0.081$	
	$a_3$	$-0.031 \pm 0.077$	
	$b_1$	$-0.015 \pm 0.050$	0.49
	$b_2$	$0.199 \pm 0.037$	
	$b_3$	$0.023 \pm 0.033$	
	$a_s$	$-0.017 \pm 0.016$	
	$A_y(90^\circ)$	$-0.036 \pm 0.051$	
13.	$a_1$	$-0.005 \pm 0.039$	4.11
	$a_2$	$-0.722 \pm 0.062$	
	$a_3$	$0.032 \pm 0.073$	
	$b_1$	$-0.055 \pm 0.095$	2.62
	$b_2$	$0.200 \pm 0.040$	
	$b_3$	$-0.059 \pm 0.076$	
	$a_s$	$-0.015 \pm 0.024$	
	$A_y(90^\circ)$	$0.025 \pm 0.056$	

## C Transition Matrix Element Analysis

Table C-1 E1 solutions for the  $^{13}\text{C}(\vec{n}, \gamma_0)^{14}\text{C}$  reaction. The quadratic nature of the E1 equations resulted in two solutions for each energy. The cross sections are defined as:

$$\sigma(s_{1/2}) = |s_{1/2}|^2$$

$$\sigma(d_{3/2}) = 2 |d_{3/2}|^2.$$

$E_n$ (MeV)	$\sigma(s_{1/2})$ (%)	$\sigma(d_{3/2})$ (%)	$\varphi_d - \varphi_s$ (deg)
7.75	38.8 ± 11.4	61.2 ± 11.6	-103 ± 6
	65.7 ± 11.4	34.3 ± 11.2	-92 ± 6
9.20	10.1 ± 4.4	89.9 ± 4.8	-69 ± 6
	74.3 ± 5.5	25.7 ± 5.1	-40 ± 7
10.00	15.5 ± 7.4	84.5 ± 7.8	-93 ± 10
	78.0 ± 8.6	22.0 ± 8.1	-61 ± 9
10.20	15.8 ± 5.7	84.2 ± 6.0	-69 ± 4
	68.3 ± 6.4	31.7 ± 6.3	-47 ± 6
11.00	12.4 ± 4.1	87.6 ± 4.6	-63 ± 5
	69.8 ± 5.5	30.2 ± 5.0	-40 ± 5
12.00	12.6 ± 4.9	87.4 ± 5.4	-55 ± 6
	67.0 ± 6.3	33.0 ± 5.9	-35 ± 6
13.00	14.7 ± 7.2	85.3 ± 8.1	-53 ± 10
	66.0 ± 9.7	34.0 ± 8.9	-37 ± 7

Table C-2 E1-E2 solutions for the  $^{13}\text{C}(\vec{n}, \gamma_0)^{14}\text{C}$  reaction. Two E1 amplitudes, the  $f_{5/2}$  E2 amplitude and two relative phases were fit. The cross sections are defined as:

$$\sigma(s_{1/2}) = |s_{1/2}|^2$$

$$\sigma(d_{3/2}) = 2 |d_{3/2}|^2$$

$$\sigma(f_{5/2}) = 3 |f_{5/2}|^2.$$

$E_n$ (MeV)	$\sigma(s_{1/2})$ (%)	$\sigma(d_{3/2})$ (%)	$\varphi_d - \varphi_s$ (deg)	$\sigma(f_{5/2})$ (%)	$\varphi_f - \varphi_s$ (deg)	$\chi_n^2$
7.75	40.48 $\pm$ 11.90	59.37 $\pm$ 12.22	-102 $\pm$ 6	0.15 $\pm$ 0.22	10 $\pm$ 17	0.7
9.20	12.06 $\pm$ 4.03	87.04 $\pm$ 4.42	-62 $\pm$ 7	0.90 $\pm$ 0.86	208 $\pm$ 8	0.9
10.00	13.55 $\pm$ 7.38	86.06 $\pm$ 7.49	-104 $\pm$ 11	0.39 $\pm$ 1.19	183 $\pm$ 17	1.3
10.20	11.69 $\pm$ 4.77	85.15 $\pm$ 5.26	-63 $\pm$ 5	3.17 $\pm$ 1.45	197 $\pm$ 7	1.7
11.00	9.73 $\pm$ 4.14	90.11 $\pm$ 4.69	-67 $\pm$ 5	0.15 $\pm$ 0.22	16 $\pm$ 18	0.7
12.00	19.74 $\pm$ 5.23	80.20 $\pm$ 5.92	-43 $\pm$ 7	0.06 $\pm$ 0.03	190 $\pm$ 86	0.6
13.00	13.74 $\pm$ 6.61	86.13 $\pm$ 7.53	-55 $\pm$ 10	0.14 $\pm$ 0.54	211 $\pm$ 29	3.9

Table C-3 E1-E2-M1 solutions for the  $^{13}\text{C}(\vec{n}, \gamma_0)^{14}\text{C}$  reaction. Two E1 amplitudes, the  $f_{5/2}$  E2 amplitude and two relative phases were fit. The  $p'_{3/2}$  M1 complex matrix element was held constant to the value determined at each energy by the direct-semidirect model calculation of Chapter 7. The cross sections are defined as:

$$\begin{aligned}\sigma(s_{1/2}) &= |s_{1/2}|^2 \\ \sigma(d_{3/2}) &= 2 |d_{3/2}|^2 \\ \sigma(f_{5/2}) &= 3 |f_{5/2}|^2 \\ \sigma(p'_{3/2}) &= 2 |p'_{3/2}|^2.\end{aligned}$$

---

$E_n$ (MeV)	$\sigma(s_{1/2})$ (%)	$\sigma(d_{3/2})$ (%)	$\varphi_d - \varphi_s$ (deg)	$\sigma(f_{5/2})$ (%)	$\varphi_f - \varphi_s$ (deg)	$\sigma(p'_{3/2})$ (%)	$\varphi_p - \varphi_s$ (deg)	$\chi_n^2$
7.75	39.43±10.13	60.08±10.48	-102±6	0.30±0.33	30±18	0.19	63	0.8
9.20	16.90±8.00	75.44±8.00	-66±5	0.45±0.17	103±46	7.21	121	1.2
10.00	13.60±5.72	81.00±6.38	-107±10	1.46±1.39	-1±15	2.78	139	1.2
10.20	11.60±5.56	85.94±5.92	-63±5	0.13±0.24	138±42	2.33	179	2.1
11.00	9.48±4.23	89.81±4.79	-66±5	0.62±0.43	19±11	0.10	192	0.7
12.00	20.03±7.00	79.91±7.00	-43±10	0.03±0.21	154±99	0.03	177	0.6
13.00	13.72±6.61	86.20±7.52	-55±10	0.07±0.38	208±44	0.02	172	3.9

---

## D Comparison to Theory

Table D-1 Direct-Semidirect Model Parameters used to fit the  
 $^{13}\text{C}(\vec{n}, \gamma_0) ^{14}\text{C}$  data.

Continuum Wave Function:

Real Well:

$$V = 60.0 + 27 \frac{N-Z}{A} - 0.3 E_{\text{c.m.}} \text{ MeV}$$

$$r = 1.14 \text{ fm}$$

$$a = 0.57 \text{ fm}$$

Imaginary Surface:

$$W_s = W_s(E) + 10 \frac{N-Z}{A} \text{ MeV}$$

$$W_s(E) = \begin{cases} 0.64 E_{\text{c.m.}}; & E_{\text{c.m.}} \leq 13.8 \text{ MeV} \\ 9.60 - 0.06 E_{\text{c.m.}}; & E_{\text{c.m.}} > 13.8 \text{ MeV} \end{cases}$$

$$r = 1.14 \text{ fm}$$

$$a = 0.50 \text{ fm}$$

Spin Orbit:

$$V_{\text{so}} = 5.5 \text{ MeV}$$

$$r = 1.14 \text{ fm}$$

$$a = 0.57 \text{ fm}$$

Coulomb Radius:

$$r_c = 1.14 \text{ fm}$$

Table D-1 Continued.

---

 Bound State Wave Function:

$$V = 53.1 \text{ MeV at } E_n = 11.0 \text{ MeV}$$

$$E_B = -8.1766 \text{ MeV}$$

$$r = 1.14 \text{ fm}$$

$$a = 0.57 \text{ fm}$$

$$V_{so} = 5.5 \text{ MeV}$$

$$C^2 S = 1.7336 \text{ (Spectroscopic Factor)}$$

## Effective Charges:

$$\epsilon_1 = \frac{-Z_t}{1 + A_t} = -0.429$$

$$\epsilon_2 = \frac{Z_t}{(1 + A_t)^2} = 0.0306$$

## Semidirect Form Factors:

## Electric Dipole:

## Isovector Volume Coupling Form Factor:

$$V = 68 \text{ MeV}$$

$$r = 1.14 \text{ fm}$$

$$a = 0.57 \text{ fm}$$

## Resonance:

Position:	15.45 MeV	17.85 MeV
-----------	-----------	-----------

Width:	1.50 MeV	1.75 MeV
--------	----------	----------

Strength:	0.26 Sum Rule	0.25 Sum Rule
-----------	---------------	---------------

---

Table D-1 Continued.

-----  
Semidirect Form Factors (continued):

## Electric Quadrupole:

## Isoscalar Surface Coupling Form Factor:

$$V = 53 \text{ MeV}$$

$$r = 1.14 \text{ fm}$$

$$a = 0.57 \text{ fm}$$

## Resonance:

$$\text{Position: } 20.0 \text{ MeV}$$

$$\text{Width: } 4.0 \text{ MeV}$$

$$\text{Strength: } 0.4 \text{ Sum Rule}$$

## Magnetic Dipole:

## Isovector Volume Coupling Form Factor:

$$V = 40 \text{ MeV}$$

$$r = 1.14 \text{ fm}$$

$$a = 0.57 \text{ fm}$$

## Resonance:

$$\text{Position: } 16.70 \text{ MeV} \qquad 17.50 \text{ MeV}$$

$$\text{Width: } 0.20 \text{ MeV} \qquad 0.20 \text{ MeV}$$

$$\text{Strength: } 0.24 \mu_0^2 \qquad 0.17 \mu_0^2$$
  
-----

## E Polarized Ion Source Microprocessor

The following pages have been extracted from the instruction manual for the polarized ion source. They contain the operating instructions for the microprocessor based interlock and control system. Primary responsibility for the design, construction, and installation of the system rested with the author of this thesis.



## OVERVIEW

The Polarized Ion Source Microprocessor is a Vector Graphics brand Z-80 based computer running with the CP/M operating system. CP/M is used to edit, compile, and load the SENSE program from disk and begin its execution. Once put into operation, the SENSE program monitors the condition of the source by interrogating various sensors located on the high and low voltage frames, and turns devices on or off if dangerous conditions arise or if previous fault conditions have become cleared. SENSE provides the user with information about the status of the source and about operations that it has performed. SENSE also provides an extensive set of commands with which the user may request information and alter the condition of the source. The user may enter commands at the microprocessor console itself or at any VAX terminal by using the XSYS program XPIS. Output information is displayed on the microprocessor console and on standard TV monitors connected to the video output of the console. No information is displayed on the user's VAX terminal when running the XPIS program (except under certain error conditions during spin flip or quench commands) but SENSE does communicate with the XPIS program itself to indicate normal completion or error completion.

## STARTUP PROCEDURE

To run the SENSE program perform the following operations:

- 1 - Insert the floppy disk containing the program into the slot in the right hand disk drive and load it by pushing the plastic lever to the right. Orient the the disk with the label toward the front and on the left.
- 2 - Push the RESET button on the front of the computer.
- 3 - Type B in response to the MON> prompt. This (B)oots the CP/M operating system.
- 4 - Type SENSE<CR> in response to the A> prompt. This loads and begins execution of the SENSE program.
- 5 - After the SENSE program has been loaded (about 10 seconds), unload the disk by pushing the lever to the right and letting it spring back to the left. Leave the floppy disk in the slot. It is bad for the disk to leave it in the loaded position for extended periods of time.
- 6 - Type SET mm/dd hh:mm:ss to set the real time clock.
- 7 - Check the sense panels and relay boxes on the high and low voltage frames to be sure the source is in a safe condition. When the light next to the power switch on either relay box is on, it means the microprocessor has control of the devices attached to that box. The switch can be used to disable microprocessor control.

## COMMANDS

The following is an alphabetical list of the commands understood by the SENSE program. The last (or only) keyword appearing on a command line may be abbreviated to as little as 3 letters. Separate all subcommands from the main commands by a space.

### IGNORE

The IGNORE command tells the microprocessor to ignore the condition of the physical sense lines. The microprocessor will not respond to changes in the ignored sense lines and will use the status information contained in the sense line status table to determine what actions to perform.

Subcommand:

- ALL - Ignore all of the sense lines.
- HIGH - Ignore the high voltage sense lines.
- LOW - Ignore the low voltage sense lines.

### INITIALIZE

The INITIALIZE command clears the sense line status table, the wait table, and the control line status table. In addition, all devices are turned "on".

### MONITOR

The MONITOR command causes SENSE to return to the CP/M monitor.

### QUENCH and UNQUENCH

Quenching of the polarized source beam is controlled by a standard control line (named QUN) and may be altered using any of the control line commands listed below. The QUENCH and UNQUENCH commands provide a more convenient notation for the operation. In addition, a message is sent to the VAX after the command has been performed indicating success or failure of the operation. Any VAX program using this command should wait for the beam to stabilize before proceeding.

### SET

The SET command sets the real time clock. The "/" and ":" need not be typed, but each numerical field must be separated by one character.

Subcommand:

- mm/dd hh:mm:ss - The current time.

### SPIN

The spin direction on the polarized source is controlled by a standard control line (named SPN) and may be altered using any of

the control line commands listed below. The SPIN command is provided to allow the spin to be "flipped" as well as being set to UP or DOWN. In addition, a message is sent to the VAX after the SPIN command has been performed indicating success or failure of the operation. Any VAX program using this command should wait for the beam to stabilize before proceeding.

Subcommand:

UP - Set spin direction to up.  
 DOWN - Set spin direction to down.  
 FLIP - Flip spin direction.  
 STATUS - Report spin direction.

### SST

The SST command causes the status of all sense lines included in the short status list to be output.

### STATUS

The STATUS command causes the microprocessor to output the status of the requested sense and/or control lines. A header is typed to label the various pieces of information.

Subcommand:

SENSE - All allocated sense lines.  
 CONTROL - All allocated control lines.  
 HSENSE - All allocated high voltage sense lines.  
 LSENSE - All allocated low voltage sense lines.  
 HCONTROL - All allocated high voltage control lines.  
 LCONTROL - All allocated low voltage control lines.  
 ALL - All sense lines and control lines including spares.

### TEST

The TEST command alters or reports the status of the sense/control line testing mechanism.

Subcommand:

ON - Turn testing on.  
 OFF - Turn testing off.  
 STATUS - Report whether testing is on or off.

### TIME

The TIME command causes the real time clock to be printed, including the month and day.

### SENSE LINE COMMANDS

The following subcommands are used to alter or report information in the sense line status table. See below for a discussion of this table. These subcommands are entered by typing the 3 letter abbreviation for the sense line followed by the subcommand. The

list of currently defined sense lines and their abbreviations is output by the STATUS ALL command.

Subcommand:

- FAULT - Set the line status to always fault.
- GOOD - Set the line status to always good.
- OPEN - Set the line status to always open.
- CLOSED - Set the line status to always closed.
- ON - Set the line status to always on.
- OFF - Set the line status to always off.
- STATUS - Report the sense line status.
- NORMAL - Restore the sense line to normal operation (no override).
- SST - Enter the sense line into the short status list.
- NOSST - Remove the sense line from the short status list.
- RESET - Perform a manual reset for the sense line.

#### CONTROL LINE COMMANDS

The following subcommands are used to alter or report information in the control line status table or to alter the state of a control line. See below for a discussion of the control line status table. These subcommands are entered by typing the 3 letter abbreviation for the control line followed by the subcommand. The list of currently defined control lines and their abbreviations is output by the STATUS ALL command.

Subcommand:

- FAULT - Set the line status to fault.
- GOOD - Set the line status to good.
- OPEN - Set the line status to open.
- CLOSED - Set the line status to closed.
- ON - Set the line status to on.
- OFF - Set the line status to off.
- UP - Set the line status to up.
- DOWN - Set the line status to down.
- STATUS - Report the control line status.
- NORMAL - Restore the control line to normal operation (no override).
- (ALWAYS) - Insert this subcommand between the control line abbreviation and one of the subcommands listed above (except STATUS and NORMAL). This causes the control line to be manually overridden and always have the indicated status.

The following commands exist in the SENSE program but do not function because the necessary hardware has not been installed.

**ALARM**

The ALARM command performs a simple alarm clock function. When the set time has arrived, the terminal will start beeping. A carriage return typed on the terminal will stop the beeping.

## Subcommand:

- SET hh:mm - Set the time.
- TIME - Print the alarm time if it has been set, else print a message.
- OFF - Turn alarm off.

**BEEP**

The BEEP command alters or reports the status of the message beep mechanism. Certain important unsolicited messages appearing on the terminal will be accompanied by "bells" being sent to the terminal until the operator types a carriage return to acknowledge reading the message.

## Subcommand:

- ON - Turn message beeping on.
- OFF - Turn message beeping off.
- STATUS - Report status of message beeping.

**DVM**

The DVM command is used to read the voltage present on one of the channels of the digital volt meter on the high voltage frame.

## Subcommand:

- xx - a channel number in the range 0 to 31.

## OVERVIEW OF THE SENSE SOFTWARE

The philosophy of the SENSE software is similar to that of the XSYSTEM. There is a collection of more or less independent subroutines operating on a common data base. The microprocessor is a single user machine running only one program organized into separate subroutines while the XSYSTEM is a multiuser machine running separate programs simultaneously. The main program of SENSE is an endless loop that checks for the completion of an input command from the user and calls subroutines periodically to monitor sense line inputs.

### SEQUENCES

The sense and control line action sequences are the heart of the SENSE program. All of the logic needed to decide the actions that are necessary in response to external conditions is contained in the sequences. The program is very general and does not need to be changed in order to make large changes in the way the microprocessor responds to events occurring on the source.

The sequences are contained in the assembly language common block SEQUEN. The sequences are not really in assembly language, rather the assembler provides a convenient notation for encoding the sequences. The EQU assembler directive is used to equate the 3 letter abbreviation for a sense or control line with its number (1-40). The DB (define byte) assembler directive is used to place the sequences of sense or control line numbers into memory.

Each sense line has two sequences, a "fault" sequence and a "good" sequence. The fault sequence contains a list of the control lines, in order, to be turned "off" if a fault occurs on the sense line. If a control line is to be turned "on" during a fault condition then the control line symbol is entered as a negative number. Turning a valve "off" means to close the valve, "on" means to open the valve. The adjective to be used in describing the operations of a control line is determined by its entry in the BCTEXT table. The operations to be performed when a sense line returns to the good condition are not necessarily the inverse of the operations performed during the execution of the fault sequence, therefore a separate "good" sequence is provided for each line. The good sequence contains a list of the devices to be turned on, with negative numbers indicating turn the device off. The sequences are of variable length and are terminated by the SQEND command. If two lines are to use the same sequence then the sequence for the second line can be defined with the EQU directive. A line with no sequence can be EQU'd to NONE. An example of a simple set of sequences is:

```

FP3F:   DB      -AUD,FV4,DP5,GV5,SQEND
FP3G:   DB      -AUD,FV4,SQEND
FP4F:   EQU     FP3F
FP4G:   EQU     FP4F
FP5F:   EQU     NONE
FP5G:   EQU     NONE

```

Additional capabilities are provided for the sequences by the sequence commands SQCOR,SQRPT,SQMAN, and WAIT#. SQMAN is used to suspend execution of a sequence until the user issues a reset command at the terminal. When the reset command is given, execution of the sequence continues with the sequence elements following SQMAN. The WAIT# command (for # between 1 and 6) provides a means of delaying execution of a sequence. The sequence element following the WAIT# command is the duration of the waiting time in minutes. A negative number for the time indicates seconds. Up to 6 wait operations (WAIT1 through WAIT6) may be encoded in a sequence. During the waiting time, the status of the sense line is not examined. If at the end of the wait the status of the sense line is unchanged, execution of the sequence continues with the sequence elements after the wait command. If the status of the sense line changes during the wait, then the sequence is reexecuted from the beginning in the opposite sense. That is, if the WAIT# command is used in a fault sequence, devices that were turned off by the execution of the sequence up to the point of the WAIT# command are turned back on. WAIT# commands occurring before the one that was just executed are ignored during the reexecution of the sequence.

One might imagine conditions under which a sense line would repeatedly change status during a waiting period. For example, close a valve and the vacuum gets good, reopen the valve and the vacuum gets bad again. Inserting a SQRPT command into a sequence immediately after a WAIT# command sets a limit on the number of times a sequence may be reexecuted. The maximum number of executions is inserted after the SQRPT command itself. Each time the status of a sense line changes during a wait period, the corresponding entry in the array SREP is incremented. If the maximum count is reached, the logical status of the line is set to fault and the line is no longer monitored. SREP is cleared any time the status does not change during the wait period or by the RESET or NORMAL subcommands of the sense line commands. For example the sequence:

```

FP1G:   DB      -AUD,WAIT1,-15,FV1,WAIT2,3,SQRPT,5,DP1,DP2,SQEND

```

means that if sense line FP1 returns to "good" after having been "fault", then turn off control line AUD, wait 15 seconds, turn on line FV1 and wait 3 minutes. If at the end of three minutes FP1 still indicates "good", then turn on DP1 and DP2 and clear the element of the array SREP corresponding to sense line FP1. If, on the other hand, FP1 now indicates "fault", then turn AUD on and FV1 off and increment the element of SREP. If the element of SREP now is equal to 5, then set the status of sense line FP1 to permanently "fault".

The SQCOR command allows the status of sense lines to be correlated

with one another in order to determine the proper response. The command is entered into a sequence by entering the command SQCOR, the number of sense lines to be examined, the names of the sense lines to examine, then the sequence elements (control lines and commands) to be executed if the correlation condition is met. The sense lines named in the command must all be "fault" in order to have a correlation, unless a sense line name appears as a negative number in which case the line must be "good". If the condition is not met, then the sequence elements which follow the SQCOR command are not executed until another SQCOR command is found or the end of the sequence is reached. The SQCOR's are therefore not nested, but are checked sequentially. Zero may be used for the number of sense lines if it is desired to have an unconditionally executed action list occur after a conditional one. Care should be used in coding WAIT statements into the action list of a SEQCOR command. It is possible, in principle, for the sense lines named in the correlation list to change during the waiting time and therefore remove the correlation. The SENSE program has no way to know if that has occurred and so the assumption is made that the other lines do not change, that is, the status at the time the sequence is being reexecuted is assumed to be the same as when the sequence was initially executed. This assumption is almost always valid for the current operating setup and in any case would not cause dangerous conditions to arise because of the constant monitoring of all sense lines. In the following simple example assume D3T and D4T are sense lines and DP3,DP4, and FRV are control lines:

```
D3TF:    DB      DP3,SQCOR,1,D4T,FRV,SQEND
D3TG:    DB      DP3,SQEND
D4TF:    DB      DP4,SQCOR,1,D3T,FRV,SQEND
D4TG:    DB      DP4,SQCOR,1,D3T,FRV,SQEND
```

If D3T or D4T indicates a fault then the corresponding DP line is turned off, but if both sense lines indicate a fault then FRV is also turned off. If D4T returns to the good condition after D3T then FRV will be turned back on, but if D4T returns to good first then FRV will not be turned back on. The use of asymmetric correlation conditions illustrated by the "good" sequences above allows time ordering of events on the source to be considered when deciding the proper response. By combining multiple SQCOR and WAIT# commands, almost any function relating sense lines to control lines can be implemented.

Control line sequences list the sense lines that should be examined before turning a device on or off. Sense lines appearing in the "on" sequence must all be "good" (unless entered as a negative number, in which case it must be fault) before the device will be turned "on". Likewise, the "off" sequence lists sense lines that must be "fault". The control sequences are checked any time a control line is to be altered, whether in response to an event on the source or to an input command. If the operator desires to override the checking, the ALWAYS option of the control line command must be used.



## DESCRIPTION OF THE PROGRAM

When the program begins execution, the main program SENSE performs various startup procedures - enables the real time clock interrupt, passes variable addresses to assembly language subroutines, clears all sense line tables to indicate no faults, and initializes variables. It then enters an endless loop that checks for the completion of an input command and then branches to one of two subroutines, SSENSE or INPUT. If no command has been entered then SSENSE is called. This subroutine examines all of the sense lines in numerical order, determines if any have changed state and if so performs the assigned fault or good sequence. If an input command has been typed (signified by IDONE nonzero) then the subroutine INPUT is called. INPUT decodes and executes the input command, calling most of the other subroutines in the process.

The Vector Graphics contains an internal 55.5 Hz clock which causes an interrupt to assembly language subroutine CLKINT 55 times a second. CLKINT maintains an internal counter which counts up to 55 and then generates a call to the calendar and clock subroutine INTER. Thus, roughly once per second the time is updated. The time is written onto the microprocessor console in the lower right corner through a series of POKES into the memory mapped display. To maintain chronological accuracy, 24 seconds are added to the clock every hour to compensate for the half-Hertz clock error. INTER also performs a test on one sense/control line pair by enabling a hardware connection between the control line output and the sense line input, blipping the control line status, and verifying that the sense line has also blipped. The test is done rapidly enough so that the control relays do not actually change state during the test. Thus, one sense/control pair is tested every second. In this manner all sense and control lines are tested every 40 seconds.

Keyboard entries are interpreted via this same clock interrupt structure. After incrementing its internal 55Hz counter, CLKINT checks the status of the flashwriter input port to see if a character has been typed within the last clock interrupt cycle. If so, it picks up the character and puts it into the array ILINE (whose address was previously passed by the call to ENABLE). If the character was a carriage return, IDONE is set as a flag to the main program that a completed command line has been input. Besides checking the flashwriter keyboard, CLKINT checks for any input on serial port C (which is connected to a dedicated VAX terminal port) and strings these characters into ILINE along with the flashwriter input. Thus either device can input a command line. Note that as the keyboard and serial port C are checked only 55 times a second, data must be input slower than this (about 30 chars per second seems to work well). It does not matter what the VAX baud rate is; but the VAX must slow down its data output to less than 30 chars per second or data will be lost.

The SSENSE subroutine performs a DO loop which picks up the current status of each sense line via a call to PSSTAT and compares it with the status read during the last cycle saved in BSSTAT. If BSSTAT is good but the line is now fault, a subloop is entered which examines the sense line several times in succession (currently six times) for noise immunity. This is necessary since a tank or frame spark can glitch the sense lines momentarily. If the sense line shows a hard fault, the fault sequence for the sense line is activated by calling EXSEQ. If the examination of a sense line shows it to have become good, EXSEQ is called to execute the SGOOD sequence. SSENSE also checks each line to see if a wait operation just has been completed for the line, and whether the status changed or not during the wait.

The sense line status table, BSSTAT, contains six fields. The first bit indicates the status of the line the last time it was examined. The second bit indicates whether or not the physical status of the sense line should be examined. If the second bit is set, the hardware line will be ignored and the first bit in the status table will be used to determine the condition of the sense line. The third bit indicates whether or not a reset command has been issued for the sense line. The bit is cleared when the reset has been performed. The fourth bit indicates the condition of the sense/control test loop for the sense/control line pair. The fifth bit indicates whether or not the sense line is to be included in the short status list. The short status list exists to allow lines that are judged likely to change status to be easily examined by the operator. The last three bits in BSSTAT are used to process wait operations. If all three bits are zero then no wait operation is related to this line. If all three bits are one then a wait operation is currently in progress. Otherwise the last three bits represent the number of a WAIT# command that has just been completed. The control line status table, BCSTAT, contains only one field. The last bit indicates whether or not the line is under manual control. Lines under manual control will not be altered in response to a status change on the source or to a type in command. They can only be changed by using the ALWAYS subcommand of the control line commands or by returning the line to NORMAL operation.

Wait operations needed during the execution of a sense line sequence are performed by the WAIT subroutine. It is not practical for the program to actually halt during the wait time because it would then be unable to respond to other commands or failures. Therefore the WAIT subroutine simply enters the wait time and the sense line number into the global arrays WTIME and WLINE. WTIME is then decremented by the real time interrupt routine INTER until it reaches zero. When this occurs the sense line status table is altered by the interrupt routine to indicate that the wait has been completed. SSENSE will note the change in the sense line status table on its next loop through the sense lines.

## SUBROUTINE DESCRIPTIONS

## CLKINT

Assembly language interrupt handler for the real time clock interrupts. CLKINT calls INTER to perform the required actions.

## DCADJ

DOUBLE PRECISION FUNCTION DCADJ(II,ONOFF,NORREV)

Return proper adjective to describe the state of a control line.

## Input:

II = Number of the sense line  
 ONOFF = ON -> Return the "on" adjective  
       = OFF -> Return the "off" adjective  
 NORREV < 0 -> Return the opposite adjective  
        > 0 -> Return the normal adjective

## Output:

The value of the function will be an 8 character string containing the proper adjective.

## DSADJ

DOUBLE PRECISION FUNCTION DSADJ(II,FAGO,NORREV)

Return proper adjective to describe the state of a sense line.

## Input:

II = Number of the sense line  
 FAGO = FAULT -> Return the "fault" adjective  
       = GOOD -> Return the "good" adjective  
 NORREV < 0 -> Return the opposite adjective  
        > 0 -> Return the normal adjective

## Output:

The value of the function will be an 8 character string containing the proper adjective.

## DVM

SUBROUTINE DVM(NUM)

Read high voltage frame dvm.

## Input:

NUM = Channel number (1-32)

## ENABLE

SUBROUTINE ENABLE(ARRAY,FLAG)

## Input:

ARRAY = LOGICAL\*1 input buffer for type in commands  
 FLAG = LOGICAL\*1 flag to use to signal completion of input

## EXCSEQ

```
SUBROUTINE EXCSEQ(II,ONOFF,ALWAYS,WASOK)
```

```
Execute a control inhibit sequence.
```

## Input:

```
II      = # of control line whose inhibit sequence is to be executed
        < 0 -> Perform opposite operation to that specified by ONOFF
ONOFF   = ON  -> Turn device "on"
        = OFF -> Turn device "off"
ALWAYS  = 0   -> Execute sequence, turn device on or off if allowed
        <> 0 -> Ignore sequence and turn device on or off
```

## Output:

```
WASOK   = Device was successfully turned on or off
```

## Local:

```
ITEM    = Item in control inhibit sequence
ISEQ    = pointer to sequence
```

## EXSEQ

```
SUBROUTINE EXSEQ(II,FAGO,ONOFF,BWAIT)
```

```
Execute a sense line action sequence.
```

## Input:

```
II      = Number of sense line whose sequence is to be executed
FAGO    = FAULT -> Execute the "fault" sequence
        = GOOD  -> Execute the "good" sequence
ONOFF   = ON    -> Turn appropriate devices "on"
        = OFF   -> Turn appropriate devices "off"
BWAIT   > 0 -> (-BWAIT) is the code for the wait command that has
        finished where the status changed during the wait
        period
        = 0 -> No wait operation has been involved for this sense
        line
        < 0 -> BWAIT is the code for the wait command that has
        finished where the status did not change during the
        wait period
```

## Local:

```
BITEM   = Item from the control sequence being executed
ISEQ    = Pointer to an item in the control sequence
TIME    = Length of wait time
DUNIT   = Units of wait time (minutes or seconds)
NCORR   = Number of sense lines to correlate status
```

## INPUT

```
SUBROUTINE INPUT
```

```
Decode and execute terminal input commands.
```

## INTER

```
SUBROUTINE INTER
```

```
Process real time clock interrupt.
```

## PCSTAT

LOGICAL FUNCTION PCSTAT(I)

Assembler language subroutine to read the value of a control line.

Input:

II = Number of the control line to read

## PSSTAT

LOGICAL FUNCTION PSSTAT(I)

Assembler language subroutine to read the value of a sense line.

Input:

II = Number of the sense line to read

## SEQUEN

Assembly language block data common block. Holds the sense and control sequence definitions and the index pointers into the sequence table.

## SENSE

PROGRAM SENSE

Main program. Variables are initialized, then an infinite loop calling SSENSE and INPUT is entered.

## SETCNT

SUBROUTINE SETCNT(II,ONOFF)

Assembler language subroutine to set a control line.

Input:

II = Control line number

ONOFF = LOGICAL\*1 value to assign to control line

## SSENSE

SUBROUTINE SSENSE

Check sense lines and respond to changes.

Local:

BWAIT = Flag for handling waits, passed to EXSEQ.

> 0 -> (-BWAIT) is the code for the wait command that has finished where the status changed during the wait period

= 0 -> No wait operation has been involved for this sense line

< 0 -> BWAIT is the code for the wait command that has finished where the status did not change during the wait period

NUSTAT = New status of sense line

## TABLES

Fortran block data common block. Contains the name, abbreviation, and adjective descriptors of the sense and control lines.

## TSSTAT

SUBROUTINE TCSTAT(II)

Type the status of one sense line.

Input:

II = Number of the control line whose status is to be typed

## TCSTAT

SUBROUTINE TSSTAT(II)

Type the status of one sense line.

Input:

II = Number of the sense line whose status is to be typed

## WAISUB

SUBROUTINE WAISUB(TIME,DUNIT,LINE,BMASK)

Set up a wait operation using the real time clock.

Input:

TIME = Length of wait time

DUNIT = Units of wait time

LINE = Location to alter to signal completion

BMASK = Mask to use to signal completion

COMMON DATA BASE

## Global Arrays

## Sense line tables

QSABBR = R\*4 Three character abbreviated name of sense line.

QSNAME = R\*4 2D(6) Twenty four character full name of sense line.

BSSTAT = L\*1 Status of sense line.

SREP = I\*2 Number of repeats executed.

BSTEXT = L\*1 Define which adjective describes sense line status.

SFAULT = I\*2 Location of start of fault sequence in SEQUEN.

SGOOD = I\*2 Location of start of good sequence in SEQUEN.

## Control line tables

QCABBR = R\*4 Three character abbreviated name of control line.

QCNAME = R\*4 2D(6) Twenty four character full name of control line.

BCSTAT = L\*1 Status of control line.

BCTEXT = L\*1 Define which adjective describes control line status.

CON = I\*2 Location of start of on sequence in SEQUEN.

COFF = I\*2 Location of start of off sequence in SEQUEN.

SEQUEN = L\*1 Array containing all of the sequences.  
 WTIME = I\*2 Remaining wait time in seconds.  
 WLINE = I\*2 Sense line number for which the wait is being performed.  
 BWMASK = L\*1 Byte to use to signal completion of the wait.  
 ILINE = L\*1 Text of the input command.

#### Global Variables

DOTEST = L\*1 Flag to enable testing of sense/control loops.  
 ITEST = I\*2 Number of next sense/control loop to test.  
 BTESTF = L\*1 Number of sense/control loop that has just changed status.  
 IDONE = L\*1 Flag to indicate an input line is completed.  
 ALERT = L\*1 Flag to enable message beeping.  
 MBEEP = L\*1 Flag to indicate message beeper is beeping.  
 ALARM = L\*1 Flag to enable alarm beeping.  
 ABEEP = L\*1 Flag to indicate alarm beeper is beeping.

#### Global Constants

NLINES = Number of sense/control lines wired.  
 NSTLOW = Start of low voltage channels.

#### Bit masks for sense line status

FAULTM = 10000000 -> Sense line is fault.  
 IGNORM = 01000000 -> Sense line is being ignored.  
 MANM = 00100000 -> A manual reset has been given for this sense line.  
 TESTM = 00010000 -> This sense/control pair tests faulty.  
 SSTM = 00001000 -> Sense line is included in short status.  
 WAITM = 00000111 -> A wait is being performed on this sense line.

#### Bit mask for control line status

CMANM = 00000001 -> Control line is under manual control.

#### Bit masks for BSTEXT, BCTEXT tables

FAGOVM = 00000001 -> Fault/good are valid adjectives for this line.  
 OPCLVM = 00000010 -> Open/closed are valid adjectives for this line.  
 ONOFVM = 00000100 -> On/off are valid adjectives for this line.  
 UPDNVM = 00001000 -> Up/down are valid adjectives for this line.

### MODIFYING THE SOFTWARE

Modifications to the program itself will be relatively rare since most of the desired changes can be accomplished by modifying the sequences and tables. Each subroutine exists as a separate file on the disk. It is only necessary to edit and recompile the subroutines being changed. A command file, SL.SUB, exists to link subroutines and block data together. Files can be edited using the SCOPE editor. SCOPE is a full screen editor with several nice features made possible by the memory mapped display. The CP/M operating system is similar in many ways to VAX/VMS and should be easy for a VAX user to learn. There is a loose leaf notebook near the microprocessor containing manuals for all of the system software.

To define a new sense line or control line in the system only the files TABLES.FOR and SEQUEN.MAC need to be altered. The table entries for the spare line that is being redefined to an active line should be changed to the appropriate values for the new function of the line.



## F SENSE Program Listing

The following pages contain the source listing for the SENSE program run on the polarized ion source microprocessor. The program is written in Microsoft FORTRAN and assembly language for the Vector Graphics brand Z80 computer running the CP/M operating system.

```

PROGRAM SENSE
C Palatined Ion Source Microprocessor Operating System
C Written by Michael Wright
C Triangle Universities Nuclear Lab
C Duke University, Duke Station, Durham, NC 27701
C
C Sense/control tables
C QBABR - Abbreviated name of sense line
C QSNAME - Full name of sense line
C BSTAT - Status of sense line
C BREP - Number of repeats executed
C BTEXT - Define which adjective describes sense line status
C BFAULT - Location of start of fault sequence
C BGOOD - Location of start of good sequence
C QCBABR - Abbreviated name of control line
C QCSNAME - Full name of control line
C BCBSTAT - Status of control line
C BCBTEXT - Define which adjective describes control line status
C BCBON - Location of start of on sequence
C BCBOFF - Location of start of off sequence
C BCBSEQUEN - Array containing all of the sequences
C
C Wait tables
C WTIME - Length of wait time in seconds
C WLINE - Number of the sense line that is being waited on
C WMASK - Byte to .AND. into BCBSTAT(WLINE) to signal completion of the wait
C
C Bit masks for status bytes
C FAULTM = 10000000 -> Sense line is fault
C IGNORM = 01000000 -> Sense line is being ignored
C MANN - 00100000 -> A manual reset has been given for this sense line
C TESTM = 00010000 -> This sense/control pair tests faulty
C SBTH = 00001000 -> Sense line is included in short status
C MAITH = 00000111 -> A wait is being performed on this sense line
C CHANNM = 00000001 -> Control line is under manual control
C FACDVM = 00000001 -> Fault/good are valid adjectives for this line
C DPCLLVM = 00000010 -> Open/closed are valid adjectives for this line
C DNDQVVM = 00000100 -> On/off are valid adjectives for this line
C UPDVM = 00001000 -> Up/down are valid adjectives for this line
C
C Number of physical sense/control lines
C NLINES = Number of sense/control lines
C NSTLOW = Start of low voltage channels
C NSHTCH = Number of high voltage sense lines used
C NCHTCH = Number of high voltage control lines used
C NBLCH = Number of low voltage sense lines used
C NCLCH = Number of low voltage control lines used
C
C Keywords to make program more readable
C FAILT = 1
C GOOD = 2
C ON = 3
C OFF = 4
C YEB = 5
C NO = 6
C
IMPLICIT INTEGER*(A,C,E,P,R,Z),REAL*(G),REAL*(D),BYTE*(B)
DIMENSION QSNAME(6,40),QBABR(40),BTEXT(40),BSTAT(40),BREP(40)
DIMENSION QCSNAME(6,40),QCBABR(40),BCBTEXT(40),BCBSTAT(40)
LOGICAL I DONE, ALERT, MBEEP, ALARM, ABEEP, DQTEST
BYTE FAULTM,IGNORM,MAITH,MANN,TESTM,SBTH,CBCHANNM
1 FACDVM,DPCLLVM,DNDQVVM,UPDVM
1 ILINE(60)
1 DIMENSION WTIME(25),WLINE(25),WMASK(25)
C
COMMON /SENSE/ QSNAME, QBABR, BTEXT, BSTAT, BREP
COMMON /CONTROL/ QCSNAME, QCBABR, BCBTEXT, BCBSTAT
COMMON /MASKS/ FAULTM,IGNORM,MAITH,MANN,TESTM,SBTH,CBCHANNM
1 FACDVM,DPCLLVM,DNDQVVM,UPDVM
COMMON /NUMBER/ NLINES, NSTLOW, NSHTCH, NCHTCH, NBLCH, NCLCH
COMMON /TIME/ WTIME, WDAY, WMO, WMIN, WSEC, WARM, WJMIN
COMMON /WAIT/ WLINE, WLINE, WMASK, WABST, DMIN, DSEC
COMMON /FLAGS/ ALERT, MBEEP, ALARM, ABEEP, DQTEST, ITEST, BTESTF
COMMON /NEWS/ FAULT, GOOD, ON, OFF, YEB, NO
COMMON /INPUT/ IDONE, ILINE
C
DATA FAULTM/-128/,IGNORM/64/,MANN/32/,TESTM/16/,SBTH/8/,MAITH/7/,
1 CHANNM/1/,FACDVM/1/,DPCLLVM/2/,DNDQVVM/4/,UPDVM/8/,
DATA FAULT/1/,GOOD/2/,ON/3/,OFF/4/,YEB/5/,NO/6/
DATA BREP/20/
C Main Program
C Cold start
C WRITE(1,1000)
1000 FORMAT(' SENSE -- Version 3.4 -- October 4,1982')
C
C Init wait table
DO 30 J=1,MAIBIZ
30 WTIME(J)=0
DO 35 I=1,NLINES
BCSTAT(I)=0
BREP(I)=0
35 BSTAT(I)=0
C
C Init flags
ALERT = .TRUE.
ABEEP = .FALSE.
MBEEP = .FALSE.
ALARM = .FALSE.
DQTEST = .TRUE.
ITEST = 2
BTESTF = 0
C
C Init real time clock
MONTH = 0
IDAY = 0
HOUR = 0
MIN = 0
SEC = 0
C
40 IDONE = 0
WRITE(1,4000)MONTH,IDAY,HOUR,MIN,SEC
4000 FORMAT(' ',12,' ',12,' ',12,' ',12,' ',12)
CALL ENABLE(ILINE, IDONE)
C
C Check sense lines
60 CALL SENSE
C
C If a test loop has changed status, print a message
IF(BTEXTF.GT.0)WRITE(1,5000)QBABR(BTEXTF),QCBABR(BCBTEXTF)
5000 FORMAT(' ',A3,' ',A3,' TEST LOOP IS NOW GOOD')
IF(BTEXTF.LT.0)WRITE(1,6000)QBABR(-1*BTEXTF),QCBABR(-1*BCBTEXTF),

```

```

1 BREV, BREV
6000 FORMAT('A3. ', A3, ' ', A3, ' TEST LOOP IS NOW ', A1, 'FAULT', A1//)
BTSTIP = 0
C
C
C IF input line is ready then execute it
IF (.IDONE.EQ.0) GOTO 60
IDONE=0
CALL INPUT
CALL POKETZ('F759', '<')
CALL POKETZ('F758', '<')
CALL POKETZ('F759', '>')
GOTO 60
END
SUBROUTINE INPUT
C INPUT. Subroutine to decode and execute terminal input commands
C
C The keyboard is interrupt driven and is always active. Input may be
C typed at any time. An interrupt routine sets the logical variable IDONE
C to true to signal the completion of an input line and puts the text of
C the line into the 80 byte array ILINE. Subroutine INPUT is then called
C by the main program to decode and process the input.
C
C The commands themselves are described elsewhere.
C
IMPLICIT INTEGER(A,C,E,P,R,Z), REAL*4(D), REAL*8(I,D), BYTE(B)
DIMENSION Q$NAME(6,40), Q$ABBR(40), B$TEXT(40), B$STAT(40), B$REP(40)
DIMENSION Q$NAME(6,40), Q$ABBR(40), B$TEXT(40), B$STAT(40)
DIMENSION W$LINE(25), W$LINE(25), B$M$ASK(25)
LOGICAL*1 IDONE, ALERT, M$BEEP, ALARM, A$BEEP, D$OTEST
BYTE FAULT, I$ONDRM, WAITM, M$ANM, T$BTH, B$TH, C$HANN,
1 FAGDVM, D$PCLVM, D$MCFVM, U$PDVM
BYTE ILINE(80), D$NCR(4), U$PCR(4), B$LANM, C$R
COMMON /CENTAB/ Q$NAME, Q$ABBR, B$TEXT, B$STAT, B$REP
COMMON /CONTAB/ Q$NAME, Q$ABBR, B$TEXT, B$STAT
COMMON /HASKB/ FAULT, I$ONDRM, WAITM, M$ANM, T$BTH, B$TH, C$HANN,
1 FAGDVM, D$PCLVM, D$MCFVM, U$PDVM
COMMON /NUMBER/ N$LINE, N$STLON, N$HIGH, N$HIGH, N$LOW, N$LOW
COMMON /TIME/ P$ONTH, I$DAY, H$OUR, M$IN, S$EC, A$ALRM, A$ALRM
COMMON /MAIL/ W$TIME, W$LINE, W$M$ASK, W$M$SIZ, D$MIN, D$SEC
COMMON /FLAGS/ ALERT, M$BEEP, ALARM, A$BEEP, D$OTEST, I$TEBT, B$TEBT
COMMON /KEYS/ FAULT, Q$OOD, Q$DN, D$FF, Y$ES, N$O
COMMON /INPUTC/ IDONE, ILINE
C
C EQUIVALENCE (Q$DNAME, ILINE(1)), (Q$ACTIN, ILINE(5)),
1 (Q$SUBCD, ILINE(8)), (Q$ALMSB, ILINE(12)), (Q$ALMSB, ILINE(7))
EQUIVALENCE (Q$NCR, D$NCR(1)), (Q$PCR, U$PCR(1))
C
C Define 3 letter codes and abbreviations
DATA Q$ON/'ON', Q$INI/'INI', Q$BTA/'BTA', Q$DVM/'DVM' //
1 Q$TIM/'TIM', Q$BET/'BET', Q$IGH/'IGH', Q$ALL/'ALL', Q$HIO/'HIO' //
1 Q$LOM/'LOM', Q$BEE/'BEE', Q$ONM/'ON', Q$XDF/'DF', Q$ALA/'ALA' //
1 Q$OFF/'OFF', Q$SST/'SST', Q$SEN/'SEN', Q$HSE/'HSE', Q$LSE/'LSE' //
1 Q$CON/'CON', Q$HCO/'HCO', Q$LCD/'LCD', Q$FAU/'FAU', Q$OOD/'OOD' //
1 Q$OPE/'OPE', Q$CLD/'CLD', Q$ORH/'ORH', Q$RES/'RES', Q$ONOR/'ONOR' //
1 Q$MOS/'MOS', Q$ALM/'ALM', Q$TES/'TES', Q$IST/'ST', Q$FLI/'FLI' //
1 Q$SPI/'SPI', Q$QUE/'QUE', Q$XUP/'UP', Q$XDD/'DD', Q$UPX/'UP' //
1 Q$DOK/'DOK', Q$FL/'FL', Q$UNQ/'UNQ', Q$SPN/'SPN', Q$QUN/'QUN' //
1 Q$SPAR/'SPAR' //
DATA Q$NCR/'0', N$, '13', ' ', U$PCR/'U', P$, '13', ' ' //
DATA D$ALM/'ALWAYS', D$N$ALM/' ', B$LANM/' ', C$R/'13/' //
DATA D$D$M/'DOWN' //

```

```

C
C ILINE(4) = BLANK
C
C Monitor command
C
C IF (Q$DNAME.EQ.Q$ON) BTOP
C
C Initialive command
C
C IF (Q$DNAME.EQ.Q$INI) GOTO 180
C
C Status command
C
C IF (Q$DNAME.EQ.Q$TA) GOTO 200
C
C Dvm command
C
C IF (Q$DNAME.EQ.Q$VM) GOTO 10
C
C VAI version of decode statement
C
C DECODE(18,1300, ILINE) CHANNEL
C
C MICROSOFT version of decode statement
C
C DECODE(18,1300) CHANNEL
C
C DECODE(18,1300) CHANNEL
C
1100 FORMAT('X', I2, ' ')
CALL DVM(CHANNEL)
RETURN
C
C Print real time clock command
C
C 10 IF (Q$DNAME.EQ.Q$TM) GOTO 20
C
C WRITE(1,1200) MONTH, IDAY, HOUR, MIN, SEC
1200 FORMAT(' ', I2, ' ', I2, ' ', I2, ' ', I2, ' ', I2, ' ')
RETURN
C
C Set real time clock command
C
C 20 IF (Q$DNAME.EQ.Q$ET) GOTO 30
C
C VAI version of decode statement
C
C DECODE(18,1300, ILINE) MONTH, IDAY, HOUR, MIN, SEC
C
C MICROSOFT version of decode statement
C
C DECODE(18,1300) MONTH, IDAY, HOUR, MIN, SEC
1300 FORMAT('X', I2, ' ', I2, ' ', I2, ' ', I2, ' ', I2, ' ')
C
C 1300 WRITE(1,1300) MONTH, IDAY, HOUR, MIN, SEC
C
C In principle this is an error message. Write(1,1400)
1400 FORMAT(' Proper format is: BET 00/00 00:00:00 //')
RETURN
C
C Ignore sense lines (including spaces) command
C
C 30 IF (Q$DNAME.EQ.Q$N) GOTO 60
C
C ILINE(11) = BLANK
C
C IF (Q$SUBCD.NE.Q$ALL.AND.Q$SUBCD.NE.Q$HIO) GOTO 50
C
C ILL = N$STLON-1
C
C DO 40 I=1, ILL
C
C 40 B$STAT(11) = B$STAT(11).OR.I$ONDRM
C
C WRITE(1,1410)
1410 FORMAT(' HIGH VOLTAGE SENSE LINES IGNORED //')
C
C IF (Q$SUBCD.NE.Q$ALL.AND.Q$SUBCD.NE.Q$LOM) RETURN
C
C DO 60 I=N$STLON, N$LINES
C
C 60 B$STAT(11) = B$STAT(11).OR.I$ONDRM
C
C WRITE(1,1420)
1420 FORMAT(' LOW VOLTAGE SENSE LINES IGNORED //')
RETURN

```

```

C
C
C      Turn message beep flag on or off command
C
180 IF (OCOMAN.NE.QBEE) GOTO 100
   ILINE(B) = BLANK
   IF (GACTIN.NE.QXDM) GOTO 90
   ALERT = TRUE
   WRITE(1,1430)
   FORMAT('MESSAGE BEEP ON')
   RETURN
1430
90 IF (GACTIN.NE.QXDF) GOTO 310
   ALERT = FALSE
   MUEEP = FALSE
   WRITE(1,1440)
   FORMAT('MESSAGE BEEP OFF')
   RETURN
C
C      Alarm command
C
100 IF (OCOMAN.NE.QALA) GOTO 122
   ILINE(10) = BLANK
   IF (GALRSB.NE.QOFF) GOTO 110
   Turn alarm off
   ALARM = FALSE
   ADEEP = FALSE
   WRITE(1,1550)
   RETURN
110 IF (GALRSB.NE.QTIR) GOTO 120
   Print alarm time
   IF (ALARM) WRITE(1,1500)ALARM,ALARMIN
1500 FORMAT('ALARM TIME IS ',12,' ',12/)
   IF (NOT ALARM) WRITE(1,1550)
1550 FORMAT('ALARM IS NOW OFF')
   RETURN
C
120 IF (GALRSB.NE.QSET) GOTO 310
   Set alarm time
   VAX version of decode statement
   DECDE(15,1600,ILINE)ALARM,ALARMIN
   MICROSOFT version of decode statement
   DECDE(10,12,1X,12)
   FORMAT(10,12,1X,12)
   ALARM = TRUE
   WRITE(1,1610)ALARM,ALARMIN
1610 FORMAT('ALARM SET TO ',12,' ',12/)
   RETURN
C
C      Turn test flag on or off command
C
122 IF (OCOMAN.NE.QTES) GOTO 130
   ILINE(8) = BLANK
   IF (GACTIN.NE.QXDM) GOTO 126
   DOTEEST = TRUE
   WRITE(1,1633)
   RETURN
126 IF (GACTIN.NE.QXDF) GOTO 127
   DOTEEST = FALSE
   WRITE(1,1666)
   RETURN
127 IF (GACTIN.NE.QXST) GOTO 310
   IF (DOTEEST) WRITE(1,1633)
1633 FORMAT('TEST IS NOW ON')
   IF (NOT DOTEEST) WRITE(1,1666)
1666 FORMAT('TEST IS NOW OFF')

```

```

RETURN
C
C      Short status command
C
130 IF (OCOMAN.NE.QBST) GOTO 330
   WRITE(1,2000)
   FORMAT('ABBR NAME LINE STATUS IGNORE',
1 ' WAITING TEST REPEATS')
   DO 140 J=1,NLINEB
   IF (QBSTAT(11).AND.QBTH).EQ.QBTH) CALL TBSTAT(11)
140 CONTINUE
   RETURN
C
C      Bpin command
C
330 IF (OCOMAN.NE.QBP1) GOTO 600
   ILINE(9) = BLANK
   DO 333 I=1,NLINEB
   IF (QCABBR(11).EQ.QBPM) GOTO 336
333 CONTINUE
   GOTO 390
336 IF (GACTIN.EQ.QXUP) GOTO 340
   IF (GACTIN.EQ.QXDO) GOTO 370
   IF (GACTIN.NE.QXFL) GOTO 380
   IF (PCSTAT(11)) GOTO 370
   Set spin direction to up
   CALL EXCBEG(11,ON,0,WASOK)
   IF (WASOK.NE.YES) GOTO 390
   WRITE(1,2200)(OCNAME(I,11),I=1,6)
   FORMAT(' ',6A4,'UP')
2200 WRITE(7,23000)
   RETURN
C
370 Set spin direction to down
   CALL EXCBEG(11,OFF,0,WASOK)
   IF (WASOK.NE.YES) GOTO 390
   WRITE(1,2300)(OCNAME(I,11),I=1,6)
   FORMAT(' ',6A4,'DOWN')
23000 WRITE(7,23000)
   RETURN
380 IF (GACTIN.NE.QXBT) GOTO 310
   CALL TCSTAT(11)
   WRITE(7,25000)
   RETURN
C
Band "error" code back to the VAX
24000 WRITE(7,24000)
   FORMAT('N')
25000 WRITE(7,25000)
   RETURN
C
C      Perform quench and unquench commands
C
600 IF (OCOMAN.NE.QQUE.AND.OCOMAN.NE.QUNQ) GOTO 150
   DO 610 I=1,NLINEB
   IF (QCABBR(11).EQ.QGUN) GOTO 620
610 CONTINUE
   GOTO 390
620 IF (OCOMAN.NE.QQUE) GOTO 630
   CALL EXCBEG(11,ON,0,WASOK)
   IF (WASOK.NE.YES) GOTO 390
   WRITE(1,2600)(OCNAME(I,11),I=1,6)
   FORMAT(' ',6A4,'ON')
26000 WRITE(7,23000)
   RETURN

```

```

630 CALL EXCBEG(II,OFF,O,WASDK)
IF (WASDK NE YES) GOTO 590
WRITE(1,27000)(GCNAME(1,II),I=1,6)
FORMAT(' ',6A4,' OFF//')
27000 WRITE(7,25000)
RETURN
C
C Insert future commands here
C
C Look for sense line command
150 ILINE(8) = BLANK
DO 160 II=1,NLINES
IF (OCOPAN EQ QBABR(II)) GOTO 320
160 CONTINUE
C
C Look for control line command
ILINE(15) = BLANK
DO 170 II=1,NLINES
IF (OCOPAN EQ QCABR(II)) GOTO 430
170 CONTINUE
C
C Invalid command or empty line
ABEEP = FALSE
MBEEP = FALSE
IF (ILINE(II) EQ CR) RETURN
WRITE(1,3000)
FORMAT(' ',53X,'Invalid command')
RETURN
C
C Initialize entire system
180 DO 190 I=1,NLINES
INIT SENSE STATUS
BSSTAT(1) = 0
SREP(1) = 0
INIT CONTROL LINE STATUS
CALL SETCNT(1,TRUE)
BCSTAT(1) = 0
190 CONTINUE
DO 195 I=1,MA181Z
195 WTIME(I) = 0
WRITE(1,3500)
FORMAT(' ',SYSTEM INITIALIZED//')
RETURN
C
C Type system status on control terminal
C
200 ILINE(11) = BLANK
IF (QSUBCO NE QBEN AND QSUBCO NE QHBE) GOTO 220
WRITE(1,2000)
C
C Do high voltage sense lines
I11=NBTL0W-1
DO 210 II=1,I11
IF (GNAME(1,II),EQ,QSPAR) GOTO 210
CALL TSSTAT(II)
CONTINUE
210
C
220 IF (QSUBCO EQ QHSE) RETURN
IF (QSUBCO EQ QLSE) WRITE(1,2000)
IF (QSUBCO NE QBEN AND QSUBCO NE QLSE) GOTO 240
C
C Do low voltage sense lines
DO 230 II=NBTL0W,NLINES
IF (GNAME(1,II),EQ,QSPAR) GOTO 230
CALL TSSTAT(II)
CONTINUE
230
C
240 IF (QSUBCO NE QCDN AND QSUBCO NE QHCD) GOTO 260
CONTINUE
C
C Do high voltage control lines
I11=NBTL0W-1
DO 250 II=1,I11
IF (GNAME(1,II),EQ,QSPAR) GOTO 250
CALL TCSTAT(II)
CONTINUE
250
C
260 IF (QSUBCO EQ QHCO) RETURN
IF (QSUBCO NE QCDN AND QSUBCO NE QLCD) GOTO 280
CONTINUE
C
C Do low voltage control lines
DO 270 II=NBTL0W,NLINES
IF (GNAME(1,II),EQ,QSPAR) GOTO 270
CALL TCSTAT(II)
CONTINUE
270
RETURN
C
C Do status of all lines including spares
280 IF (QSUBCO NE QALL) GOTO 310
WRITE(1,2000)
C
C All sense lines
DO 290 II=1,NLINES
CALL TBSTAT(II)
C
C All control lines
DO 300 II=1,NLINES
CALL TCSTAT(II)
RETURN
C
C Invalid subcommand
310 WRITE(1,4000)
4000 FORMAT(' ',53X,'Invalid subcommand')
RETURN
C
C Perform sense line actions
C
C Type out status
320 IF (QACTIN NE QBTA) GOTO 340
WRITE(1,2000)
CALL TSSTAT(II)
RETURN
C
C Do other sense line actions
C
C Make line fault
340 IF (QACTIN NE QFAU) GOTO 350
IF ((IBTEXT(II),AND FAQOVR) EQ 0) GOTO 440
WRITE(1,5000)(GNAME(1,II),I=1,6)
FORMAT(' ',6A4,' FAULT//')
BSSTAT(II) = FAULT OR IQDRM
CALL EXBEG(II,FAULT,OFF,O)
RETURN
C
C Make line good
350 IF (QACTIN NE QGGO) GOTO 360
IF ((IBTEXT(II),AND FAQOVR) EQ 0) GOTO 440
WRITE(1,6000)(GNAME(1,II),I=1,6)
FORMAT(' ',6A4,' GOOD//')
BSSTAT(II) = IQDRM
CALL EXBEG(II,GOOD,DN,O)

```

```

RETURN
C
C 360 Make line open
IF (GACTIN.NE.GDPE) GOTO 370
IF ((BTEXT(11).AND.OPCLVH).EQ.0) GOTO 440
WRITE(1,7000)(OSNAME(1,1),I=1,6)
FORMAT(' ',6A4,' OPEN')
BSSTAT(11) = FAULT OR IONDRM
CALL EXSEQ(11,FAULT,OFF,0)
RETURN
7000
C
C 370 Make line closed
IF (GACTIN.NE.OCLD) GOTO 380
IF ((BTEXT(11).AND.OPCLVH).EQ.0) GOTO 440
WRITE(1,8000)(OSNAME(1,1),I=1,6)
FORMAT(' ',6A4,' CLOSED')
BSSTAT(11) = IONDRM
CALL EXSEQ(11,GOOD,ON,0)
RETURN
8000
C
C 380 Make line on
IF (GACTIN.NE.ONX AND GACTIN.NE.ONCR) GOTO 390
IF ((BTEXT(11).AND.ONPVRH).EQ.0) GOTO 440
WRITE(1,9000)(OSNAME(1,1),I=1,6)
FORMAT(' ',6A4,' ON')
BSSTAT(11) = FAULT OR IONDRM
CALL EXSEQ(11,FAULT,OFF,0)
RETURN
9000
C
C 390 Make line off
IF (GACTIN.NE.OFF) GOTO 400
IF ((BTEXT(11).AND.ONPVRH).EQ.0) GOTO 440
WRITE(1,10000)(OSNAME(1,1),I=1,6)
FORMAT(' ',6A4,' OFF')
BSSTAT(11) = IONDRM
CALL EXSEQ(11,GOOD,ON,0)
RETURN
10000
C
C 400 Reset sense line
BSSTAT(11) = BSSTAT(11).OR.MANN
BSSTAT(11) = BSSTAT(11).AND.(NOT.FAULT)
SREP(11) = 0
WRITE(1,11000)(OSNAME(1,1),I=1,6)
FORMAT(' ',6A4,' MANUAL RESET')
CALL EXSEQ(11,GOOD,ON,0)
RETURN
11000
C
C 410 Stop manual override of status
IF (GACTIN.NE.ONOR) GOTO 420
BSSTAT(11) = BSSTAT(11).AND.(NOT.IONDRM)
SREP(11) = 0
WRITE(1,12000)(OSNAME(1,1),I=1,6)
FORMAT(' ',6A4,' NORMAL')
RETURN
12000
C
C 420 Include line in short status list
IF (GACTIN.NE.OST) GOTO 430
BSSTAT(11) = BSSTAT(11).OR.BSTM
WRITE(1,13000)(OSNAME(1,1),I=1,6)
FORMAT(' ',6A4,' INSERTED INTO SHORT STATUS LIST')
RETURN
13000
C
C 430 Remove line from short status list
BSSTAT(11) = BSSTAT(11).AND.(NOT.BSTM)
WRITE(1,14000)(OSNAME(1,1),I=1,6)
FORMAT(' ',6A4,' REMOVED FROM SHORT STATUS LIST')
RETURN
14000
C
C 440 Insert future sense line actions here
C
C 440 Invalid sense line action
WRITE(1,15000)
15000 FORMAT(' ',53X,'Invalid sense line action')
RETURN
C
C 450 Perform control line actions
C
C 450 IF (GACTIN.NE.OSTA) GOTO 470
Type out status
CALL TCSTAT(11)
RETURN
C
C Put line under manual control else
470 IF (GACTIN.NE.DALH) GOTO 480
GACTIN = DALH
DALWAY = DALW
ALSTAT = CHANN
GOTO 490
480 DALWAY = DNDALH
ALSTAT = 0
C
C Make line on
490 IF (GACTIN.NE.ONX AND GACTIN.NE.ONCR) GOTO 500
IF ((BTEXT(11).AND.ONPVRH).EQ.0) GOTO 540
CALL EXSEQ(11,ON,ALSTAT,WASOK)
IF (WASOK.NE.YES) RETURN
BCSTAT(11) = BCSTAT(11).OR.ALSTAT
WRITE(1,16000)(OSNAME(1,1),I=1,6),DALWAY
FORMAT(' ',6A4,' ON',AB/)
16000 RETURN
C
C Make line off
500 IF (GACTIN.NE.OFF) GOTO 510
IF ((BTEXT(11).AND.ONPVRH).EQ.0) GOTO 540
CALL EXSEQ(11,OFF,ALSTAT,WASOK)
IF (WASOK.NE.YES) RETURN OR ALSTAT
BCSTAT(11) = BCSTAT(11).OR.ALSTAT
WRITE(1,17000)(OSNAME(1,1),I=1,6),DALWAY
FORMAT(' ',6A4,' OFF',AB/)
17000 RETURN
C
C Make line open
510 IF (GACTIN.NE.OPE) GOTO 520
IF ((BTEXT(11).AND.OPCLVH).EQ.0) GOTO 540
CALL EXSEQ(11,ON,ALSTAT,WASOK)
IF (WASOK.NE.YES) RETURN
BCSTAT(11) = BCSTAT(11).OR.ALSTAT
WRITE(1,18000)(OSNAME(1,1),I=1,6),DALWAY
FORMAT(' ',6A4,' OPEN',AB/)
18000 RETURN
C
C Make line closed
520 IF (GACTIN.NE.OCLD) GOTO 523
IF ((BTEXT(11).AND.OPCLVH).EQ.0) GOTO 540

```

```

COMMON /CONTAB/ GCNAME,GCABBR,BCTEXT,BCSTAT
COMMON /WASOK/  FAULTM,IGNDRM,WAITH,MANN,TESTM,BBTH,CHANNP,
1              FADVM,OPCLVM,NSLDM,NCHTOH,NSLDM,KCLDM
COMMON /NUMBER/ NLINEB,NSLDM,NSLDM,NCHTOH,NSLDM,KCLDM
COMMON /FLACS/  ALERT,MBEEP,ALARM,ABEEP,DOTEST,ITEBT,BTEBT
COMMON /KEYS/   FAULT,GOOD,ON,OFF,YES,NO

C      DATA  BREV/20/
C      DO 60 I1=1,NLINEB
C      Set repeat count for noise immunity
C      IREPT=6
C      See if we are performing a wait on this line
C      BWAIT = BBSSTAT(I1).AND.WAITH
C      IF (BWAIT.EQ.WAITH) GOTO 60
C      Bat BWAIT = I111 1111 where xxx is the wait number
C      IF (BWAIT.NE.O) BWAIT = BWAIT.OR (.NOT.WAITH)
C      Bat MUSTAT to be the new status as determined by bbsstat(I1) or by
C      bstat(I1) depending on the IGNORE bit in bbsstat(I1).
C      MUSTAT = BSSTAT(I1).AND.FAULTM
C      IF ((BSSTAT(I1).AND.IGNDRM).NE.O) GOTO 5
C      MUSTAT = FAULTM
C      IF (PBSTAT(I1)) MUSTAT = MUSTAT.XOR.FAULTM
C      IF (BSTAT(I1).LT.O) then reverse the value of MUSTAT
C      IF (BTEXT(I1).LT.O) MUSTAT = MUSTAT.XOR.FAULTM
C      See if status has changed since last examination
C      IF (MUSTAT.EQ.(BSSTAT(I1).AND.FAULTM)) GOTO 40
C      Examine IREPT times for noise immunity
C      Loop takes an estimated 200 microseconds
C      IREPT=IREPT-1
C      IF (IREPT.GT.O) GOTO 1
C      New status is different from old status
C      Set "fault" bit of bstat to "fault" bit of mustat
C      BSSTAT(I1) = BSSTAT(I1).AND(.NOT.FAULTM)
C      BBSSTAT(I1) = BBSSTAT(I1).OR.MUSTAT
C      IF (MUSTAT.EQ.O) GOTO 20
C      Sense line is now fault
C      IF (BWAIT.NE.O) GOTO 10
C      No wait operation is involved
C      DAQJ = DSADJ(I1,FAULT,1)
C      WRITE(1,1000)(GCNAME(I,1),I=1,6),BREV,DAQJ,BREV
C      FORMAT(' ',6A4,'AL,AB,A1/')
C      CALL EXSEQ(I1,FAULT,OFF,BWAIT,WASOK)
C      IF (ALERT) MBEEP = .TRUE.
C      GOTO 60
C      Has just finished waiting
C      DAQJ = DSADJ(I1,FAULT,1)
C      WRITE(1,2000)(GCNAME(I,1),I=1,6),BREV,DAQJ,BREV
C      FORMAT(' ',6A4,'NOH',AL,AB,A1/')
C      BWAIT = .BWAIT
C      CALL EXSEQ(I1,GOOD,OFF,BWAIT,WASOK)
C      GOTO 60
C      Sense line is now good
C      IF (BWAIT.NE.O) GOTO 30
CALL EXSEQ(I1,OFF,ALSTAT,WASOK)
IF (HASOK.NE.YES) RETURN
BCSTAT(I1) = BCSTAT(I1).OR.ALSTAT
WRITE(1,19000)(GCNAME(I,1),I=1,6),DALWAY
FORMAT(' ',6A4,'CLOSED',AB/)
RETURN
19000
C      Make line up
C      523 IF (OACTIN.NE.OUPX).AND.GACTIN.NE.OUPCR) GOTO 526
C      IF ((BTEXT(I1).AND.UPDNVM) EQ O) GOTO 540
C      CALL EXSEQ(I1,ON,ALSTAT,WASOK)
C      IF (HASOK.NE.YES) RETURN
C      BCSTAT(I1) = BCSTAT(I1).OR.ALSTAT
C      WRITE(1,19300)(GCNAME(I,1),I=1,6),DALWAY
C      FORMAT(' ',6A4,'UP',AB/)
C      RETURN
19300
C      Make line down
C      526 IF (OACTIN.NE.ODOM) GOTO 530
C      IF ((BTEXT(I1).AND.UPDNVM) EQ O) GOTO 540
C      CALL EXSEQ(I1,OFF,ALSTAT,WASOK)
C      IF (HASOK.NE.YES) RETURN
C      BCSTAT(I1) = BCSTAT(I1).OR.ALSTAT
C      WRITE(1,19600)(GCNAME(I,1),I=1,6),DALWAY
C      FORMAT(' ',6A4,'DOWN',AB/)
C      RETURN
19600
C      Remove line from manual control
C      530 IF (OACTIN.NE.ONOR) GOTO 540
C      BCSTAT(I1) = BCSTAT(I1).AND(.NOT.CHANNP)
C      WRITE(1,20000)(GCNAME(I,1),I=1,6)
C      FORMAT(' ',6A4,'NORMAL')
C      RETURN
20000
C      Insert future control line actions here
C      C
C      C
C      Invalid control line action
C      540 WRITE(1,21000)
C      21000 FORMAT(' ',53X,'Invalid control line action')
C      RETURN
C      END
C      SUBROUTINE GBEMBE
C      GBEMBE: subroutine to perform sense/control function
C      C
C      C Local:
C      C > 0 -> (-BWAIT) is the code for the wait command that has finished
C      C where the status changed during the wait period
C      C = 0 -> No wait operation has been involved for this sense line
C      C < 0 -> BWAIT is the code for the wait command that has finished
C      C where the status did not change during the wait period
C      C MUSTAT - New status of sense line
C      IMPLICIT INTEGER(A-C,E-P,R-Z),REAL*4(Q),REAL*8(D),BYTE(B)
C      DIMENSION GCNAME(6,40),GCABBR(40),BTEXT(40),BSSTAT(40),BREP(40)
C      DIMENSION GCNAME(6,40),GCABBR(40),BTEXT(40),BSSTAT(40)
C      LOGICALAL1 ALERT,MBEEP,ALARM,ABEEP,DOTEST
C      BYTE      FAULTM,IGNDRM,WAITH,MANN,TESTM,SSIM,CHANNP,
1              FADVM,OPCLVM,ONOFFV,UPDNVM,MUSTAT
C      LOGICALAL1 PSBSTAT,PCSTAT
C      COMMON /SENTAB/ GCNAME,GCABBR,BTEXT,BBSSTAT,BREP

```

```

C No wait operation is involved
DADJ = DSADJ(11,GOOD,1)
WRITE(1,1000)(OSNAME(1,11),I=1,6),DADJ
FORMAT('...',6A4,AB/)
CALL EXSEQ(11,GOOD,ON,BWAIT,WASOK)
GOTO 60

C
C Has just finished waiting
DADJ = DSADJ(11,GOOD,1)
WRITE(1,2000)(OSNAME(1,11),I=1,6),DADJ
FORMAT('...',6A4,AB/)
BWAIT = -BWAIT
CALL EXSEQ(11,FAULT,ON,BWAIT,WASOK)
GOTO 60

C Sense line status is unchanged
IF (BWAIT.EQ.0) GOTO 60

C Has just finished waiting
IF (NBSTAT.EQ.0) GOTO 30

C Sense line is still fault
DADJ = DSADJ(11,FAULT,1)
WRITE(1,3000)(OSNAME(1,11),I=1,6),BREV,DADJ,BREV
FORMAT('...',6A4,BTILL,AB,AB/)
CALL EXSEQ(11,FAULT,OFF,BWAIT,WASOK)
GOTO 60

C Sense line is still good
DADJ = DSADJ(11,GOOD,1)
WRITE(1,3000)(OSNAME(1,11),I=1,6),DADJ
FORMAT('...',6A4,BTILL,AB/)
CALL EXSEQ(11,GOOD,ON,BWAIT,WASOK)
GOTO 60

C CONTINUE
RETURN
SUBROUTINE EXSEQ(II,FAOD,ADROFF,BWAIT)
C EXSEQ. subroutine to execute a sense/control sequence
C Input
C II = Number of sense line whose sequence is to be executed
C FAOD = FAULT -> Execute the "fault" sequence
C GOOD = GOOD -> Execute the "good" sequence
C ON = ON -> Turn appropriate devices "on"
C OFF = OFF -> Turn appropriate devices "off"
C BWAIT > 0 -> (-BWAIT) is the code for the wait command that has finished
C where the status changed during the wait period
C > 0 -> No wait operation has been involved for this sense line
C < 0 -> BWAIT is the code for the wait command that has finished
C where the status did not change during the wait period
C Local
C BITEM = Item from the control sequence being executed
C IREQ = Pointer to an item in the control sequence
C ITIME = Length of wait time
C DUNIT = Units of wait time (minutes or seconds)
C NCDIR = Number of sense lines to correlate status
C ISEQ2 = Pointer to the item following the end of a correlation list
C ISEQ2 = ISEQ2 + 1
IMPLICIT INTEGER(A,C,E,P,R,Z),REAL*4(O),REAL*8(D),BYTE(B)
DIMENSION OSNAME(6,40),OSABBR(40),BTEXT(40),BSSTAT(40),SREP(40)
DIMENSION OSNAME(6,40),GCABBR(40),BCTEXT(40),BCSTAT(40)

```

```

DIMENSION SFAULT(40),BGOOD(40),CON(40),COFF(40)
BYTE SEQUEN(2000)
BYTE FAULTM,IGNDRM,WAITM,MANN,TEBTH,BBTH,CMANN,
FAGDVM,DFCLVM,DNOFVM,UPDNVM
BYTE SEGEN,SEGMAN,GEORPT,SECKDR,WAITM,WAIT&
CORCON /CENTAB/ OSNAME,OSABBR,BTEXT,BSSTAT,BREP
CORCON /CONTAB/ OSNAME,GCABBR,BCTEXT,BCSTAT
CORCON /GEOPTR/ SFAULT,BGOOD,CON,COFF
CORCON /SECDM/ SEQUEN
CORCON /SECOND/ SEGEN,SEGMAN,GEORPT,SECKDR,WAITM,WAIT&
CORCON /MASAB/ FAULTM,IGNDRM,WAITM,MANN,TEBTH,BBTH,CMANN,
FAGDVM,DFCLVM,DNOFVM,UPDNVM
CORCON /NUMBER/ MLINE,NSTLOM,NSHIOH,NCHIOH,NBLOW,NCLON
CORCON /KEYS/ FAULT,GOOD,ON,OFF,YES,NO
CORCON /WAIT/ WTIME,MLINE,BPMASK,WA1BIZ,DMIN,DBEC
DATA BREV/20/
1500 = BGOOD(11)
IF (FAOD.EQ.FAULT) IREQ = SFAULT(11)
3 DNOFF = ADROFF
BWAIT = BWAIT
10 ITEM = SEGEN(IREQ)
ITEM = BITEM
IITEM = IABS(IITEM)
ISEQ = ISEQ+1
IF (IITEM.LT.0) GOTO 10
IF (BWAIT.LT.0) GOTO 10
C We are not stepping to a wait command, change control line
IF (BCSTAT(IITEM).NE.CMANN) GOTO 20
C Line is under manual control
WRITE(1,1000)(OSNAME(1,11),I=1,6),BREV,BREV
FORMAT('...',6A4,AB,AB,AB) UNDER MANUAL CONTROL',AB/)
GOTO 10
C Turn line on or off
CALL EXSEQ(IITEM,DNOFF,0,WASOK)
IF (WASOK.NE.YES) GOTO 10
C Line is not blocked
DADJ = DSADJ(IITEM,DNOFF,IITEM)
WRITE(1,2000)(OSNAME(1,11),I=1,6),DADJ
FORMAT('...',6A4,AB/)
GOTO 10
C Process end of sequence command
30 IF (BITEM.NE.BEEND) GOTO 40
C Clear MANUAL ( and IGNDRM )
IF ((BSSTAT(11).AND.MANN).EQ.MANN) BSSTAT(11) = BSSTAT(11).AND.
(.NOT.MANN)
BSSTAT(11) = BSSTAT(11).AND.(.NOT.IGNDRM)
RETURN
C Process manual command
40 IF (BITEM.NE.SEGMAN) GOTO 60
IF ((BSSTAT(11).AND.MANN).NE.MANN) GOTO 50
GOTO 10
C Have manual reset
C Need manual reset
50 WRITE(1,3000)BREV,BREV

```



```

3000 FORMAT(' ',A1,'REQUIRES MANUAL RESET',A1/)
RETURN
C
C Process wait command
60 IF (BITEM.LT.WAIT) OR (BITEM.GT.WAIT) GOTO 110
BITEM = BITEM OR (.NOT.WAIT)
IF (BWAIT.NE.O) GOTO 80
C
C Execute a wait
TIME = SEQUEN(ISEQ)
DUNIT = DRIN
IF (TIME.GT.O) GOTO 70
TIME = TIME
DUNIT = DSEC
WRITE(1,4000)TIME,DUNIT
FORMAT('WAIT',I5,' ',A8/)
BSSTAT(1) = BSSTAT(1) OR WAIT
CALL WAITBUS(TIME,DUNIT,I,BITEM)
RETURN
C
C Executed wait command found, status changed during wait
C
C Stop processing sequence
80 BSSTAT(1) = BSSTAT(1) .AND. (.NOT.(WAITM.OR.MANM))
ISEQ = ISEQ+1
BITEM = SEQUEN(ISEQ)
ISEQ = ISEQ+1
IF (BITEM.NE.SEMPTY) RETURN
C
C Process a repeat command
IEM = SEQUEN(ISEQ)
ISEQ = ISEQ+1
C
C Increment repeat count
SREP(1) = SREP(1)+1
C
C Allowable number of repeats exceeded
SREP(1) = SREP(1)+1
BSSTAT(1) = FAULTM.OR.IONDRM
WRITE(1,5000)(GBNAME(I),I),I=1,6),BREV,BREV
FORMAT(' ',A4,' ',A1,'MAXIMUM REPEAT COUNT EXCEEDED',/)
C
C Reexecute sequence from start
ONOFF = DFF
BWAIT = O
ISEQ = SFAULT(1)
GOTO 5
C
C Executed wait command found, status did not change during wait
C
C Stop skipping, resume normal processing
90 IF (BITEM.NE.BWAIT) GOTO 100
BWAIT = O
BSSTAT(1) = BSSTAT(1) .AND. (.NOT.WAITM)
C
C Continue skipping to find executed wait command.
100 ISEQ = ISEQ+1
BITEM = SEQUEN(ISEQ)
IF (BITEM.EQ.SEND) GOTO 30
IF (BITEM.NE.SEMPTY) GOTO 10
C
C Repeat counter if line is not being ignored
IF ((BSSTAT(1) .AND. (IONDRM).EQ.O) SREP(1) = O
ISEQ = ISEQ+2
GOTO 10
C
C 3000 Process correlate command
110 IF (BITEM.NE.SEMPTY) GOTO 10
120 NCDRR = SEQUEN(ISEQ)
ISEQ = ISEQ+1
IF (BWAIT.LT.O) GOTO 200
IF (BWAIT.LT.O) GOTO 200
C
C Examine correlated sense lines
DO 130 I=1,NCDRR
ITEM = SEQUEN(ISEQ)
ISEQ = ISEQ+1
IF (ITEM.LT.O) GOTO 125
IF ((BSSTAT(ITEM).AND.FAULTM.NE.FAULTM) GOTO 150
GOTO 130
125 IF ((BSSTAT(-1)ITEM).AND.FAULTM.EQ.FAULTM) GOTO 130
130 CONTINUE
C
C Have correlation, continue processing control sequence
GOTO 10
C
C No correlation, if no wait, flush rest of this correlate command
150 ISEQ = ISEQ+2
IF (BWAIT.GT.O) GOTO 180
160 BITEM = SEQUEN(ISEQ)
ISEQ = ISEQ+1
IF (BITEM.EQ.SEND) RETURN
IF (BITEM.EQ.SEMPTY) GOTO 120
GOTO 160
C
C No correlation, look for changed wait, if so then pretend correlation
180 BITEM = SEQUEN(ISEQ)
ISEQ = ISEQ+1
IF (BITEM.EQ.SEMPTY) GOTO 120
IF (BITEM.EQ.SEMPTY) AND (BITEM.LE.WAITM)
1 BITEM = BITEM OR (.NOT.WAITM)
IF (BITEM.EQ.SEMPTY) GOTO 190
GOTO 180
190 ISEQ = ISEQ+2
GOTO 10
C
C Skip test of correlation, continue skipping for an unchanged wait
200 ISEQ = ISEQ+2
GOTO 10
END
SUBROUTINE EXCSEQ(A11,ADNOFF,ALWAYS,MAJOR)
C
C EXCSEQ: subroutine to execute a control inhibit sequence
C
C Input:
C I1 = Number of control line whose inhibit sequence is to be executed.
C O -> Perform opposite operation to that specified by ONOFF
C ONOFF = ON -> Turn device "on"
C = OFF -> Turn device "off"
C ALWAYS = O -> Execute sequence then turn device on or off if allowed
C < O -> Ignore sequence and turn device on or off
C
C Output:
C MAJOR = Device was successfully turned on or off
C
C Local:
C IEM = Item in control inhibit sequence
C ISEQ = pointer to sequence

```



```

IF (HOUR NE. 24) GOTO 3
HOUR = 0
IDAY = IDAY+1
IF (IDAY LE. MONTH(MONTH)) GOTO 3
IDAY = 1
MONTH = MONTH+1
IF (MONTH EQ 13) MONTH = 1
C
C Print clock time
C
3 CALL POKE(Z,F778', HOUR/10+Z'.30')
CALL POKE(Z,F779', HOUR-10+(HOUR/10)+Z'.30')
CALL POKE(Z,F77A', Z'.3A')
CALL POKE(Z,F77B', MIN/10+Z'.30')
CALL POKE(Z,F77C', MIN-10+(MIN/10)+Z'.30')
CALL POKE(Z,F77D', Z'.3A')
CALL POKE(Z,F77E', SEC/10+Z'.30')
CALL POKE(Z,F77F', SEC-10+(SEC/10)+Z'.30')
C
C Decrease wait time
C
DO 20 I=1,MAIBIZ
IF (WTIME(I) NE. 1) GOTO 10
Wait is completed, signal the main program
WTIME(I) = 0
LINE = MLINE(I)
8SSTAT(LINE) = 8SSTAT(LINE).AND.8UMASK(I)
10 IF (WTIME(I).GT.1) WTIME(I) = WTIME(I)-1
20 CONTINUE
C
C Check alarm time
C
IF (.NOT.(ALARM.AND.(ALARM EQ. MIN).AND.(ALARM EQ. HOUR))) GOTO 23
ABEEP = .TRUE.
ALARM = .FALSE.
Sound the alarm if needed
25 IF (ABEEP) WRITE(2,1000)BEEP
1000 FORMAT(' ',BA1)
C
C Sound the message beep
C
IF (M8EEP) WRITE(2,1000)B8EEP
C
C Test one sense/control line
C
IF (.NOT. (DOIEBT OR (8TESTF.NE. 0))) GOTO 90
The test cannot be done if the sense line is already false.
27 IF (8SSTAT(I)EQ. 0) GOTO 80
OLDC = 8SSTAT(I)EQ. 0) GOTO 80
LINE = 1
Set for 7.5 msec delay
IDELAY = .300
IF (ITEST LT. N8TLOW) GOTO 29
LINE = N8TLOW
IDELAY = 1
29 CALL SETCNT(LINE,.FALSE)
Wait for slow optical circuits
DO 30 J=1,IDELAY
30 CONTINUE
OLDS = 8SSTAT(I)EQ. 0)
CALL SETCNT(I)EQ. 0)
Wait for slow optical circuits
DO 30 J=1,IDELAY
50 CONTINUE

```

```

NEWS = 8SSTAT(I)EQ. 0)
Restore lines
CALL SETCNT(I)EQ. 0)EQ. 0)
CALL SETCNT(LINE,.TRUE)
Do not return until line has settled
DO 55 J=1,IDELAY
55 CONTINUE
C
IF (NEWS EQ. 0) GOTO 70
Test loop is good
IF ((8SSTAT(I)EQ. 0).AND. (TESTM.NE. TESTM)) GOTO 80
Has changed since last looked at
8SSTAT(I)EQ. 0) = 8SSTAT(I)EQ. 0).AND. (.NOT. TESTM)
8TESTF = ITEST
GOTO 80
Test loop is fault
70 IF ((8SSTAT(I)EQ. 0).AND. (TESTM.NE. 0) GOTO 80
Has changed since last looked at
8SSTAT(I)EQ. 0) = 8SSTAT(I)EQ. 0).OR. TESTM
IF (ALERT) M8EEP = .TRUE.
8TESTF = -ITEST
Increment test line counter
8TEST = ITEST+1
8SIP low voltage test line
IF (ITEST EQ. N8TLOW) GOTO 80
IF (ITEST.GT. MLINE8) ITEST=2
C
C Reenable one hertz interrupt
C
90 CALL ENINTR
90 CONTINUE
END
SUBROUTINE TCSTAT(II)
C
TCSTAT: Type the status of one sense line
C
Input
C
II = Number of the control line whose status is to be typed
C
IMPLICIT INTEGER(A,C,E,P,R-Z),REAL(G),REAL*8(D),BYTE(B)
DIMENSION GCNAME(6,40),GCABBR(40),BCTEXT(40),BCSTAT(40)
BYTE FAULTM,IONDRM,MAITH,MANM,TESTM,8BTRM,CHANNM,
FADVM,OPCLVM,DNDQVM,UPDNVM
LOGICALAL1,PCSTAT,8SSTAT
COMMON /CNTAB/ GCNAME,GCABBR,BCTEXT,BCSTAT
COMMON /MASKS/ FAULTM,IONDRM,MAITH,MANM,TESTM,8BTRM,CHANNM
COMMON /KEYS/ FADVM,OPCLVM,DNDQVM,UPDNVM
COMMON /MODE/ FAULT,GOOD,ON,OFF,YES,NO
C
DATA BREV/20/,BINUL/0/
C
Read physical status and reverse if BCTEXTCO
IF (PCSTAT(II).AND.(BCTEXT(II).GT. 0)) GOTO 10
IF ((PCSTAT(II).EQ. 0).AND.(BCTEXT(II).LT. 0)) GOTO 10
DSTAT = DCADJ(II,OFF,1)
GOTO 20
10 DSTAT = DCADJ(II,ON,1)
C
Set reverse video flag if line is different from normal
20 8PBT = BINUL

```

```

C      IF((PCBTAT(11),EQ,0).AND.(BCTEXT(11).AND.UPDVM).EQ,0))BPBT=BREV
C      Write status line
C      IF ((BSTAT(11).AND.CHANN).EQ.CHANN) GOTO 30
1000  WRITE(1,1000)OCABR(11),GCNAME(1,11),I=1,6),BPBT,DBSTAT,SPBT
      FORMAT('A3,2X,6A4,A1,AB,A1/'),
      RETURN
30    WRITE(1,2000)OCABR(11),GCNAME(1,11),I=1,6),BPBT,DBSTAT,SPBT,
      BREV,BREV
2000  FORMAT('A3,2X,6A4,A1,AB,A1/'),A1,UNDER MANUAL CONTROL',A1/
      RETURN
      SUBROUTINE YBSTAT(11)
C      YBSTAT: Type the status of one sense line
C      Input:
C      I1 = Number of the sense line whose status is to be typed
C
C      IMPLICIT INTEGER*(A,C,E,P,R-Z),REAL*(G),REAL*(D),BYTE*(B)
      DIMENSION OSNAME(6,40),QBABR(40),BTEXT(40),BSTAT(40),BREP(40)
      BYTE      FAULTM,IONORM,WAITH,MANN,TESTH,SBTH,CHANN,
      LOGICAL*1 PBSTAT,PCBTAT
C      COMMON /SENAB/ OSNAME,QBABR,BTEXT,BSTAT,BREP
C      COMMON /HABKB/ FAULTM,IONORM,WAITH,MANN,TESTH,SBTH,CHANN,
C      COMMON /NUMBER/ NLINE,NBTLOW,NBHIGH,NCHTCH,NBLLOW,NCLLOW
C      COMMON /NEVB/ FAULT,GOOD,ON,OFF,YES,NO
C      DATA OND/'NO',OFF/'YES',
C      DATA FAULT/'FAULT',GOOD/'GOOD',
C      DATA BREV/'0',BNUL/'0/
C
10    IF (PBSTAT(11).AND.BTEXT(11).GT,0) GOTO 10
      IF ((PBSTAT(11).EQ,0).AND.BTEXT(11).LT,0) GOTO 10
      DLNE = DSADJ(11),FAULT,1)
      BLNR = BREV
      GOTO 20
      IF ((BTEXT(11).AND.UPDVM).NE,0) BLNR = BNUL
      GOTO 20
      DSADJ(11),GOOD,1)
      DLNE = BNUL
      GOTO 20
      IF ((BSTAT(11).AND.FAULTM).NE,FAULTM) GOTO 30
      BSTAT = DSADJ(11),FAULT,1)
      BSTR = BREV
      GOTO 40
      IF ((BTEXT(11).AND.UPDVM).NE,0) BSTR = BNUL
      GOTO 40
      BSTAT = DSADJ(11),GOOD,1)
      BSTR = BNUL
      GOTO 50
      IF ((BSTAT(11).AND.IONORM).EQ,IONORM) GOTO 50
      BION = OND
      BICR = BNUL
      GOTO 60
      GION = OYEB
      GICR = BREV
      GOTO 70
      IF ((BSTAT(11).AND.WAITH).EQ,WAITH) GOTO 70
      QMATI = QND
      GOTO 80
      QMATI = OYEB
      GOTO 80
      IF ((BSTAT(11).AND.TESTH).EQ,TESTH) GOTO 90
      BTEST = DGOOD
      BIST = BNUL

```

```

90    DTEST = DFAULT
      BIST = BREV
100   WRITE(1,1000)QBABR(11),QBNAME(1,11),I=1,6),BLNR,DLNE,BLNR,
      BSTR,DBSTAT,BSTR,BIOR,GIOR,QMATI,BTBT,DTEST,BTBT,BREP(11)
1000  FORMAT('A3,2X,6A4,A1,AB,2A1,A7,A1,2X,A1,A3,A1,4X,A3,
      RETURN
      END
      SUBROUTINE WAIBUS(TIME,DUNIT,LINE,BHABK)
C      WAIT: subroutine to execute a wait using the real time clock
C      Input:
C      TIME = Length of wait time
C      DUNIT = Units of wait time
C      LINE = Location to alter to signal completion
C      BHABK = Mask to use to signal completion
C
C      IMPLICIT INTEGER*(A,C,E,P,R-Z),REAL*(G),REAL*(D),BYTE*(B)
      DIMENSION WTIME(25),WLINE(25),QBABR(40),BTEXT(40),BSTAT(40),BREP(40)
      COMMON /WAIT/ WTIME,WLINE,BHABK,WAIBZ,DMIN,DBEC
C      Look for free slot in table
      DO 10 I=1,WAIBZ
      IF (WTIME(I).NE,0) GOTO 10
      Enter wait operation into table
      IF (DUNIT.EQ,DMIN) TIME = TIME*60
      WTIME(I) = TIME
      WLINE(I) = LINE
      BHABK(I) = BHABK
      RETURN
10    CONTINUE
      Table is full
      WRITE(1,1000)
1000  FORMAT('Wait table is full, no wait performed.')
      RETURN
      END
      DOUBLE PRECISION FUNCTION DCADJ(11,ONOFF,NORREV)
C      DCADJ: Return proper adjective to describe the state of a control line
C      Input:
C      I1 = Number of the sense line
C      ONOFF = ON -> Return the "on" adjective
C      NORREV = OFF -> Return the "off" adjective
C      NORREV < 0 -> Return the opposite adjective
C      NORREV > 0 -> Return the normal adjective
C      OUTPUT:
C      The value of the function will be an @ character string containing the
C      proper adjective
C      IMPLICIT INTEGER*(A,C,E,P,R-Z),REAL*(G),REAL*(D),BYTE*(B)
      DIMENSION GCNAME(6,40),OCABR(40),BTEXT(40),BSTAT(40)
      BYTE      FAULTM,IONORM,WAITH,MANN,TESTH,SBTH,CHANN,
      LOGICAL*1 PADDVM,DPCLVM,ONOFFVM,UPDVM
      COMMON /CNTAB/ GCNAME,OCABR,BTEXT,BSTAT

```

```

COMMON /MABK/  FAULT, IONRM, WAIT, MANN, TESTM, SBTH, CMANN,
1  FAGOV, OPCLVM, DNQFV, UPDNVM
COMMON /KEYS/  FAULT, GOOD, DN, OFF, YES, NO
DATA DOPEN/  OPEN  //, DCLOSE/  CLOSED //
DATA DON/    DN   //, DOFF/    OFF   //
DATA DUP/    UP   //, DDOWN/    DOWN //
C
C Decide which type of adjective to return
IF (NORREV, OT, 0, AND, DNQFV, EQ OFF) GOTO 10
IF (NORREV, LT, 0, AND, DNQFV, EQ DN) GOTO 10
C
C Assign adjective
IF ((BCTEXT(11)) AND DNQFV) NE, 0) DCADJ = DON
IF ((BCTEXT(11)) AND OPCLVM) NE, 0) DCADJ = DOPEN
IF ((BCTEXT(11)) AND UPDNVM) NE, 0) DCADJ = DUP
RETURN
10 IF ((BCTEXT(11)) AND DNQFV) NE, 0) DCADJ = DOFF
IF ((BCTEXT(11)) AND OPCLVM) NE, 0) DCADJ = DCLOSE
IF ((BCTEXT(11)) AND UPDNVM) NE, 0) DCADJ = DDOWN
RETURN
END
DOUBLE PRECISION FUNCTION DBADJ(11), FAGQ, NORREV)
C
C DBADJ: Return proper adjective to describe the state of a sense line
C
C Input:
C 11 = Number of the sense line
C FAGQ = FAULT -> Return the "fault" adjective
C NORREV < 0 -> Return the "good" adjective
C NORREV > 0 -> Return the opposite adjective
C
C Output:
C The value of the function will be an 8 character string containing the
C proper adjective.
C
IMPLICIT INTEGER*2(A,C,E,P,R,Z), REAL*4(I), REAL*8(D), BYTE(B)
DIMENSION GSNAM(6,40), GBABR(40), BTEXT(40), BBSTAT(40), BREF(40)
FAULT, IONRM, WAIT, MANN, TESTM, SBTH, CMANN,
1  FAGOV, OPCLVM, DNQFV, UPDNVM
COMMON /BENTAB/ GSNAM, GBABR, BBTEXT, BBSTAT, BREF
COMMON /NUMBER/ NLINES, NSTLOW, NCHIGH, NCHLOW, NSLOW, NCLDM
DATA  NLINES/47, NSTLOW/23, NCHIGH/24, NCHLOW/19,
1  NSLOW/14, NCLDM/11/
C
C INITIALIZE SENSE/CONTROL TABLES
C
DATA GBNAM/
1 'HIGH', VOL, 'TAGE', STA, 'TUB
1 'FORE', PUMP, 1, P, 'REB', 'URE
1 'DUP', LASH, 'ATRO', 'N BD', 'X VA', 'CURN
1 'CESI', 'UM B', 'DI V', 'ACU', 'H
1 'COIL', BOX, 'VAC', 'UUM
1 'DIFF', 'USIO', 'N PU', 'HP 1', 'THE', 'RHAL
1 'DIFF', 'USIO', 'N PU', 'HP 2', 'THE', 'RHAL
1 'DIFF', 'USIO', 'N PU', 'HP 3', 'THE', 'RHAL
1 'DIFF', 'USIO', 'N PU', 'HP 4', 'THE', 'RHAL
1 'PROB', 'E WA', 'TER
1 'AND', 'E WA', 'TER
1 'ARC', 'RESI', 'STOR', 'WAT', 'ER
1 'SPAR', 'E BE', 'NSE', 'A
1 'SOUR', 'CE M', 'AONE', 'T WA', 'TER
1 'SPAR', 'E BE', 'NSE', 'C
1 'SPAR', 'E BE', 'NSE', 'D
1 'SPAR', 'E BE', 'NSE', 'E
1 'SPAR', 'E BE', 'NSE', 'F
1 'SPAR', 'E BE', 'NSE', 'O
1 'SPAR', 'E SE', 'NSE', 'H
1 'STAN', 'DBY', 'MODE
1 'SPAR', 'E SE', 'NSE', 'J
1 'OPER', 'ATIN', 'O MO', 'DE
1 'LOW', 'VOLT', 'AGE', 'BTAT', 'US
1 'FORE', PUMP, 3, P, 'REB', 'URE
1 'DIFF', 'USIO', 'N PU', 'HP 3', 'THE', 'RHAL
1 'MIR', 'DR B', 'DI V', 'ACU', 'H
1 'CHIL', 'LER', 'FAIL', 'URE
1 'OIL', 'PRES', 'SURE
1 'OIL', 'TEMP', 'ERAT', 'URE

```

```

COMMON /MABK/  FAULT, IONRM, WAIT, MANN, TESTM, SBTH, CMANN,
1  FAGOV, OPCLVM, DNQFV, UPDNVM
COMMON /KEYS/  FAULT, GOOD, DN, OFF, YES, NO
DATA DOPEN/  OPEN  //, DCLOSE/  CLOSED //
DATA DON/    DN   //, DOFF/    OFF   //
DATA DUP/    UP   //, DDOWN/    DOWN //
C
C Decide which type of adjective to return
IF (NORREV, OT, 0, AND, DNQFV, EQ OFF) GOTO 10
IF (NORREV, LT, 0, AND, DNQFV, EQ DN) GOTO 10
C
C Assign adjective
IF ((BCTEXT(11)) AND DNQFV) NE, 0) DCADJ = DON
IF ((BCTEXT(11)) AND OPCLVM) NE, 0) DCADJ = DOPEN
IF ((BCTEXT(11)) AND UPDNVM) NE, 0) DCADJ = DUP
RETURN
10 IF ((BCTEXT(11)) AND DNQFV) NE, 0) DCADJ = DOFF
IF ((BCTEXT(11)) AND OPCLVM) NE, 0) DCADJ = DCLOSE
IF ((BCTEXT(11)) AND UPDNVM) NE, 0) DCADJ = DDOWN
RETURN
END
DOUBLE PRECISION FUNCTION DBADJ(11), FAGQ, NORREV)
C
C DBADJ: Return proper adjective to describe the state of a sense line
C
C Input:
C 11 = Number of the sense line
C FAGQ = FAULT -> Return the "fault" adjective
C NORREV < 0 -> Return the "good" adjective
C NORREV > 0 -> Return the opposite adjective
C
C Output:
C The value of the function will be an 8 character string containing the
C proper adjective.
C
IMPLICIT INTEGER*2(A,C,E,P,R,Z), REAL*4(I), REAL*8(D), BYTE(B)
DIMENSION GSNAM(6,40), GBABR(40), BTEXT(40), BBSTAT(40), BREF(40)
FAULT, IONRM, WAIT, MANN, TESTM, SBTH, CMANN,
1  FAGOV, OPCLVM, DNQFV, UPDNVM
COMMON /BENTAB/ GSNAM, GBABR, BBTEXT, BBSTAT, BREF
COMMON /NUMBER/ NLINES, NSTLOW, NCHIGH, NCHLOW, NSLOW, NCLDM
DATA  NLINES/47, NSTLOW/23, NCHIGH/24, NCHLOW/19,
1  NSLOW/14, NCLDM/11/
C
C INITIALIZE SENSE/CONTROL TABLES
C
DATA GBNAM/
1 'HIGH', VOL, 'TAGE', STA, 'TUB
1 'FORE', PUMP, 1, P, 'REB', 'URE
1 'DUP', LASH, 'ATRO', 'N BD', 'X VA', 'CURN
1 'CESI', 'UM B', 'DI V', 'ACU', 'H
1 'COIL', BOX, 'VAC', 'UUM
1 'DIFF', 'USIO', 'N PU', 'HP 1', 'THE', 'RHAL
1 'DIFF', 'USIO', 'N PU', 'HP 2', 'THE', 'RHAL
1 'DIFF', 'USIO', 'N PU', 'HP 3', 'THE', 'RHAL
1 'DIFF', 'USIO', 'N PU', 'HP 4', 'THE', 'RHAL
1 'PROB', 'E WA', 'TER
1 'AND', 'E WA', 'TER
1 'ARC', 'RESI', 'STOR', 'WAT', 'ER
1 'SPAR', 'E BE', 'NSE', 'A
1 'SOUR', 'CE M', 'AONE', 'T WA', 'TER
1 'SPAR', 'E BE', 'NSE', 'C
1 'SPAR', 'E BE', 'NSE', 'D
1 'SPAR', 'E BE', 'NSE', 'E
1 'SPAR', 'E BE', 'NSE', 'F
1 'SPAR', 'E BE', 'NSE', 'O
1 'SPAR', 'E SE', 'NSE', 'H
1 'STAN', 'DBY', 'MODE
1 'SPAR', 'E SE', 'NSE', 'J
1 'OPER', 'ATIN', 'O MO', 'DE
1 'LOW', 'VOLT', 'AGE', 'BTAT', 'US
1 'FORE', PUMP, 3, P, 'REB', 'URE
1 'DIFF', 'USIO', 'N PU', 'HP 3', 'THE', 'RHAL
1 'MIR', 'DR B', 'DI V', 'ACU', 'H
1 'CHIL', 'LER', 'FAIL', 'URE
1 'OIL', 'PRES', 'SURE
1 'OIL', 'TEMP', 'ERAT', 'URE

```

```

1 'SPAR', 'E CO', 'NITRO', 'L L',
1 'SPAR', 'E CO', 'NITRO', 'L M',
1 'SPAR', 'E CO', 'NITRO', 'L N',
1 'SPAR', 'E CO', 'NITRO', 'L O',
DATA OCABRR/
1 'HVT', 'DP1', 'DP2', 'DP3', 'DP4', 'FRC', 'SCA', 'ARC',
1 'FV1', 'FV2', 'FV3', 'CCB', 'QV1', 'QV2', 'QV3', 'QV4',
1 'BCB', 'SPN', 'GUN', 'SCE', 'BCF', 'BCO', 'BCH', 'BCI',
1 'LVT', 'MCP', 'DCP', 'DP5', 'BCJ', 'FV4', 'AUD', 'FRV',
1 'BRS', 'CML', 'QV5', 'BCK', 'BCL', 'BCM', 'BCN', 'BCD',
DATA BCTEXT/
1 -124.04.04.04.04.04.04,
1 02.02.02.04.02.02.02.02,
1 02.08.04.04.04.04.04,
1 -124.04.04.04.04.02.-124.04,
1 04.02.02.04.04.04.04.04/
END

```

C

C

```

1 'MATE', 'R PR', 'ESSU', 'RE',
1 'MATE', 'R TE', 'MPER', 'ATUR', 'E',
1 '30 D', 'EGRE', 'E WA', 'TER', 'PRES', 'BURE',
1 '30 D', 'EGRE', 'E WA', 'TER', 'PRES', 'BURE',
1 '30 D', 'EGRE', 'E WA', 'TER', 'PRES', 'BURE',
1 'SAFE', 'TY I', 'NIE', 'LOCK', 'TEMP',
1 'SPAR', 'E SE', 'NSE', 'L',
1 'SPAR', 'E SE', 'NSE', 'M',
DATA QSABRR/
1 'HVS', 'FPI', 'FR2', 'DBV', 'CSV', 'CBV', 'DIT', 'DZT',
1 'DZT', 'DAT', 'PR4', 'ANN', 'BSA', 'BMM', 'BSC',
1 'SSD', 'SSE', 'SSF', 'SBM', 'SBY', 'SSJ', 'DPR',
1 'LVS', 'FP3', 'DST', 'MBV', 'CHL', 'DLP', 'DLT', 'MAP',
1 'MAT', 'P30', 'T30', 'P80', 'T80', 'BIL', 'BSL', 'BSM',
-128-80het, -127=81het, -126=82het, etc
DATA B5TEXT/
1 -127.01.01.01.01.01.01.01,
1 01.01.01.01.01.02.01.02,
1 02.02.02.02.02.-124.02.-124,
1 -127.01.01.01.01.01.01.01,
1 01.01.01.01.01.01.02.02/
DATA GCNAME/
1 'HIGH', 'VOL', 'TAGE', 'TEB', 'T',
1 'DIFF', 'USID', 'N PU', 'MP 1',
1 'DIFF', 'USID', 'N PU', 'MP 2',
1 'DIFF', 'USID', 'N PU', 'MP 3',
1 'DIFF', 'USID', 'N PU', 'MP 4',
1 'FRED', 'N CD', 'MPRE', 'SBOR',
1 'SPAR', 'E CO', 'NITRO', 'L A',
1 'ARC', 'CURR', 'ENT', 'L',
1 'FDR', 'LINE', 'VAL', 'VE 1',
1 'FDR', 'LINE', 'VAL', 'VE 2',
1 'FDR', 'LINE', 'VAL', 'VE 3',
1 'COIL', 'CUR', 'RENT', 'B',
1 'GATE', 'VAL', 'VE 1',
1 'GATE', 'VAL', 'VE 2',
1 'GATE', 'VAL', 'VE 3',
1 'GATE', 'VAL', 'VE 4',
1 'SPAR', 'E CO', 'NITRO', 'L B',
1 'SPIN', 'DIR', 'ECTI', 'ON',
1 'QUEN', 'CH',
1 'SPAR', 'E CO', 'NITRO', 'L E',
1 'SPAR', 'E CO', 'NITRO', 'L F',
1 'SPAR', 'E CO', 'NITRO', 'L G',
1 'SPAR', 'E CO', 'NITRO', 'L H',
1 'SPAR', 'E CO', 'NITRO', 'L I',
1 'LDN', 'VOL', 'AGE', 'TEST',
1 'MATE', 'R CI', 'RCUL', 'ATIO', 'N PU', 'MP',
1 'DIL', 'CIRC', 'ULAT', 'IDN', 'PUMP',
1 'DIFF', 'USID', 'N PU', 'MP 5',
1 'SPAR', 'E CO', 'NITRO', 'L J',
1 'FDR', 'LINE', 'VAL', 'VE 4',
1 'AUDI', 'D AL', 'ARM',
1 'FRAM', 'E VO', 'LTAD', 'E',
1 'SPIN', 'ROT', 'ATIO', 'N SO', 'LENT', 'OD',
1 'CITY', 'WAT', 'ER L', 'INE',
1 'GATE', 'VAL', 'VE 5',
1 'SPAR', 'E CO', 'NITRO', 'L K',

```

C

C

C

C



```

LDAX D
CALL DBRM
ADI 20H
STA PSB1+1
IN 0
ANA B
ANA A
JZ PASS2
MOV A,OFFH
MOV C,A
LDA CLAS
CPI 3
JMP PASS2
MOV A,B
OFFH
C
JMP CLOUT
LDA CLAB
CPI 3
JMP PASS2
MOV A,C
LDA CLAS
CPI 3
JMP PASS2
ORA B
CLOUT: OUT 0
RET 0
CLAB: DB 0

; SUBROUTINE TO GENERATE PORT AND BIT #
; ENTERS WITH LINE NUMBER IN A
; RETURNS WITH PORT # IN A AND CORRECT BIT SET IN B
DBRM: DCR A
MOV B,7H
MOV C,A
ANA B
MOV B,A
MOV A,C
RAR
RAR
RAR
ANI 1FH
MOV C,A
CPI 3
JMP DBRP
INR C
MOV A,1H
INR B
DBRP: INR B
DBLP: JZ DBOT
RLC
JMP DBLP
MOV B,A
MOV A,C
STA CLAB
RET
END

; SEQUEN: Action sequence definitions
; TITLE SEQUEN P18 MICRO ACTION SEQUENCES
COMMON /SEQCMD/
;DEFINE SENSE AND CONTROL LINE NAMES
MVS EQU 1
FPI EQU 2
FP2 EQU 3
DBV EQU 4
CSV EQU 5
CBV EQU 6
D1T EQU 7
D2T EQU 8
D3T EQU 9

```

```

; LOAD PARAM VALUE
; GENERATE PORT AND BIT
; ADD OFFSET ADDRESS TO PORT
; PLANT PORT
; READ PORT
; MASK OUT BIT
; CHECK IF ZERO
; YES
; ELSE SET ALL ONES
; SAVE IN C
; PICK UP PORT #
; JUMP IF 0, E, 2
; ELSE COMPLEMENT RESULT
; RESULT IN A FOR LOGICAL FUNCTION RETURN
; PUT INTO (HL) FOR INTEGER FUNCTION RETURN
; EXIT
; READS CONTROL LINE STATUS
; FUNCTION PCSTAT(1)
; WHERE T IS (INTEGER*1) CONTROL LINE NUMBER
ENTRY PCSTAT
PCSTAT: XCHG
LDAX D
CALL DBRM
ADI 20H
STA PCB1+1
IN 0
ANA B
ANA A
JZ PCB2
MOV A,OFFH
MOV C,A
LDA CLAB
CPI 3
JMP PCB3
MOV A,C
OFFH
MOV C,A
MOV H,A
MOV L,A
RET

; BET CONTROL LINE
; CALL SETCNT(I,L)
; WHERE I IS (INTEGER*1) CONTROL LINE NUMBER
; L IS (LOGICAL*1) VALUE TO SET PORT TO
ENTRY SETCNT
SETCNT: XCHG
LDAX D
CALL DBRM
ADI 20H
STA CLIN+1
STA CLOUT+1
XCHG
IN 0
MOV C,A
LDA D
ANA A

```









```
FV4DF--SEQSTR*1
DW
AUDDF--SEQSTR*1
DW
FRVDF--BEQSTR*1
DW
SRSDF--SEQSTR*1
DW
CMLDF--SEQSTR*1
DW
CVJDF--SEQSTR*1
DW
SCSDF--SEQSTR*1
DW
SCSDF--BEQSTR*1
DW
SCSDF--SEQSTR*1
DW
SCSDF--SEQSTR*1
DW
SCSDF--SEQSTR*1
DW
END
```

## BIOGRAPHY

Michael Carl Wright

- PERSONAL: Born March 20, 1955, Conway, Arkansas
- EDUCATION: Bachelor of Arts with High Honors in Mathematics  
University of Tennessee, 1977
- POSITIONS: Teaching Assistant, Duke University, 1977-1978  
Research Assistant, Duke University, 1978-1983
- MEMBERSHIPS: Phi Beta Kappa, Sigma Xi
- PUBLICATIONS: "Proton Capture in the 19 MeV Region of  $^{12}\text{C}$ ", M. C. Wright,  
N. R. Roberson, H. R. Weller, D. R. Tilley, and Dean  
Halderson, Phys. Rev. C25 (1982) 2823.
- ABSTRACTS: "The  $^{13}\text{C}(\vec{n}, \gamma_0)^{14}\text{C}$  Reaction", M. C. Wright, H. Kitazawa,  
N. R. Roberson, H. R. Weller, M. J. Jensen, and D. R. Tilley,  
Bull. Am. Phys. Soc. 28 (1983) 650.